IDENTIFICATION AND CHARACTERISATION OF GANGLION CELL LOSS IN OPTIC NEUROPATHIES

Prema Sriram
B S (Optometry)

Australian School of Advanced Medicine
Faculty of Human Sciences
Macquarie University

A thesis submitted to Macquarie University in fulfillment of the requirements for the degree of Doctor of Philosophy

May 2014

Supervisors
Prof Stuart L Graham
A/Prof Alexander Klistorner
Dr Hema Arvind

TABLE OF CONTENTS

	Page
Declaration of Originality	5
Acknowledgements	6
Thesis Summary	7
Thesis Outline	8
List of Abbreviations	10
Chapter 1: Introduction to ganglion cells	
1.1 Anatomy of the retina	13
1.1.1 Cellular organization of the retina	13
1.1.2 General histological organization of the retina	17
1.2 Anatomy of the Optic Nerve Head and Retinal Nerve Fibre layer	22
1.3 Anatomy and physiology of the Retinal Ganglion cells	25
1.4 Axonal loss in different diseases	27
1.4.1 Glaucoma	28
1.4.2 Multiple Sclerosis	31
1.5 Methods of assessment of ganglion cell function	38
1.5.1 Structural tests	
a. Disc photography	39
b. Scanning laser ophthalmoscopy	42
c. Optical coherence tomography	46
d. Scanning laser photography	50
1.5.2 Functional tests	
a. Standard Automated Perimetry	51

b. Short Wavelength Automated Perimetry 56

c. Frequency Doubling Technology Perimetry 62

d. Electroretinogram 68

i. Oscillatory potentials in glaucoma 70

ii. Photopic negative response in glaucoma 71

iii. Scotopic threshold response in glaucoma 72

iv. Pattern Electroretinogram 72

v. Multifocal Electroretinogram 76

vi. Visual Evoked Potential 78

Chapter 2: Structural and Functional Identification of Early Glaucoma

2.1 Introduction 94

2.2 Aim of the study 95

2.3 Methods 95

2.4 Results 98

2.5 Discussion 102

Chapter 3: Reproducibility of multifocal VEP latency using different stimulus presentations

3.1 Abstract 106

3.2 Introduction 107

3.3 Methods 108

3.4 Results 112

3.5 Discussion 114

Chapter 4: Optic Neuropathy in Multiple Sclerosis

4.1 Introduction 118

4.2 Methods 119

4.3 Results 120

4.3.1 MS Non Optic Neuritis eyes 122

4.3.2 Optic Neuritis eyes 131

4.4 Discussion 133

Chapter 5: Transsynaptic retinal degeneration in optic neuropathies: Optical Coherence Tomography study

5.1 Abstract 137

5.2 Introduction 138

5.3 Materials and methods 139

5.4 Results 141

5.4.1 Glaucoma group 141

5.4.2 Multiple sclerosis group 144

5.5 Discussion 146

Chapter 6: Conclusion 149

References 152

Appendix I (Ethics approval)

DECLARATION OF ORIGINALITY

I hereby declare that this thesis is my original work, as supported by chapters published in various peer reviewed journals, except where acknowledgement has been made below and where due reference has been in the text. To the best of my knowledge, this thesis does not contain material that has been accepted for the award of any other degree or diploma at the University or any other tertiary institution. An Ethics committee approval was obtained from the University of Sydney and Macquarie University (HREC Approval number: 05- 2009/11594) prior to commencement of the study. All the experiments included in this thesis were performed at Save Sight Institute, University of Sydney and Australian School of Advanced Medicine, Macquarie University.

I give consent for the thesis to be made available for photocopying and loan if accepted for the award of the degree.

Prema Sriram

May 2014

ACKNOWLEDGEMENTS

I wish to express my gratitude and thankfulness to my supervisors Prof Stuart Graham, A/Prof Alexander Klistorner and Dr Hema Arvind for their support and guidance throughout my research. Their encouragement, enthusiasm and valuable suggestions have been a great source of motivation for improvement.

I would also like to thank Dr John Grigg, Ophthalmologist and neurologists Dr Con Yiannikus, Dr Raymond Garrick, Dr Michael Barnett and Dr John Parratt who have helped me recruit patients for my study.

I thank my friends Deepa Viswanathan and Radha Govind for having cheered and motivated me during tough challenges in the last 4 years.

I wish to acknowledge Macquarie University for having offered support in terms of funding under the International Macquarie Research Excellence Scholarship (iMQRES) scheme.

I also wish to thank Glaucoma Australia for having funded my study

Finally, last but not the least, I would like to thank my parents, husband and my children for their never-ending love, trust and support. Without them I would have never gotten through this journey and completed this thesis.

THESIS SUMMARY

This thesis explores the identification of ganglion cell loss in optic neuropathies, and utilizes new technologies. Two commonly prevalent optic neuropathies have been studied – Glaucoma, which is common among the older population and Mutiple Sclerosis (MS) associated optic neuropathy, which is more prevalent in the younger population.

The aim of the glaucoma study was to identify the combination of the tests would identify very early loss of ganglion cells. Knowledge of this impact will then allow clinicians to identify patients with early glaucomatous damage and start treatment before evident visual field loss. The study revealed that Heidelberg retina tomograph (HRT) and Low contrast multifocal visual evoked potential (LLA mfVEP) were two sensitive tests in detecting patients with preperimetric and early glaucomatous defects. The aim of the MS study was to identify ganglion cell loss in patients with MS with or without previous history of Optic Neuritis (ON). The study also aimed to prove if the eye is a primary site of neurodegeneration in patients with multiple sclerosis. This could possibly shed some light in the pathological changes in the eye that occurs with MS related neurodegeneration. The results of the study indicated the presence of a trans neuronal degeneration, which could be retrograde (from optic radiation to retina) or anterograde (from retina to visual cortex). We also proved the absence of retrograde degeneration since the ERG changes were of similar magnitude in both ON and NON eyes of MS patients.

THESIS OUTLINE

Chapter 1: INTRODUCTION

The introduction includes a brief overview of the retinal structure, anatomy of the Optic Nerve Head (ONH), ganglion cells and their axons. Ganglion cell losses in different diseases, with detailed review on two specific diseases– glaucoma and MS have been included. Different methods to assess ganglion cell loss have also been discussed in detail.

Chapter 2: STRUCTURAL AND FUNCTIONAL IDENTIFICATION OF EARLY GLAUCOMA

This chapter describes a major study that investigated the various diagnostic tests used in clinical glaucoma practice. The study aimed to determine the diagnostic test(s) that identified earliest ganglion cell loss in glaucoma. Results of the study have been discussed in detail.

Chapter 3: REPRODUCIBILITY OF MULTIFOCAL VEP LATENCY USING DIFFERENT STIMULUS PRESENTATIONS

This study was performed to assess the reproducibility of latency of multifocal visual evoked potential (mfVEP) recorded using different stimulus presentations, and to identify the peak with least variability. Results of this study have been discussed in detail in this chapter.

Chapter 4: OPTIC NEUROPATHY IN MULTIPLE SCLEROSIS

This chapter involves a comprehensive functional and structural assessment of the entire visual pathway in MS to evaluate possible association of both proximate (outer retinal) and distal (optic tract and optic radiation) pathology with loss of ganglion cell and its axons. Results of this study

have been discussed.

Chapter 5: TRANSSYNAPTIC RETINAL DEGENERATION IN OPTIC NEUROPATHIES: OPTICAL COHERENCE TOMOGRAPHY STUDY

This study was performed to determine if there was any loss of INL secondary to the loss of GCL in patients with long standing ganglion cell loss in conditions such as glaucoma and ON associated with multiple sclerosis. Results of this study have been discussed in detail in this chapter.

Chapter 6: CONCLUSIONS

The results of all the studies conducted as part of this thesis has been summarised in this chapter. A section on future directions from this study has also been included.

LIST OF ABBREVIATIONS

1. ANCOVA	Analysis of Covariance
2. ANOVA	Analysis of Variance
3. APP	Amyloid Precursor Protein
4. BBB	Blood Brain Barrier
5. BonY	Blue on Yellow
6. CDMS	Clinically Definite Multiple Sclerosis
7. CNS	Central Nervous System
8. CNTGS	Collaborative Normal Tension Glaucoma Study
9. CR	Coefficient of reliability
10. CSLO	Confocal Scanning Laser Ophthalmoscope
11. EEG	Electroencephalogram
12. EGPS	European Glaucoma Prevention Study
13. EMGT	Early Manifest Glaucoma Trial
14. ERG	Electroretinogram
15. ERP	Event Related Potential
16. FDT	Frequency Doubling Technology
17. GCL	Ganglion Cell Layer
18. GON	Glaucomatous Optic Neuropathy
19. GPA	Guided Progression Analysis
20. HFA	Humphrey Field Analyser
21. HRT	Heidelberg Retina Tomograph
22. HTG	High Tension Glaucoma
23. ICC	Intra Class Coefficient

24. INL	Inner Nuclear layer
25. IOP	Intra Ocular Pressure
26. IPL	Inner Plexiform Layer
27. LGN	Lateral Geniculate Nucleus
28. LLA	Low Luminance Achromatic
29. MD	Mean Deviation
30. mfERG	Multifocal Electroretinogram
31. mfVEP	Multifocal Visual Evoked Potential
32. MRA	Moorefield Regression Analysis
33. MRI	Magnetic Resonance Imaging
34. MS	Multiple Sclerosis
35. NAWM	Normal Appearing White Matter
36. NIRS	Near Infra Red Spectroscopy
37. NON	Non Optic Neuritis
38. OCT	Optical Coherence Tomography
39. OHT	Ocular Hypertension
40. OHTS	Ocular Hypertension Study
41. ON	Optic Neuritis
42. ONH	Optic Nerve Head
43. ONHC	Optic Nerve Head Component
44. ONTT	Optic Neuritis treatment Trial
45. OP	Oscillatory Potential
46. OPL	Outer Plexiform Layer
47. PERG	Pattern Electroretinogram
48. PET	Positron Emission Tomography

49. PhNR	Photopic Negative Response
50. PO	Pattern Onset
51. POAG	Primary Open Angle Glaucoma
52. PPMS	Primary progressive Multiple Sclerosis
53. PR	Pattern Reversal
54. PXEG	Pxeudoexfoliation Glaucoma
55. RGC	Retinal Ganglion Cell
56. RNFL	Retinal Nerve Fibre Layer
57. RPE	Retinal Pigment Epithelium
58. RRMS	Relapsing Remitting Multiple Sclerosis
59. SAFE	Structure and Function Evaluation Study
60. SAP	Standard Automated Perimetry
61. SD	Standard Deviation
62. SD-OCT	Spectral Domain Optical Coherence Tomography
63. SITA	Swedish Interactive Threshold Algorithm
64. SLP	Scanning Laser Polarimetry
65. SNR	Signal to Noise Ratio
66. SPMS	Secondary Progressive Multiple Sclerosis
67. STR	Scotopic Threshold Response
68. SWAP	Short Wavelength Automated perimetry
69. TTX	Tetrodotoxin
70. UHR-OCT	Ultra High Resolution Coherence Tomography
71. VEP	Visual Evoked Potential

CHAPTER 1: INTRODUCTION TO RETINA

1.1 ANATOMY OF THE RETINA

The retina is the best-studied part of the human brain. Embryologically it is a part of the Central Nervous System (CNS),[1-5] but is readily accessible to examination and can be investigated with relative ease by both scientists and clinicians. Moreover, an estimated 80% of all sensory information in humans is thought to be of retinal origin,[6] indicating the importance of retinal function for the ability to interact with the outside world.

1.1.1 CELLULAR ORGANIZATION OF THE RETINA

The major cellular components of the retina are the RPE cell, the photoreceptor cells, the interneurons, the ganglion cells, and the glial cells (Figure 1).

a. RETINAL PIGMENT EPITHELIUM

Like the sensory components of the neuroretina, the RPE cell is of neuroectodermal embryonic origin.[1-5, 7, 8] Each adult human retina contains about 3.5 million RPE cells[9] whose diameters vary four- fold between 14 mm in the central retina and 60 mm in the peripheral retina.[10] The density of RPE cells is greater in the fovea (5,000 cells/mm2) than in the periphery (2,000 cells/mm2).[11] In the central retina, where RPE cells are most tightly packed, they take the shape of regular hexagonal tiles that form a single layer of cuboidal epithelium. Tight junctions between adjacent RPE cells form the outer blood- retina barrier, an important physiologic barrier to the free flow of molecules between the leaky choriocapillaris and the photoreceptors of the neuroretina.[12-18] The flow of the subretinal fluid through the RPE has been reported to reflect active transport of ions or difference in oncotic pressure and plays an important role in the attachment of the retina to the

RPE.

b. PHOTORECEPTORS

The photoreceptors are the sensors of the visual system that convert the capture of photons into a nerve signal in a process called phototransduction.[19] The human retina contains approximately four to five million cones and 77–107 million rods.[19-21] Only cones are found in the foveola, whereas rods predominate outside the foveola in the remaining fovea and the entire peripheral retina. Among the three cone photoreceptors, red cones (63% or 2.9 million) are more common than green (32% or 1.4 million) and blue cones (5% or 0.2 million).[22] Each photoreceptor consists of an outer segment (photopigment), inner segment (mitochondria, endoplasmatic reticulum), a nucleus, an inner fibre (analogous to an axon), and the synaptic terminal.[23] The inner fibre is the axon of the photoreceptor cell and transmits the photoreceptor cell signals to the OPL via its synaptic terminals. Due to the absence of inner nuclear layer cells in the foveola, the inner foveolar fibres have to travel to the OPL in the surrounding macula to make synaptic contact.

c. INTERNEURON CELLS

Interneurons in the inner nuclear retinal layer connect the photoreceptor layer with the ganglion cell layer. These interneurons consist of the bipolar, horizontal, amacrine, and interplexiform cells, which form complex neuroretinal circuitries in the Outer Plexiform layer (OPL) and Inner Plexiform Layer (IPL) to process the photoreceptor signal and transmit this information to the ganglion cell layer (GCL). In the simplest case, the photoreceptor cell is directly connected to a ganglion cell via a bipolar cell. *Bipolar cells* receive input from either rods or cones.[6, 25, 26] Cone bipolar cells may make contact with as few as one cone, while rod bipolar cells may receive input from up to 70 rods. Depending

on their response to glutamate, bipolar cells are classified as being hyper-polarising (OFF-centre) or depolarising (ON-centre). Photoreceptors also interact with horizontal cells in the OPL.[27] Three types of horizontal cells have been described in the human retina.[28, 29] Amacrine cells are mainly found in the inner nuclear layer, although some are seen in the GCL and the IPL as well.[30] There are as many as 30 different types of amacrine cells, though the functional significance of each of these is not fully understood.[21] Another interneuron in the inner nuclear layer – the *interplexiform cell* – has processes extending into the IPL and OPL. Thus, on their way to the ganglion cell, visual signals are transmitted and modified by bipolar, horizontal, amacrine, and interplexiform cells as part of the visual processing within the retina.[27]

d. GANGLION CELLS

The ganglion cells are responsible for transmitting visual information from the retina to the brain. The ganglion perikarya are located in the GCL, while their dendrites make contact with bipolar and amacrine cells in the IPL. Up to 20 different ganglion cell types have been described in the human retina – the two best known types are the midget and the parasol cells, which make up about 80% of ganglion cell population.[21] The midget ganglion cell (also known as P or b cell) receives input from midget bipolar cells at a ratio of up to one-to-one in the fovea. It is a small cell with a relatively small dendritic arbor. The parasol ganglion cell (M or a cell) has a much more extensive dendritic arbor that resembles an opened umbrella in histological preparations of the retina. Midget and parasol cells project to the parvocellular and magnocellular layers of the Lateral Geniculate Nucleus (LGN), respectively.[31, 32] Because of the anatomic distance between the retina and the brain, the ganglion cell axons require effective mechanisms for transport of metabolites and organelles away from (anterograde) and back to (retrograde) the ganglion cell nucleus. Axonal transport occurs at slow (<10 mm/

day), high (hundreds of mm/day), or intermediate velocities.

e. GLIAL CELLS

Four glial cell types are found in the retina: Muller cells, astrocytes, micoglia, and occasionally, oligodendrocytes. Muller cells are the main glial cells of the retina.[33-36] Their perikarya are located in the inner nuclear layer with cell processes that span the entire neuroretina.[33] The proximal extensions of Muller cells expand and flatten to form so-called endfeet whose basal lamina forms the inner limiting membrane.[37] Distally, Muller's extensions give rise to the outer limiting membrane by forming a series of junctional complexes. Lateral extensions of Muller cells surround the retinal neurons. Muller cell processes also cover retinal blood vessels. They play a crucial role in maintaining the local environment that allows the visual process to function optimally. Astrocytes are thought to derive from stem cells in the optic nerve and are found in the superficial layers of the neuroretina where they surround ganglion cells, nerve fibres, and superficial retinal blood vessels.[38] Microglia enter the retina from the circulation.[38] They are phagocytic and part of the reticuloendothelial system. They are usually found in small numbers in the nerve fibre layer, but are mobile and can reach any part of the retina. Oligodendrocytes give rise to the myelin sheath in the peripheral nervous system. Though normally unmyelinated, retinal nerve fibres occasionally are seen to be myelinated, indicating that oligodendrocytes can reach the retina in certain conditions.

1.1.2 GENERAL HISTOLOGICAL ORGANIZATION OF THE RETINA

The retina is the neurosensory component of the eye. Its outer part is supplied by a vascular layer, the choroid, and protected by a tough outer layer, the sclera. The cellular elements of the retina are arranged and adapted to meet the functional requirements of the different

regions of the retina (Figure 1).

a. Bruch's Membrane

This membrane separates the choriocapillaris from the RPE. It is an elastic membrane composed of five layers: the basement membrane of the choriocapillaris, an outer collagenous layer, a central elastic layer, an inner collagenous layer, and the basement membrane of the RPE. It stretches from the optic disc at the posterior pole to the ora serrata anteriorly and varies in thickness between 2 and 4 μm at the posterior pole and 1– 2 μm at the ora serrata. With age, Bruch's membrane grows thicker and its ultrastructure becomes less distinct.

b. Retinal Pigment Epithelial layer

Each eye contains about 3.5 million RPE cells,[9] which are held together by junctional complexes to form a continuous epithelial monolayer. The tight junctions (zonulae occludentes) between these RPE cells separate the choriocapillaris from the photoreceptors of the outer retina, thus creating the outer blood-retina barrier, a selective barrier between the outer retina and its choroidal blood supply.[12-18] This barrier helps to control the extracellular milieu and maintain the function of the outer retina.

c. Photoreceptor Layer

Rods and cones are tightly stacked together into a single pallisading layer of photoreceptors.[19, 20, 23, 39-41] This thin, subcellular stratum is the only light-sensitive part of the neuroretina and the site of phototransduction. All other layers of the neuroretina collectively serve to process and transmit these nerve signals.

d. External Limiting Membrane

This is not a true membrane, but created by junctional complexes between adjacent Muller cells as well as between Muller and photoreceptor cells. The subretinal space is a potential space lying between the outer blood retina barrier and the external limiting membrane.[42-43]

e. Outer Nuclear Layer

The outer nuclear layer contains the nuclei of the photoreceptor cells and is thickest in the foveolar area. The human retina contains approximately four to five million cones and 77–107 million rods.[19-21]. The maximum rod density is found in the "rod ring" about 4.5 mm, or 20–25°, from the foveola. The absence of rods from the foveola ("rod-free zone") accounts for the physiological central scotoma that is experienced under extreme scotopic conditions.

f. Outer Plexiform Layer

In the OPL, photoreceptor cells of the outer nuclear layer form connections with the bipolar and horizontal cells of the inner nuclear layers. This is an important initial processing step in the retina: Individual cone photoreceptor signals are connected in such a way that they give rise to concentric receptive fields with an antagonistic centre- surround organisation. These signals are then transmitted to the next layer of processing, the IPL, by bipolar cells.[44, 45]

g. Inner Nuclear Layer

This layer harbours the nuclei of not less than five different types of cells: the horizontal, the bipolar, the amacrine, the interplexiform, and the Muller cells. The horizontal cells are located along the outer limit of the inner nuclear layer facing the OPL, whereas the amacrine faces the IPL. The nuclei of the bipolar, interplexiform, and Muller cells take up intermediate

positions.[21, 27, 33]

h. Inner Plexiform Layer

The IPL is the second retinal processing layer with net- works between bipolar, amacrine, and ganglion cells. The IPL shows sublayering into six lamina. This enables the parallel representation and processing of the photoreceptor input through specific interactions between the bipolar, amacrine, and ganglion cells in each of the six lamina of the IPL.[45] The visual message leaving the retina is in the form of ganglion cell spike discharges that occurs either when a spot of light stimulated the retina (ON discharge to light) or when the spot of light was turned off (OFF discharge). The OFF-centre bipolar chains excited OFF ganglion cells, and ON-centre bipolar cell chains excited ON ganglion cells. To keep the ON and OFF channels separate through the ganglion cells to the brain, the IPL is divided into two functionally discrete sublaminae, called **a** (the two strata below the amacrine cell bodies) and **b** (the other three strata stretching to the ganglion cell bodies). The interactions are only allowed between basal-contacting cone bipolar types and one set of ganglion cells in sublamina **a**, whereas invaginating- contacting cone bipolar cells can interact only with another set of ganglion cells branching in sublamina **b**.

i. Ganglion Cell Layer

This layer contains about 1.2 million ganglion cells as well as a number of other cell types, Inner Limiting Membrane and Vitreoretinal Interface including “displaced” amacrine cells, astrocytes, enthothelial cells, and pericytes.[19, 38, 46] The thickness of the GCL is greatest in the perifoveal macula consisting of between eight and ten rows of nuclei (60–80 μm), decreases to a single row outside the macula (10–20 μm), and is absent from the foveola itself.[24, 47] The small midget and the larger parasol cells make up 80% of the GCL and behave as either ON or OFF cells depending on the location of their dendrites in the ON or OFF-regions of the IPL. The ON-OFF centre-

surround organisation of receptive fields that was first created in the OPL is thus maintained at the ganglion cell level.[20,21,45]

j. Nerve Fibre Layer

Ganglionic axons travel towards the optic nerve head within the nerve fibre layer. Thin and difficult to discern in the far periphery, the nerve fibre layer becomes thicker towards the disc as a result of the convergence of all retinal ganglion axon fibres on the optic disc. The axons are accompanied by astrocytes in the nerve fibre layer and are separated into small bundles by the cellular processes of Muller cells and the internal limiting membrane.[25,48]
The exact cross- sectional ordering of the axonal fibres of the peripheral and central ganglion cells in the retina remains controversial.[26,36]
Temporal to the disc lies the macula, which has the highest density of ganglion cells. Axons from the macula project straight to the disc, forming the papillomacular "bundle." The remaining axons of the temporal retina reach the optic disc only by arcing around the papillomacular bundle. As a result, all temporal ganglion cell axons originating from outside the macula are compressed into the superotemporal and inferotemporal sectors of the optic nerve, above and below the temporal entry of the papillomacular bundle fibres. The superior and inferior nerve fibre bundles are therefore much thicker (almost 200 mm) compared to the papillomacular bundle (65 mm) and easier to see on clinical examination, especially in red- free light. Nasally, axons enter the nasal half of the optic disc more or less straight from their retinal location. In addition, ganglion axon fibres do not cross the horizontal meridian (the horizontal raphe) in the temporal retina.

k. Inner Limiting Membrane and Vitreoretinal Interface

The innermost processes of the Muller cell enlarge and flatten on the vitreal side to form the

inner limiting membrane. Vitreous collagen fibrils insert into this membrane of the retina, so rendering the retina vulnerable to vitreoretinal traction force. [37]

Figure 1: Overview of retinal structure

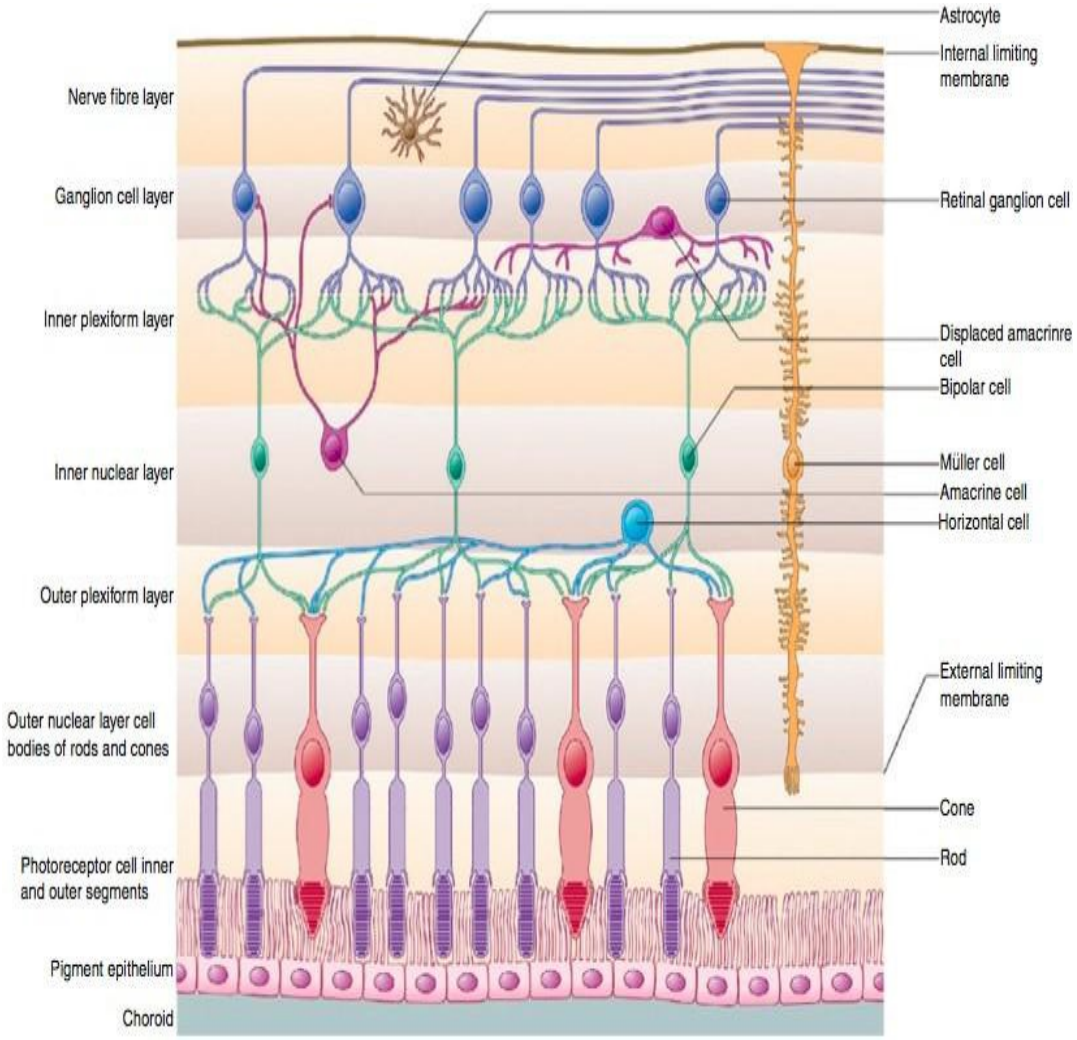

1.2 ANATOMY OF THE OPTIC NERVE HEAD AND RNFL

The retinal ganglion axon fibres travel within the nerve fibre layer to converge on the optic nerve head (also termed the optic disc) while obeying strict retinotopic organisation. The adult optic nerve head is typically elliptical in shape, having a slightly greater mean vertical (1.9 mm) than mean horizontal (1.7–1.8 mm) diameter,[19] though its size and shape can vary greatly even in healthy eyes.[19, 46, 49-51] RGC axons converge at the ONH in an organised pattern. Axons coming from the nasal, superior and inferior retina have a relatively straight course towards the ONH, while axons coming from the temporal regions of the retina describe an arcuate course around the macular region, resulting in a horizontal raphe temporal to the macula (Figure 2). Axons that originate from the fovea run, somewhat, directly to the temporal edge of the ONH and form the papillo- macular bundle.[24] Arteries and veins that originate from the central retinal vessels lie superficially in the RNFL, and are partially covered by nerve fibres.

Figure 2: Diagram of the optic nerve fibres of the right eye

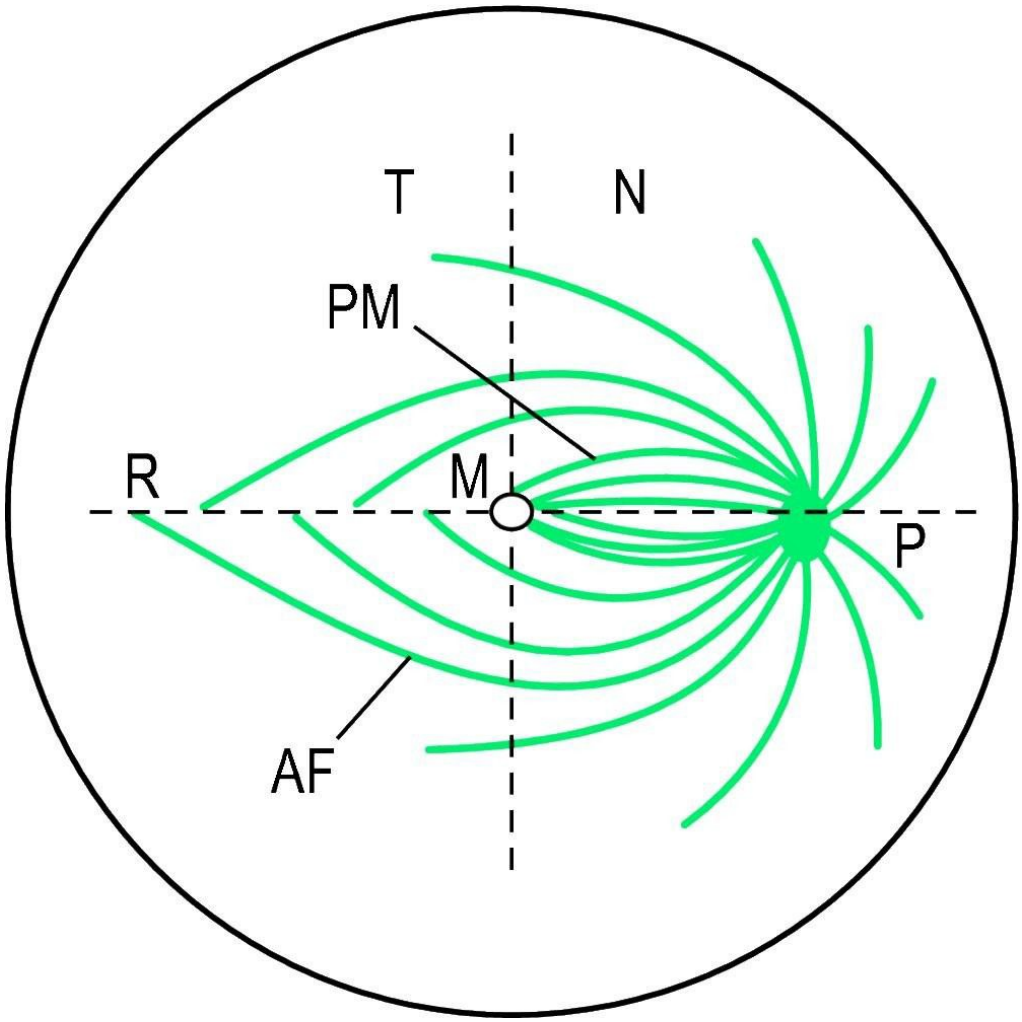

(M, macula; P, optic disc; R, retinal raphe; PM, papillomacula fibres; AF, arcuate fibres; T, temporal side; N, nasal side)

The central RGC axons are located in the inner part of the optic nerve rim whilst peripheral RGC axons are found in the outer layers of the optic disc rim. The central part of the optic nerve head that contains no retinal fibres and appears optically empty forms the optic cup. The relationship between disc and cup size (the cup- disc ratio) can vary widely in healthy eyes.[51]

All retinal ganglion axons pass through the optic nerve head, which consists of three parts: the pre-laminar portion (between the lamina cribrosa and the vitreous), the lamina cribrosa, and the postlaminar portion. Surrounded by astrocytes in the prelaminar portion, the axon bundles stream through the foramina of the lamina cribrosa, which is made of condensations of scleral collagen, to enter the postlaminar portion where oligodendrocytes and connective tissue become part of the glial structure. A number of histological structures delineate the prelaminar optic nerve head from the vitreous, the retina, and the choroid. In the oligodendrocyte-containing postlaminar portion, the axon fibres become myelinated and the optic nerve ensheathed by the meninges.

After passing through the optic nerve head, the retinal axons travel in the intraorbital (about 30 mm), the intracanalicular (5–12 mm), and the intracranial portions of the optic nerve (8–19 mm). At the optic chiasm, the nasal fibres decussate to join the temporal fibres of the contralateral optic nerve to form the optic tract, which projects to the LGN, the pretectal nuclei, the superior colliculus, the hypothalamus, and possibly other brain structures.[19]

Because all retinal ganglion cell (RGC) axons and all retinal blood vessels have to pass through the optic disc, relatively small lesions at the optic disc and in the optic nerve can have devastating clinical effects.[52, 53] Pathology affecting these ganglionic axons along their anatomic course between the retina and the brain gives rise to characteristic visual

field defects[54, 55] and patterns of neural rim loss and pallor[50, 56-59] that help to localise lesions clinically.

1.3 ANATOMY AND PHYSIOLOGY OF THE RETINAL GANGLION CELLS

Cone receptors consist of three cell types known as long, medium and short wavelength (L, M, and S) that are located in the outermost layer of the retina, and are connected to the ganglion cells by bipolar cells. A complex interconnected network is created with horizontal cells located between the cones and bipolar cells, and amacrine cells in between bipolar and ganglion cells.[60]

Bipolar cells connect, compare, and relay information from cone photoreceptors to ganglion cells. Complex networks of horizontal and amacrine cells assist in the collection and comparison of information received from cones. Cone photoreceptors that provide input to a ganglion cell through bipolar cells are called the receptive field of that ganglion cell. Two types of bipolar cells have been identified. The first polarises in the same way that cones polarise, i.e., hyper-polarisation in reaction to light; these are called "Off" cells. The other type, the "On" cells, polarises in the reverse direction. This difference arises from different glutamate receptors on the surface of these cells. In the fovea, where visual acuity is highest, most cones connect with one "Off" and one "On" bipolar cell.[71, 72] In the periphery, the number of On/Off cells increases. Overall, such a structure creates a receptive field, which for example, can detect an edge or create a centre/surround organisation.[73]

Ganglion cells are the final output neurons of the vertebrate retina. They collect information about the visual world from bipolar cells and amacrine cells (retinal interneurons). This

information is in the form of chemical messages sensed by receptors on the ganglion cell membrane. Transmembrane receptors, in turn, transform the chemical messages into intracellular electrical signals. These are integrated within ganglion-cell dendrites and cell body, and 'digitized', probably in the initial segment of the ganglion-cell axon, into nerve spikes. Nerve spikes are a time-coded digital form of electrical signalling used to transmit nervous system information over long distances, in this case through the optic nerve and into brain visual centres.

Ganglion cells are also the most complex information processing systems in the vertebrate retina. It is a general experimental truth that an organism as a whole cannot behaviourally respond to visual stimuli that are not also detectable by individual ganglion cells. Different cells become selectively tuned to detect surprisingly subtle 'features' of the visual scene, including colour, size, and direction and speed of motion. These are called 'trigger features'. Even so signals detected by ganglion cells may not have a unique interpretation. Equivalent signals might result from an object changing brightness, changing shape, or moving. It is up to the brain to determine the most likely interpretation of detected events and, in the context of events detected by other ganglion cells, take appropriate action.

Several physiologically and morphologically distinct types of ganglion cells exist. One, known as the magno cell, responds rapidly to stimulation, has thick axons with more myelin and large receptive fields (i.e., collects information from several cones). Another type known as the parvo cell, has thin axons with less myelin, responds slowly to stimuli and has smaller receptive fields. In the LGN, distinct layers of magno and parvo cells have been identified using several staining methods. Magno cells collect information from all types of cones; hence they detect "luminance" and can signal motion, stereopsis and depth. The parvo system

is used for detection of "chromatic" modulation and thus the form and material of an object. Their processing pathways also differ: magno cell information is processed through the "where" pathway to the parieto-occipital cortex, while information from parvo cells is mostly processed through the "what" pathway in the infero temporal-occipital cortex.[61] One other major type of ganglion cells is known as the konio cell. Konio cells are much less in number than the other two types and form three tiny separate layers in between the magno and parvo cells in the LGN (although up to 6 koniocellular layers have been reported – ref??). Structurally, they are smaller than parvo cells. The physiological response of konio cells is not as well studied as the other two cell types, while they may play a role in seasonal mood changes[62] and colour constancy mechanism.[63,64] Seasonal mood changes might as well be affected by the recently-found ganglion cells known as melanopsin containing retinal ganglion cells (mRGC).[65]

Data processing in the visual system starts in the eye itself, distinguishing it from any other organ in the body.[60] While the eye itself is not considered as a part of the CNS, the multilayered structure of the retina enables early processing of the retinal cone responses. The information generated by cone photoreceptors in the retina is compressed and transferred to higher processing centres through the magno, parvo and konio cells. These ganglion cells, which travel from the retina to the LGN and then to the primary visual cortex, have different structural and functional characteristics, and are organized in distinct layers in the LGN and the primary visual cortex.

Ganglion cell axons terminate in brain visual centres, principally the LGN and the superior colliculus. The axons are directed to specific visual centres depending of the visual 'trigger features' they encode. The optic nerve collects all the axons of the ganglion cells. In man this optic nerve bundle contains more than a million axons.

The optic nerve, with its 1.6 million fibres, carries information from about 4 million cones.[74] Therefore, data compression occurs at the retinal level. In the model of L, M and S cone responses in natural environments, a mathematically optimised solution for data compression matches the physiological response of the three types of ganglion cells.[75]

"Data decompression" seems to take place in the cortex, since the 1.6 million ganglion cells connect to about 120 million neurons in the visual cortex.[76] Therefore, lesions in each of the three compressed pathways cause considerable functional loss as compared to lesions in other areas of the CNS.

1.4 AXONAL LOSS IN DIFFERENT DISEASES

As mentioned above, since all RGC axons and all retinal blood vessels have to pass through the optic disc, relatively small lesions at the optic disc and in the optic nerve can have devastating clinical effects.[52, 53] Pathology affecting these ganglionic axons along their anatomic course between the retina and the brain gives rise to characteristic visual field defects[54, 55] and patterns of neural rim loss and pallor[50, 56-59] that help to localise lesions clinically. Evidence has accumulated that these three pathways show characteristic patterns of malfunction in MS,[66, 67] Glaucoma, Parkinson's,[68] Alzeimer's disease[69-70] and several other disorders. There are about 7 to 12 other types of ganglion cells including a photosensitive ganglion cell.[65] However, these cell types are much less frequent and do not create distinct layers in the LGN.

The most common conditions associated with axonal loss are firstly glaucoma, which is more

common in the older population (discussed in detail in chapter 2) and secondly optic neuritis (ON), which is more common in the younger population. An episode of ON can occur in the majority of patients having multiple sclerosis, which is an inflammatory demyelinating condition of the CNS. Hence this thesis looked at patients with MS(discussed in detail in chapter 4) and not clinically isolated cases of optic neuritis, where the cause is unknown.

1.4.1 Glaucoma

The term "Glaucoma" refers to a group of progressive optic neuropathies, which result in the slow degeneration of the RGCs and optic nerve atrophy.[77] Clinically it is characterised by a specific pattern of changes at the optic nerve head associated with corresponding visual field loss.[77] It is usually associated with elevated Intra Ocular Pressure (IOP), however it is not a necessary finding for the diagnosis. Adult glaucoma may be classified as ***primary*** or ***secondary*** depending on the presence or absence of associated ocular pathology contributing to the elevation of IOP. Adult primary glaucoma is also classified as being of the ***open-angle*** or ***angle-closure*** type, according to the manner by which aqueous outflow is impaired.

Primary open angle glaucoma (POAG) is the most common type of glaucoma, and is one of the leading causes of blindness worldwide. The disease is largely asymptomatic, the visual loss starts usually in the periphery, is insidious and slowly progressive.[56] Disc and field changes do not always occur in tandem, with structural changes often preceding field loss, although the reverse is seen in some situations. If the IOP is never documented as being elevated, the condition may be termed normal tension glaucoma (NTG).

Axonal degeneration of RGCs and apoptotic death of their cell bodies are observed in glaucoma, in which the reduction of IOP is known to slow progression of the disease. The mechanisms of degeneration of neuronal cell bodies and their axons may differ. The axons

of RGCs are approximately 50 mm in length and form synapses with cells in the LGN of the thalamus. The axons are arranged in bundles separated and ensheathed by glial cells. Upon exiting through the lamina area, the axons become myelinated with oligodendrocytes. Glaucomatous optic neuropathy (GON), the second leading cause of blindness worldwide, is therefore defined as a neurodegenerative disease characterized by structural damage to the optic nerve and the slow progressive death of RGCs.[78, 79]

NATURAL HISTORY OF GLAUCOMA

The lack of symptoms in POAG plays a large role in delaying its detection and diagnosis. Typically, POAG is slowly progressive, remaining asymptomatic until late. By the time POAG becomes symptomatic, severe and irreversible damage has usually occurred to the visual field in one or both eyes. The rate of progression of the visual field defect varies in patients, and treatment efficacy is variable. Some patients' progress despite aggressive therapy.[80]

The incidence of blindness 20 years after the initial diagnosis of POAG has been estimated at 27% for one eye and 9% for both eyes in a primarily white population.[82] Data from population-based, cross-sectional studies revealed that for patients with POAG, the mean change in visual field testing for European-derived, Hispanic, African- derived and Chinese was –1.12, –1.26, –1.33 and –1.56 dB/year, respectively. The differences in the mean deviation (MD) were not statistically significant by ethnicity. Because some participants were treated, the data cannot be used to represent the natural history of POAG.[82]

Data from individuals in the Early Manifest Glaucoma Trial (EMGT) randomised to the no-treatment group shed light on the natural course of newly detected POAG and can be used to predict the likelihood of visual loss from glaucoma. After 4 years of follow-up, 49% of the

individuals without treatment progressed, compared with 30% with treatment (an average IOP lowering of 25%).[83, 84] After 6 years of follow-up, 68% of the untreated patients showed definite visual field progression, with an overall median time to progression of 42.8 months. The study also revealed a very large variation in time to progression among the subjects. This variability in clinical course was also found by the Collaborative Normal Tension Glaucoma Study (CNTGS). Similar to the EMGT,[85] the CNTGS documented the natural course of untreated NTG.[86] The study specifically focused on patients with glaucomatous optic nerve damage and visual field loss accompanied by IOP in the normal range. While some believe that NTG represents a distinct variety of glaucoma from POAG, the two most likely represent a continuum of glaucomas. Most cases progressed slowly, requiring several years to demonstrate progression; in other cases, deterioration manifested within 1 year.

Because the course of glaucomatous progression is highly variable, identifying factors that predict progression can help guide clinical practice and patient treatment and monitoring. In the EMGT, faster and greater progression was noted in older patients (≥68 years of age) when compared with younger patients. Frequent disc haemorrhages predict faster progression, as did bilateral disease and greater visual field loss at initial diagnosis, as measured by perimetric mean deviation (MD). Pseudo-exfoliation (PXF) glaucoma, when compared with NTG and HTG, was also noted to be a more aggressive disease, with a mean progression rate corresponding to full-field blindness within 10 years. In addition, glaucoma patients with higher IOP are more likely to progress rapidly than those with IOP <21. NTG patients progressed more slowly and had a lower risk of rapid evolution to blindness. Therefore, the immediacy and aggressiveness of therapy for these patients may be less than that for patients with HTG and PXF glaucoma. That being said, high intra-group variability exists and, therefore, treatment should be guided by individual presentation.

The EMGT and the CNTG are the only two prospective studies that studied large groups of people with glaucoma without treatment. These two studies have provided important data on the natural course of POAG and on its risk factors for progression. Patients need to be monitored carefully after being diagnosed with glaucoma to determine the rapidity of glaucoma progression. Individualised treatment plans must be tailored to patients and to their rate of progression.

1.4.2 Multiple sclerosis

MS is a chronic inflammatory neurodegenerative disease of the CNS. Axonal loss is now accepted as the major cause of irreversible neurological disability in MS.[87] Acute inflammation results in axonal transection and ultimately axonal and neuronal loss. Evidence exists that the demyelination processes in MS affects magno and parvo pathways, in a specific order.[61] The visual system represents an ideal model to study axonal loss and factors associated with it due to the fact that it sub-serves a single class of functions, which are easily identifiable and measurable *in vivo*. Thus, axonal loss in the absence of acute inflammation can be assessed by measuring retinal nerve fibre layer (RNFL) thickness and amplitude of the Visual Evoked Potentials (VEP), while latency of the VEP and its progressive change are indicative of de/remyelination along visual pathway.

PATHOLOGY OF AXONAL INJURY IN MULTIPLE SCLEROSIS

When MS pathology was defined at the end of the nineteenth century, whether the primary lesion in the CNS affected myelin or axons was controversial. Marburg in 1906 pointed out that the hallmark of the MS lesions is primary demyelination with relative sparing of axons. Fromann (1878), mainly concentrating on spinal cord lesions, emphasized axonal transection and loss within lesions and tract degeneration. In contrast, Charcot (1880), focusing more on brain lesions, defined MS as a demyelinating disease, and acknowledged the presence of

axonal injury and loss.[91] Detailed morphological studies performed at the turn of the nineteenth century showed clearly that primary demyelination is the key and most characteristic pattern of tissue damage in MS lesions.

While demyelination is still considered the most characteristic histopathological feature of MS, a significant association has been recently found between permanent functional deficit and loss of axons and it is now believed that axonal injury constitutes the basis for neurological disability in MS. It has been established that axonal loss is an early event in the disease pathogenesis and is not limited to long-standing chronic MS lesions. By using Amyloid Precursor Protein (APP), Ferguson et al[92] were able to demonstrate axonal damage within acute MS lesions. This was confirmed by Trapp et al,[93] who used confocal laser microscopy to study axonal transection in early MS lesions. Kornek et al[94] later demonstrated that massive axonal injury may even occur during the first few weeks after onset of demyelination. Post- mortem studies have shown that axonal loss can be detected in the normal appearing white matter and cortical grey matter, suggesting a more diffuse pathology than previously considered.

Pathologic studies implicate acute inflammatory demyelination as a principal cause of axonal transection and subsequent axonal degeneration. There are various mechanisms of axonal damage in acute lesions. The inflammatory microenvironment contains a multitude of substances produced by activated immune and glial cells that potentially injure axons, including proteolytic enzymes, cytokines, oxidative products, and free radicals. Inflammation induces aberrant glutamate homeostasis and production of nitric oxide and can also affect energy metabolism and the viability of affected cells. Acute axonal damage may occur via mechanical compression caused by increased extracellular pressure from inflammation-

induced edema. Severe swelling in the CNS can lead to herniation or compression damage. Inflammation can also result in the disruption of normal vascular function, which could lead to ischemic-mediated axonal damage.

Axons transected during acute inflammation continue to degenerate over the following months, which results in MRI detected white matter atrophy. Acute inflammation and brain atrophy, however, do not proceed in parallel. It takes up to a year for atrophy to be fully manifested. It was also suggested that permanent demyelination in the absence of active inflammation may contribute to axonal degeneration by making axons more vulnerable to physiological stress. Significant slow-burning axonal damage was found by Kornek at el[94] even in plaques, completely devoid of active myelin destruction in cases where no active lesion was detected. However, this slow burning process was absent when a plaque remyelinated. Chronic demyelination of axons results in alterations in neurofilament spacing as a result of changes in phosphorylation status and axolemmal redistribution of ion channels. Lack of trophic support from myelin or myelin forming cells may also cause degeneration of chronically demyelinated axons. Disruption of normal axon-myelin interaction is another factor believed to contribute to induction of axonal degeneration. Functional oligodendrocyte pathology alone (in the absence of inflammation) can cause significant axonal loss and progressive neurologic disability. Therefore, while axonal loss is not caused by demyelination *per se*, the loss of myelin may have detrimental effect on axons through the variety of mechanisms and as a result has indirect effect on progress of disability.

In addition, it has been recently demonstrated that there is an apparent dissociation between lesion load and degree of white matter neurodegeneration and therefore, inflammatory demyelination alone cannot explain increasing neurological disability in MS. Thus, recently,

Bitsch et al[95] investigated relations between axonal injury, demyelination, and inflammation in MS tissue obtained by biopsy. Axonal injury, as identified by APP accumulation, and reduced axonal density were observed in active lesions, but also in inactive and remyelinated MS lesions. Because APP accumulation correlated with the number of macrophages and CD8+ T lymphocytes, but not with expression of putative mediators of demyelination such as tumor necrosis factor and inducible nitric oxide synthase, investigators suggested that axonal damage in MS lesions might not be directly proportional to demyelinating activity. Study of diffuse axonal injury in MS patients with low cerebral lesion load and no disability also suggests that axonal and/or tissue injury begins very early in the course of MS and might be at least partially independent of cerebral demyelination. A similar conclusion was reached by. Zivadinov and Zorzon[96] based on review of 10 studies investigating relationship between Gd-enhancing lesions and brain atrophy.

One of the possible explanations for the relatively poor correlation between inflammation and development of brain atrophy was offered by Lassman (New information on inflammatory changes in MS. ECTRIMS, 2008) and is based on neuropathological studies. He suggested that, while the acute inflammatory process is associated with a disturbance of the blood brain barrier (BBB), there is, in parallel, a gradual accumulation of inflammation trapped inside the CNS, behind a closed and repaired BBB (so called compartmentalized inflammation), which leads to slow expansion at the borders of pre-existing lesions. Such lesions reveal an inactive plaque core that is surrounded by a rim of profound microglia activation. At the lesion border, located within the zone of microglia activation, evidence for ongoing demyelination and axonal injury is often seen. These findings suggest that in focal white matter plaques there is a slow, but continuous progression of demyelination and axonal injury within the plaque margins, reflecting a slow expansion of the pre- existing lesions. This slow plaque

growth may represent a pathologic substrate of gradual worsening of pre-existing clinical deficits. A similar conclusion was advocated by Patani et al,[97] who found evidence of ongoing inflammation at the border of majority of the white matter lesions. A recent study by Henderson et al also demonstrated preceding loss of oligodendrocytes in tissue bordering an expanding MS lesion. While there is also a possibility of diffuse NAWM inflammation in MS, it has only been reported in progressive (SP or PP) forms of the disease.

VISUAL SYSTEM IN MULTIPLE SCLEROSIS

The visual system is highly susceptible to damage in MS.

The optic nerve is particularly vulnerable, as ON is the presenting symptom of MS in approximately 20% of patients. The Optic nerve treatment trial (ONTT) reported that the risk of development of MS after an episode of isolated unilateral ON is 38% at 10 years[98] and 50% at 15 years.[99] Another study reported that 54% of patients with ON go on to develop MS after 30 years.[100] Up to 75% of female patients and 35% of male patients initially presenting with ON ultimately develop MS.[101] The most significant contribution of imaging in the setting of demyelinating ON is in imaging the brain. This is due to the fact that the most valuable predictor for the development of subsequent MS is the presence of white matter abnormalities. In a patient with demyelinating ON, the presence of even a single, 3 mm-diameter, T2-signal lesion seen on MRI increases the probability that additional neurological manifestations sufficient for a diagnosis of MS will develop.

Optic radiation lesions are also common in MS and the occipital gray matter is also targeted by MS.[102, 103, 104] In addition, recent studies[105,106] demonstrated significant damage of outer- retina in MS patients.

The visual system comprises a chain of hierarchically organized and synaptically linked

neurons, which maintain strong topographic connectivity between retina and primary visual cortex. Owing to recent technological advances, many components of the visual system became now accessible to *in vivo* structural and functional measurements. Therefore, the visual system represents an ideal model to study axonal loss and factors associated with it due to the fact that it sub-serves a single class of functions.[107] Thus, axonal loss in an absence of acute inflammation can be assessed by measuring RNFL thickness and amplitude of the Visual Evoked Potentials (VEP), while latency of the VEP and its progressive change is indicative of de/remyelination along visual pathway (with exclusion of outer retina and extra-striate cortex).

The RGCs, in particular, have attracted researcher's attention recently. RGC represent typical neurons and therefore are analogous to the brain grey matter, while RGC axons are analogous to the brain white matter. The neuronal and axonal loss of RGC, therefore, can be used as a model to study MS-related neurodegeneration of the CNS. A major advantage of using RGC is that their cellular and axonal loss can now be measured by Spectral Domain Optical Coherence Tomography (SDOCT) with high level of precision.[108]

In addition, the effect of chronic demyelination of the optic nerve on RGC loss can be studied using latency of mfVEP,[109] while the effect of trans-neuronal degeneration or primary retinal pathology on RGC loss can be examined using structural and functional assessment of neighbouring cellular structures of the visual pathway.[105,110,111]

Numerous studies reported that acute inflammation of the optic nerve as seen in optic neuritis, (ON) results in damage and subsequent loss of significant number of RGC axons. Among the normals, mean RNFL thickness thinned by approximately 2.0 μm for every decade of increased age. After a single episode of ON the thickness of RNFL, which comprises the

intra-ocular (non- myelinated) part of the optic nerve and consists of RGC axons is reduced on average by about 20%.[108] This is followed by degeneration of RGC bodies.[112]

The clinical course of demyelinating ON initially involves an episode of demyelination followed, in the majority of cases, by near-full recovery; recurrent attacks are also compatible with good visual function.[113] However a small group of patients will have a poor visual outcome after a single attack and progressive visual loss can be seen in MS. The pathogenesis of demyelinating ON is thought to involve an inflammatory process that leads to activation of peripheral T-lymphocytes which cross the BBB and cause a delayed type hypersensitivity reaction culminating in axonal loss. Clinical recovery reflects the combined effects of demyelination with conduction block and axonal injury on the one hand, and remyelination with compensatory neuronal recruitment on the other. However, irreversible axonal damage occurs early in the disease process. A study using ocular coherence tomography (OCT) demonstrated that axonal injury is common in ON[114] and observed RNFL thinning in 74% of individuals within 3 months of acute ON.

In this and another cross-sectional study of MS patients with ON,[115] RNFL was significantly reduced in the affected eye when compared with fellow eyes or disease-free controls. These and other studies[116] have correlated RNFL thinning with impaired visual function. OCT can be employed to monitor such progressive axonal loss in both primary and secondary progressive MS.[117]

An increasing number of studies[118-130] have demonstrated significant axonal and neuronal loss of RGC in MS patients with no history of ON (MS-NON). A recently published meta-analyses showed an average RNFL thinning of 7 μm (i. e. about 7%) in MS-NON eyes.[108]

Correlation of RNFL thickness with stage of MS, brain atrophy, degree of disability and disease duration found in a number of cross-sectional studies incited considerable interest in using an assessment of the anterior visual pathway as a structural marker of CNS neurodegeneration in MS[119, 120, 124, 126, 127, 129, 131-133] and was even suggested as a possible outcome for future neuroprotection trials. [124, 126, 134] Progressive axonal loss of optic nerve fibers in MS-NON eyes has been recently demonstrated by Talman et al[121] in the longest up to date follow up study of 299 patients who were monitored for up to 4 years. The authors reported that each year of follow-up was associated, on average, with 2.0 μm decreases in RNFL thickness.

However, the pathological basis of the RNFL reduction in the MS-NON eyes at present is not clear. There is a possibility that some loss of RNFL and RGC may be caused by sub- clinical inflammation in the optic nerve or lesions of the optic tract. However, lesions of the optic tract in MS are rare,[111, 135] while true presence of sub-clinical inflammation in the optic nerve has never been proven.

This raises the possibility that other mechanisms such as primary retinal pathology or trans-neuronal degeneration may also be involved in RGC axonal loss. Of relevance a recent histological study have demonstrated significant pathological changes of retinal cells distal to RGC, including bipolar cells and photoreceptors.[106] While structural (OCT based) *in vivo* assessment of outer retina produced conflicting results,[136, 137] functional analysis based on electroretinography (ERG) demonstrated reduced function of outer retina in MS patients. RGC can also potentially be affected by changes in proximal part of the visual pathway. The neurons closest to RGC are located in LGN and their axons form the optic radiation, which is known to be a frequent site of MS lesions.[103, 138] Loss of RGC and their axons following axonal transection above the LGN, however, would require trans-neuronal degeneration.

1.5 METHODS OF ASSESSMENT OF GANGLION CELL FUCNTION[84]

Most of the available information on RGCs originates from animal models. In animals, electrophysiology has been the main method for assessing ganglion cell function. Recording electrical activity can be performed at the intracellular level, the extracellular level, or using multiple electrodes with tens or even hundreds of concurrent activity recordings. Noninvasive methods used in humans include behavioural and psychophysical techniques combined with functional imaging, such as functional magnetic resonance imaging (fMRI), positron emission tomography (PET)) scan and near infrared spectroscopy (NIRS). Noninvasive electrophysiological data from humans using electroencephalography (EEG) or EEG during presentation of stimuli, known as event- related potentials (ERP), have been valuable for evaluation of ganglion cell function.

Behavioural techniques include simple tasks, such as contrast sensitivity measurement, designed to distinctively stimulate magno, parvo, or konio cells. Stimuli containing only luminance information (i.e., with no chromatic modulation) selectively stimulate magno cells, while chromatic modulation without any luminance changes elicits a response from parvo and konio cells. Since parvo cells mainly receive input from L and M cones in an excitatory/ inhibitory combination, a combination of chromatic stimuli that selectively excite L and M cones can excite parvo cells. Such stimuli may consist of two colours close to dark red and dark green with the same luminance levels (isoluminant). Konio cells, on the other hand, seem to compare inputs from S cones with L and M cone inputs. Therefore, an isoluminant stimulus combining violet/blue with greenish yellow would selectively provoke a response from konio cells. Behavioural techniques have been used in combination with EEG recordings as well as functional imaging methods. The low temporal resolution of functional imaging methods has been a major obstacle for their use in combination with behavioural tasks.

In humans, the tests selected for evaluation of the ganglion cells and the nerve fibre layer would vary depending on the underlying cause.

1.5.1 STRUCTURAL TESTS

a. *Disc Photography*

Stereoscopic ONH photography (Figure 3) is a simple and low-cost method providing a three-dimensional full-color view of the ONH; in practice, it is the most commonly utilized technique to objectively document structural damage in glaucoma suspects.[139] Stereoscopic views of the optic nerve via ophthalmoscopy or slit-lamp biomicroscopy, documented by drawings in the patient's chart, are also an important method to detect glaucomatous neuropathy. However, due to the inherent subjectivity of a qualitative assessment, there is considerable variability in classifying the ONH as normal or glaucomatous both within and between graders.[140, 141] Even among glaucoma specialists, there can be high intra- and interobserver variability in clinically assessing the optic disk.[142] Optic disk damage based on photograph assessment has been used as an endpoint in three randomized clinical trials (level I evidence): the OHTS, the EMGT, and the European Glaucoma Prevention Study (EGPS). These studies have shown that by standardizing optic disk evaluation, photographs can be reproducibly evaluated.[143, 144] Other level II studies have also overcome some of this variability by using a variety of methods to standardize optic disk evaluation.[139, 145-148]

Recently, there have been tremendous advances in the development of computer-based technologies with the ability to provide reproducible, quantitative assessments of the ONH. An advantage of subjective assessment over quantitative analysis is a comprehensive evaluation of the ONH, including parameters that cannot be quantified, such as disk hemorrhages and pallor. In fact, given the wide range of normal variations of the ONH,

qualitative variables have been shown to have higher specificity than quantitative parameters in separating normal from glaucomatous eyes. Furthermore, subjective ONH evaluation provides the clinician with the opportunity to assess the impact of other nonglaucomatous processes that may impact functional testing.

Manual, subjective examination of the ONH via ophthalmoscopy, slit-lamp biomicroscopy or stereoscopic optic nerve head photography remain mainstays in the evaluation of a glaucoma patient, with objective documentation of optic disk damage preferred whenever possible.[149]

Figure 3: Stereo photos of the optic disc (normal)

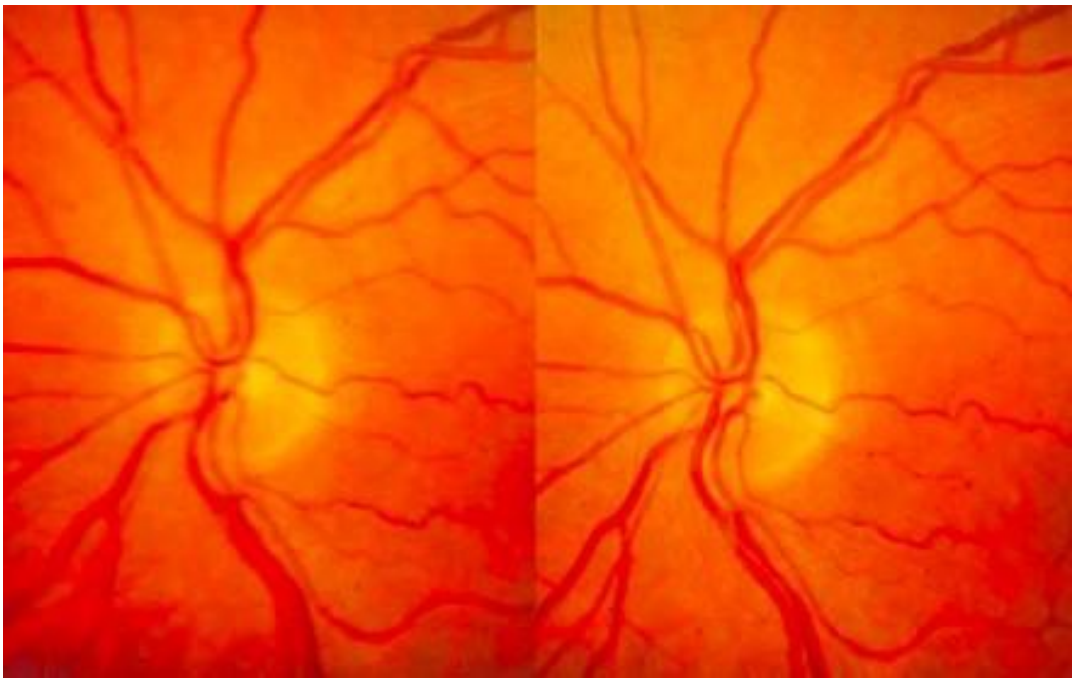

b. ***Scanning Laser Ophthalmoscopy (SLO)***

Confocal Scanning laser Ophthalmoscopy (CSLO)[150] is a real-time imaging technique that produces multiple coronal optical cross-sections of the retina and optic nerve head (ONH), which are then combined to give a three-dimensional image of the optic nerve head (ONH). It is based on the principle of spot illumination and spot detection. The system uses a pair of conjugated pinholes located in front of the light source and the light detector components. This pair ensures that only light reflected from a defined focal plane will reach the light detector. The device moves the focal plane to acquire sequential images. Reconstructing the series of scans at the various focal planes creates a three- dimensional topographic representation of the surface that is scanned.

The Heidelberg Retina Tomograph (HRT; Heidelberg Engineering, Heidelberg, Germany) is a widely used CSLO device. The HRT uses a diode laser beam (wavelength, 670 nm) and captures a series of 32 sequential two-dimensional scans in a total acquisition time of 1.6 seconds. The optical transverse resolution of the HRT is 10 μm and the axial resolution 62.5 μm.

The operator is required to trace the ONH margin. Based on this contour line, the HRT operation software automatically defines the reference plane. This plane is located 50 μm posterior to the mean surface height along a 6-degree arc at the inferotemporal region of the contour line. The reference plane is then used as a topographic cut-off. Structures below the plane are defined as optic cup and structures above the plane as neuroretinal rim. Among several stereometric parameters generated are disc area, cup area, rim area, cupdisc area ratio, cup volume, rim volume and cup depth. Measurements with the HRT have been found to be highly reproducible in numerous studies.[151, 152] Three versions of the HRT have been available-of these, HRT III is the most recent and HRT II is the previous version. Most

planimetric data using the HRT available today has been obtained with the HRT II. One method of HRT-II software analysis, Moorefield's Regression Analysis (MRA), uses a program that compares the subject's optic nerve and RNFL parameters to a normative database of 112 subjects, all of whom were white and had ametropia of less than 6 diopters.[153] (Figure 4) The HRT III was designed to incorporate a new, expanded, race- specific database to account for this problem. This new normative database consists of 733 eyes of caucasians and 215 eyes of African-Americans.[154]

This database was found to increase sensitivity with comparable specificity among caucasian patients, but increased sensitivity at the expense of specificity among Afican- American patients. The operator-marked contour line is an important source of variability in HRT measurements. Hatch et al[155] assessed the interobserver agreement of HRT parameters reflecting the variation in contour line placement. The interobserver agreement was substantially better for parameters not dependent on the contour line than for those that are dependent on the contour line.

In many cases, the HRT analyses incorporate blood vessels into the neuroretinal rim. This inclusion has been suggested as the reason for the higher HRT rim measurements when compared with the findings of optic disk photograph planimetric evaluation.[156, 157] The ease of use and widespread availability of the HRT have made it a useful tool to obtain normative optic disc measurements on large numbers of people[158, 159] However, the HRT does not directly make linear measurements i.e., linear disc diameters, cup diameters or cup-disc ratios, which are the most commonly assessed clinical parameters. This is one of the drawbacks of using the HRT to obtain normative planimetric measurements.

Though the HRT is the most popular CSLO, there are other CSLOs based on the same

principle – the Rodenstock CSLO and TopconSS CSLO. The latter has been used mainly in Japan and Korea. Advantages of HRT include good image quality through undilated pupils (though dilation may be necessary at times), and the ability to upgrade existing machines with newer software, allowing the clinician to build upon long-term databases. Most importantly, the sophisticated registration capability of HRT to superimpose baseline and follow-up images allows for automated detection of change to the ONH. The use of HRT in the ancillary study to OHTS has resulted in a well-characterized data set, beneficial for future investigations of this technique.

Figure 4: Example of a HRT report showing Moorefield Regression Analysis

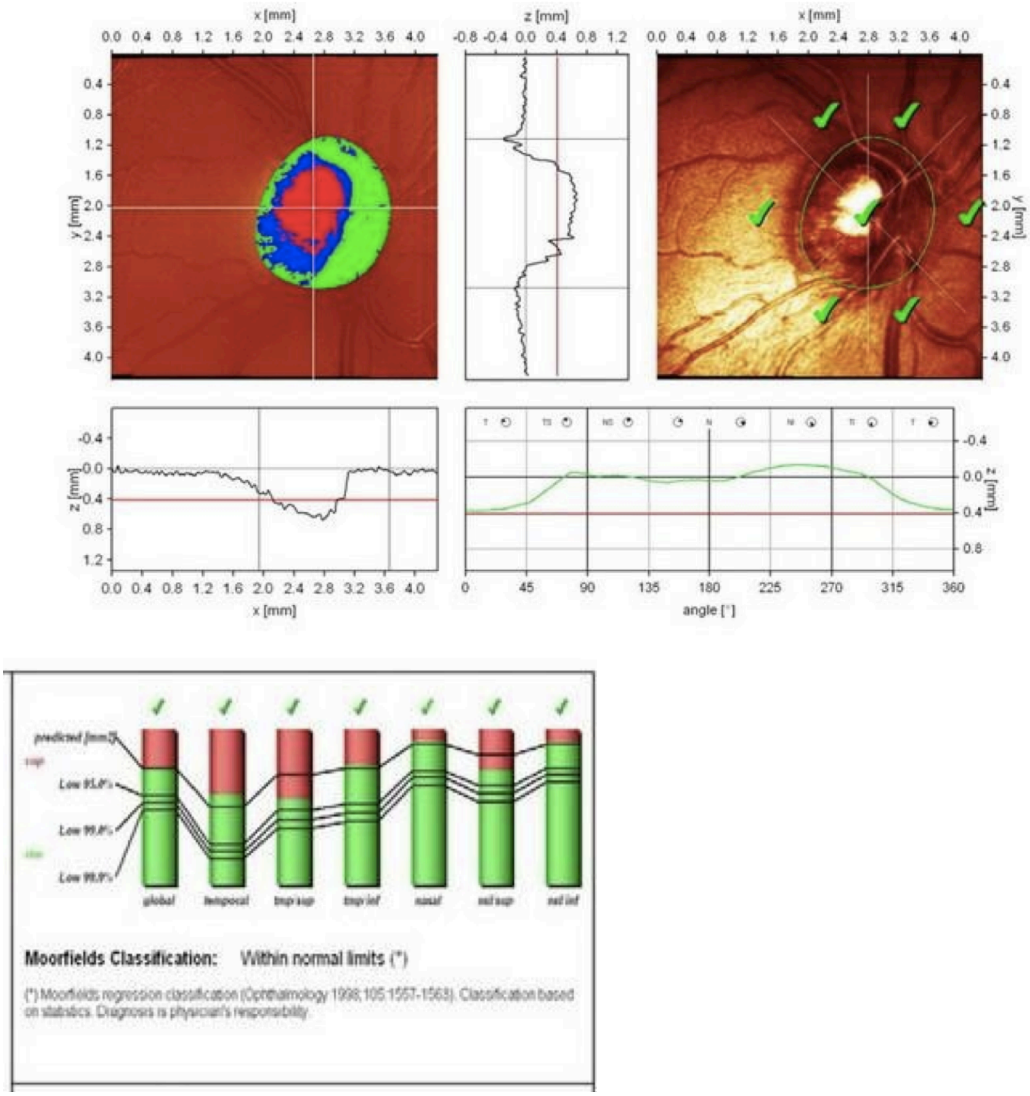

c. Optical Coherence Tomography (OCT)

The OCT permits high-resolution cross-sectional imaging of the human retina using light. It is based on the principle of Michelson interferometry. OCT is a noninvasive, non- contact technique that uses a light source consisting of a near-infrared, low coherence superluminescent diode laser (wavelength 850 nm) split at a 50/50 beam splitter into two arms. One arm sends light to the actual sample (the eye), and the other sends light to a reference mirror. The distance between the beam-splitter and reference mirror is continuously varied. When the distance between the light source and retinal tissue is equal to the distance between the light source and reference mirror, the reflected light from the retinal tissue and reference mirror interacts to produce an interference pattern. The interference pattern is detected and then processed into a signal. The signal is analogous to that obtained by A-scan ultrasonography using light as a source rather than sound. A two-dimensional image is built (analogous to a series of stacked A-scans) as the light source is moved across the retina. A transverse sequence of longitudinal measurements is used to construct a false colour topographic image of tissue microsections that appears remarkably similar to histological sections. The OCT image can be displayed on a gray scale where more highly reflected light is brighter than less highly reflected light. Alternatively, it can be displayed in colour whereby different colours correspond to different degrees of reflectivity. On the OCT scanners currently commercially available, highly reflective structures are shown with bright colours (red and white), while those with low reflectivity are represented by darker colours (black and blue). Those with intermediate reflectivity appear green. Digital processing aligns the A-scans to correct for eye motion. Digital smoothing techniques are used to further improve the signal-to-noise ratio. The newer generation of OCT-spectral domain OCTs[160] utilize the spectral properties of light to obtain very high resolution scans in rapid acquisition times. Their axial resolutions are claimed to be about 4 microns. However, it is still early days with

these machines and further data may become available over time.

The ONH scan of the OCT3 which makes planimetric measurements is composed of six radial scans across the optic disc and centred at the optic disc centre. With the six cross-sectional line scans, the ONH analysis measures the amount of nerve fibre at the optic nerve head. The termination of the RPE on either side of the ONH is identified as the disc margins. The distinction between the optic cup and neural rim is made at a line parallel to the line joining the 2 ends of the RPE across the optic disc, with an anterior offset of 150 microns. The cup offset is 150 μm by default and is adjustable. The placement of the disc reference points is also adjustable. Contour diagrams of the optic disc and optic cup are displayed as created from the data obtained from all six radial scans. The individual radial scan analysis gives rim area in vertical cross-section, average nerve width at the disc, disc diameter, cup diameter, horizontal rim length, and cup offset. The optic nerve head analysis results give vertically integrated rim area volume, horizontally integrated rim width, disc area, cup area, rim area, cup/disc area ratio, cup/disc horizontal ratio, and cup/disc vertical ratio.

Very high axial resolution and automatic definition of both disc and cup margins are inherent strengths of this method - however, limited transverse sampling may be a source of error. It is likely that the unscanned areas between the linear spokes and the unsampled points along each spoke also contribute to variation in OCT measurements. Also, errors in automatic detection of the disc margin in 53% of cases was reported in one study.[161] The commonly used time domain OCT (Stratus OCT; Carl Zeiss Meditec, Inc., Dublin CA) till a few years ago had ~10-micron axial image resolution.

Limitations of OCT include the need to dilate some patients who undergo OCT, as well as the

lack of an ethnicity-specific normative database and progression analysis software, although the latter are currently in production. In addition, the Stratus OCT does not have the ability to automatically register follow-up to baseline scans to ensure that the measurements are obtained at the same location for analysis of change. As for all optical imaging technologies, image quality may be compromised in patients with ocular opacities.

Newer developments in OCT technology have enabled increases in scanning speed to 20,000–50,000 A-scans/second in commercial devices, allowing the creation of three- dimensional datasets. This technology, known variously as Fourier-domain OCT, spectral OCT, frequency-domain OCT, and high-speed, high-resolution OCT, has recently become commercially available. Three-dimensional imaging promises to permit registration from scan session to session, and to allow arbitrary analysis of three-dimensional datasets. Further, recent development of an ultrahigh-resolution (UHR) OCT in commercially available high speed OCT devices enables intraretinal imaging comparable to conventional histopathology, including visualization of the GCL, photoreceptor layers, and RPE. UHR OCT uses a femtosecond laser light source to obtain axial resolutions of ~ 3 mm in the human eye.[162, 163]

Studies comparing UHR OCT with standard OCT imaging found that ultrahigh- resolution enables improved visualization of intraretinal morphology and may enhance the clinical utility of standard OCT imaging for glaucoma.[164]

The Spectralis OCT (Spectralis HRA + OCT, Heidelberg Engineering, Heidelberg, Germany; Software version 5.3.3.0) is one such newly developed spectral domain OCT. It uses a superluminescent light emitting diode for the spectral-domain OCT and a CSLO to provide images of the microstructure of the retina. The light-emitting diode has a wavelength of 870 nm and an infrared scan simultaneously to assess the RNFL thickness. For this purpose, the

instrument uses 1,024 A-scan points from a 3.45 mm circle centered on the optic nerve head. The acquisition rate is 40,000 A-scans per second at a digital axial resolution of 3.9 μm. The advantage of this OCT is that it uses an eyetracking system, which adjusts the scanner in case of eye movement, and provides a clear motion free image. This also ensures that the same region of the RNFL is scanned. (Figure 5)

Figure 5: Example Spectralis report of a normal subject

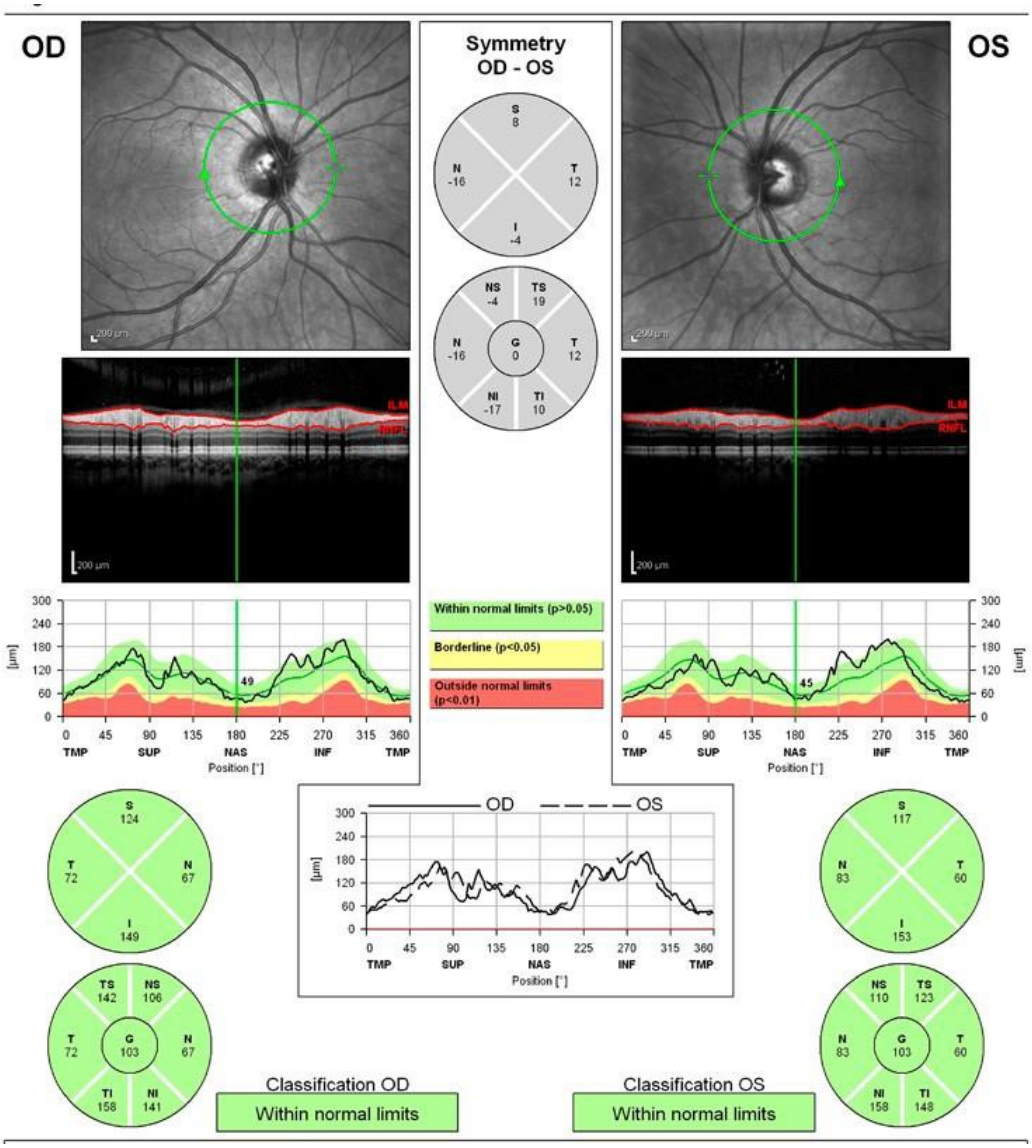

d. Scanning Laser Polarimetry (SLP)

SLP is a non-invasive method to objectively measure the RNFL; RNFL thickness corresponds to a decrease in the GCL from the fovea to the optic disk. SLP has gained popularity as a potential diagnostic tool for glaucoma particularly in response to studies indicating that RNFL damage may precede optic nerve damage in early glaucoma.[165] The instrument consists of CSLO with a polarized laser beam; when the polarized light passes through the birefringent RNFL, a measurable phase shift is created, which can be correlated to the RNFL thickness.[166]

SLP was first commercially available as the GDx Nerve Fiber Analyzer (Laser Diagnostic Technologies, Inc., San Diego, California). This instrument contained a fixed anterior segment compensating device to compensate for the polarization effects of other ocular birefringent structures, such as the cornea and lens. In light of evidence that the parameters for corneal compensation are different for different subjects,[167] a new device with variable corneal compensation (GDx-VCC) (Zeiss Meditec, Dublin, CA) has been developed to allow for individualized eye-specific compensation of anterior segment birefringence. Several studies have shown that the addition of VCC to GDx substantially enhances its discriminating power for glaucoma detection[168, 169] and correlation with visual field loss.[170, 171]

GDx VCC has been shown to have good diagnostics accuracy, with reported area-under- the-curve values (AUCs) for glaucoma detection ranging from 0.90 to 0.978.[172-174] Recent data suggests that GDx-VCC may be useful for earlier glaucoma diagnosis. In a cross- sectional analysis by Medeiros et al, the GDx-VCC was able to detect structural abnormalities in preperimetric eyes with progressive optic disk changes as compared to controls.[148]

Limitations of older SLP devices include fixed corneal compensation; newer models such as the GDx-VCC and GDx-ECC individualize anterior segment birefringence compensation.

Anterior and posterior segment pathology does affect the accuracy of SLP measurements. Unreliable values for RNFL thickness have been reported in patients with media opacities, ocular surface diseases, peripapillary atrophy, and in those who have had keratorefractive surgery.[175] The presence of vitreous opacities, optic nerve crescents, and other nonglaucomatous retinal distortions may induce erroneous RNFL measurements.[175]

Additionally, some GDx-VCC scans are characterized by problematic atypical birefringence patterns (ABPs); ABPs result from artifact introduced by the device's attempt to compensate for poor noise-to-signal ratio.[176] An updated technique, enhanced corneal compensation (ECC), was developed to reduce this artifact. Recent studies found that GDx-ECC significantly reduces the frequency and severity of ABPs and improves the correlation between RNFL measures and visual function as compared to GDx- VCC.[166, 177, 178] As with many rapidly advancing technologies, the need to upgrade hardware with each advancement to the GDx has made it challenging for clinicians to follow patients over time with SLP. Although progression software is now available, images must be acquired with the current generation of instruments to be included in the analysis. Additional research is still needed on the new GDx-ECC to evaluate its utility as a diagnostic test for glaucoma, and to evaluate progression analysis in large longitudinal cohorts.

1.5.2 FUNTIONAL TESTS

a. Standard Automated Perimetry (SAP)

As the damage that results from glaucoma is largely irreversible, it is imperative to accurately identify pathological changes early, as they are at risk of continuous injury. Early detection and consequent treatment will delay the progression of glaucomatous neuropathy and

permanent functional impairment.

The temporal relationship between the structural changes of the disease at the optic nerve head and the functional development of the visual field defect varies with the disease severity. As glaucoma progresses, the exact nature of this relationship becomes more complex. At the end stage of the disease, functional measures of assessment may prove to be more sensitive, as the optic disc approached total cupping.[179]

Johnston et al[180] in a cross sectional review of structure and functional changes that occur in glaucoma, suggest that there is a strong correlation between subjective assessment of the optic disc photography and standard automated perimetry. Overall, these cross sectional studies assessed the neuro retinal rim, vasculature, peripapillary changes and the RNFL defects with the presence, site and severity of the visual field defects. The correlation between morphological change and visual dysfunction was demonstrated with both the global visual field indices and more regionally, comparing rim changes to the scotoma site.[180]

SAP evaluates differential light sensitivity using a small (0.47 degree) white flash (200 msec) on a dim (31.5 asb) white background. Because all the primary RGC types responsible for vision respond to this stimulus, SAP is a nonselective test. Due to the inherent redundancy of the visual system, SAP may not provide adequate sensitivity to detect early glaucomatous changes.[181] In some patients, a significant amount of ganglion cell loss has occurred (25–50%) before SAP can detect functional deficits.[182] Another concern with SAP, and all visual function tests described here, is its high test–retest variability, particularly in regions of visual field deficits, making it difficult to assess whether the visual field is worsening on serial examination.[183, 184] For example in the OHTS, the majority of initial visual field abnormalities detected by SAP were not confirmed on repeat visual field testing[185] and the study endpoint

was reset in year 2 to require three consecutive abnormal results rather than the initially proposed two. Similarly, the EMGT study required progression on three consecutive fields to reach endpoint.[186]

Gordon et al[187] presented the risk factor analysis for the Ocular hypertension treatment Study (OHTS). This is a critical study that has had a sweeping impact on the clinical management of OHT. It was found that nearly 50% of the patients converted to glaucoma based on the optic disc criteria alone[187] therefore necessitating the need for baseline optic disc photographs. However half the patients also progressed based on visual fields.[187] The mean cup area was higher in the converted group,[187] suggesting that perhaps these patients had early changes in disc morphology at baseline.

In another study Johnston et al,[188] in the Structure and Function Evaluation Study (SAFE), evaluated the prognostic significance of structural changes in the optic nerve on the development of visual field defects. This longitudinal study assessed 295 patients over 6 years. Progression was defined using 6 progression criteria of conventional perimetry. The incidence of field progression was significantly higher in subjects defined as having glaucomatous optic discs at baseline, indicating that structural changes were likely to be present before visual field changes.[188] In contrast to the above studies, the EMGT randomly allocated subjects with early glaucomatous changes into a treatment group and a control group and demonstrated that the vast majority of subjects (51% of controls and 41% treatment group) progressed based on visual fields using glaucoma change probability, compared with only 1% treated group and no controls progressing on the optic disc photographs.[187] Therefore, it could be suggested that field progression may occur more readily than structural change and that perimetry is still an important clinical technique for assessing progression.

Many factors influence the variability of visual field results, such as patient performance and

reliability, fixation losses, fatigue, learning effects, changes in pupil size, improper refractive correction, and true physiological variability. In a multifactor model of variability in SAP or SWAP fields, Blumenthal and colleagues found the three most important contributors were defect severity, location of defect, and patient's diagnosis.[188] However, all factors together accounted for only one-third of the variability found. Some improvements in both test time and the variability of SAP have been made by applying the Swedish interactive thresholding algorithm (SITA), a strategy that significantly decreases testing time (to 4–5 min) without compromising accuracy for detecting visual field defects as compared to much longer full-threshold testing.[189] SITA STANDARD has become the standard for clinical use with the Humphrey Visual Field Analyzer (HFA; Carl Zeiss Meditec, Inc.). Additionally, it is the only visual field test that offers an analysis for identifying progression of existing defect, the guided progression analysis (GPA) on the HFA, which is based on the progression analysis developed for the EMGT.[186] (Figure 6)

Figure 6: Example HFA report of a patient with early glaucoma

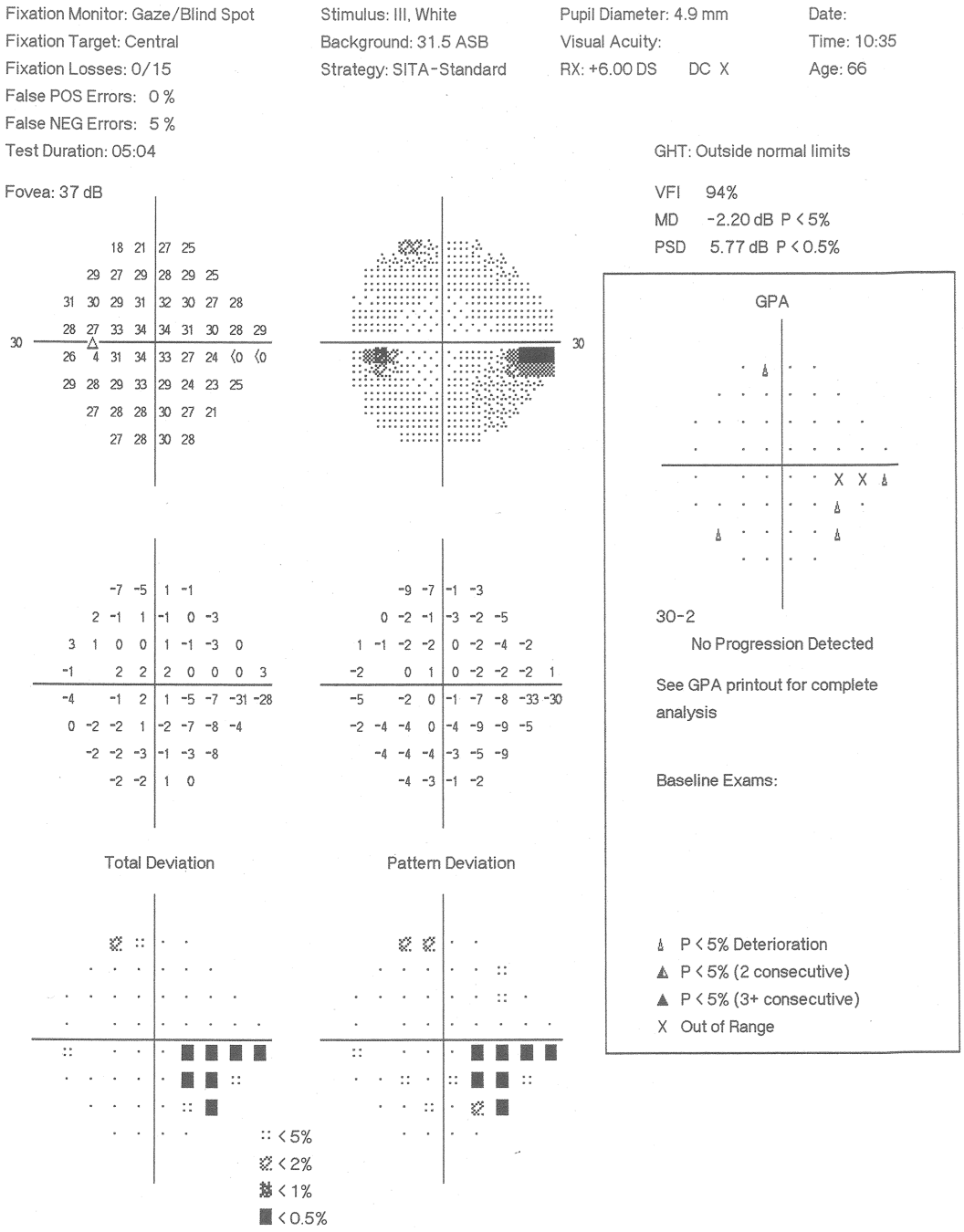

b. Short Wavelength Automated Perimetry (SWAP)

Short wave automated perimetry (SWAP, Humphrey Field Analyser, Humphrey system, Dublin, CA) differs from SAP as the stimulus consists of a blue light stimulus (peak wavelength 440 nm, Goldmann size V) that approximates the peak response of the blue cones. This is projected onto a high luminance yellow background (570-590 nm, 100 cd/m^2) that the patient has been adapted to for 3 minutes. It is designed to test the short wavelength sensitive pathway, by selectively stimulating a sub-population of the blue cones via the bistratified RGCs to target the koniocellular sub layers of the LGN.[190] The background simultaneously adapts the medium red (M) and long green (L) wavelength cones as well as saturates rod activity.[191] The instigation for the development of SWAP as a visual field test was based on reports that glaucoma was associated with colour vision deficiencies demonstrated in patients affected by glaucoma more than 25 years ago[192-194] and it is the clinical application of the technique developed by Stiles to assess the blue- yellow chromatic channel.[195, 196]

As mentioned above, the utility of SWAP is currently based on the reduced redundancy hypothesis. The concept that early functional damage can be most readily identified by testing a subset of ganglion cells that exhibit sparse neural representation,[197] with lower degrees of overlap between adjacent receptive fields, as this may demonstrate detectable functional deficits earlier in the disease process.

Early histological studies in primates and humans suggested that large diameter optic nerve fibres are selectively lost in glaucoma.[198, 199] The rationale for use of SWAP in glaucoma was therefore based upon the fact that one ganglion cell type that mediates the koniocellular pathway exhibit large cell diameters than the midget cells projecting to the parvocellular layers of theLGN.[190] The selective loss hypothesis of Quigley and colleagues[198] has subsequently been questioned in early glaucoma.[197] Consequently, it has been suggested that any given ganglion cell type which exhibits less functional redundancy, such as the small

bistratified ganglion cell involved in SWAP processing, may exhibit damage more readily even if there are greater losses for other ganglion cell types.[197] The degree of isolation of the koniocellular pathway is ideal for glaucomatous patients exhibiting mild loss. In more extensively damaged areas the defect can still theoretically be monitored using the stimulus although the response is mediated through the achromatic luminance channel, the same channel that responds in white on white SAP.

In recent years, there has been considerable interest in SWAP as a potential means for identifying visual field loss prior to conventional white on white perimetry and also for detecting progressive field loss in advance of white on white perimetry.[200-209] Since SWAP has the potential ability to detect early glaucomatous damage there has been research into the prevalence of defects on SWAP in ocular hypertensive patients. Ocular hypertensive patients at higher risk of developing glaucoma end to show greater prevalence of SWAP defects than those at risk.[200, 205] Sample et al investigated high risk, medium risk and low risk glaucoma suspects, based on the cup disk ratio and IOP, all with normal SAP. The high risk group had more damage in SWAP than in the medium and low risk groups.[205] Although the prevalence of detecting a field defect on SWAP is higher than SAP in OHT, the incidence rates is the same between the two tests.[210] This suggests that both tests are identifying the same damage but that one is detecting it earlier.

In those with established glaucomatous SAP visual field loss, the area of visual field loss is larger on SWAP.[200, 205, 209] Johnson et al, found that over 5 years, SWAP defects were found to be 80% larger and twice as large as those classified into the stable group and 3-4 times as large in the progressive group.[209] Therefore, large defects on SWAP may be predictive of glaucoma progression on SAP.

SWAP defects correlate well with the structural changes of the ONH in those with glaucoma.[211, 212] There is increased prevalence of SWAP defects in those with optic nerve damage compared to those without.[211] Correlations between SWAP and RNFL imaging or optic disc imaging are stronger than those found with SAP.[213, 214] and it can predict a higher proportion of patients with progressive optic disc damage based on serial photographs.[215] However, increasing evidence from comparative studies suggests that functional abnormality detected by SWAP is actually preceded by structural abnormalities of the optic nerve head and or RNFL,[203, 216-218] this suggests that ONH imaging may be of greater clinical value in the detection of early disease.

Longitudinal studies have been performed by two independent laboratories showing that SWAP defects may occur up to 3-5 years before there are abnormalities seen on SAP.[203, 205, 209, 215, 219] The first studies indicating the clinical ability of SWAP to predict progression in glaucoma, were by Johnson et al. In 1993 they investigated OHT patients over 5 years detected with normal SAP.[207] OHT patients had abnormal SWAP results at the outset with normal SAP. Of these patients 5 subsequently developed corresponding SAP abnormalities indicating an ability to detect early change.[203] A second study validated SWAP as a tool to identify early glaucoma progression, 32 glaucomatous eyes
underwent SWAP and SAP annually over a 5 year period and were classified as either stable or progressing. These results were confirmed by a series of cross-sectional studies.[212-215] Girkin et al, conducted a prospective study of glaucoma patients over 4 years; the patients were also defined as stable or progressing. 22 of the 47 patients had progressed and SWAP obtained a better area under the curve in comparison to SAP and therefore SWAP may improve the early detection of glaucoma.[215]

Since then SWAP has been reported to provide a clinical advantage, some studies indicate that progression of glaucomatous field loss can be detected 1-3 years prior to SAP,[200, 209] at a greater rate (approximately twofold) of progressive field loss.[201] In eyes with established defects the rate or progression is faster than with SAP.[209] The defects are predictive of both the onset and location of subsequent field loss with white on white perimetry.[203, 205, 206, 209] However a recent report showed no advantage of SWAP over SITA SAP.

Satisfactory test quality can be influenced by media opacity such as the aging lens or corneal scarring. The lens becomes more yellow with time as cataract develops and the absorption of short wave sensitive light increases. This acts as a blue filter that generally diffusely depresses the height of the hill of vision derived by SWAP.[191] It is best to interpret the results in light of this and assess the pattern standard deviation and pattern deviation plots.[201, 220, 221] It has been stated that it accounts for 63% of the variability of SWAP.[201] Sample et al solved this problem by applying statistical analysis to factor out the lens effects that were found to be consistent across the field.[222]

The short-term variation (variation in threshold values for the same point on the field) for SWAP has been shown to be 25-30% higher than for SAP. Long term variability (test-retest variation) full threshold variability for normals and glaucomas is higher than SAP,[223, 224] which makes it difficult to interpret true progression of pathology as a greater change is needed over time before it can be reliably judged as progression. There is also a higher range of sensitivities within the tested areas (the hill of vision has a steeper shape than SAP and FDT),[225] which enlarges the confidence intervals for those indices that do not take into account the hill of vision and reduces the diagnostic ability of the test.

The longer test duration (usually 12-15 minutes) including prior adaptation to the yellow stimulus[207] is an important limitation. Both the increased test time and variability has largely been overcome by with the introduction of SITA-SWAP. This reduces the test time to about 3-6 minutes, correlates well with the full threshold SWAP results, has lower inter-subject variability rates, however it has significantly higher normal thresholds of sensitivity.[220, 221]

It is still subjectively more difficult to see the Blue on Yellow (BonY) stimulus than white on white SAP, which potentially increases fatigue. There is also a learning effect,[208] which must be taken into consideration when analysing results and occurs even with those expert at SAP. (Figure 7) In advanced cases, the test is limited by the perimeters dynamic range, there is a lower level of perceived luminance of the target, therefore it is limited in monitoring advanced cases of glaucoma and these should be followed by SAP.

Figure 7: Example SWAP report of a patient with early glaucoma

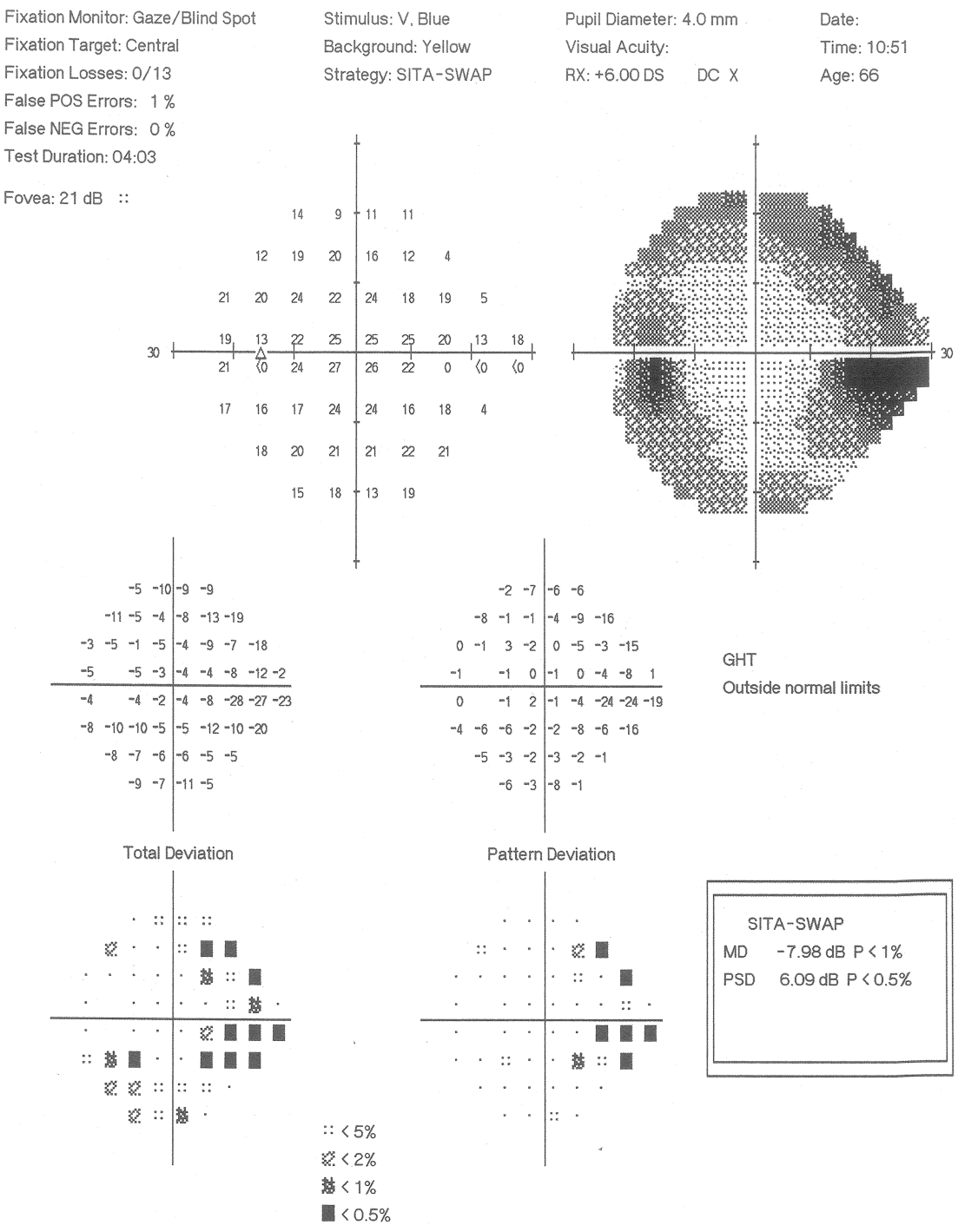

c. Frequency Doubling Technique Perimetry

FDT determines the contrast sensitivity for detecting the frequency-doubling stimulus. The frequency doubling effect occurs when a vertical sine wave pattern of low spatial frequency (0.25-0.50 cyc/degree) undergoes high temporal frequency counterphase flickering (12-25 Hz) and results in the appearance of twice as many as light and dark bars as there are physically present.[226]

Researchers have attributed this illusion predominantly to a subset of the magnocellular system,[227, 228] which is primarily involved in motion and flicker detection. It has been suggested that it is mediated by the non linear response properties of the parasol ganglion cells (My) which project to the magnocellular layers of the LGN.[229] These cells compromise only 3-5% of all RGCs, a deficit would be manifest if only a small portion of these cells are affected, due to the reduced redundancy in the coverage of a given location.[230, 231] The FDT was designed to emphasis the response characteristics of the parasol ganglion cells and the magnocellular pathway.[232]

The FDT perimeter (Humphrey Zeiss Systems, CA with frequency doubling technology from Welch Allyn, Skaneates Falls, NY) uses both suprathreshold and threshold strategies. The contrast sensitivity for the frequency-doubled stimulus is modified in each location to calculate threshold sensitivity. Targets are presented at 19 test areas located within the central 24 degrees eccentricity. Threshold strategies take 4-5 minutes, where as suprathreshold takes less than 1 minute per eye and are used mainly for glaucoma screening.

Maddess and Henry initially suggested that this technique could be useful to distinguish between those with glaucoma and those that were normal, by measuring the contrast

sensitivity obtained for the frequency doubled stimuli.[227] The instrument utilized 10 degree targets to test contrast sensitivity using spatial frequency undergoing counterphase flicker at high temporal frequency.[230, 232, 233]

Maddess and Henry investigated ocular hypertensive patients and normal subjects and tested them on the FDT and SAP. The OHT patients only detected stimuli when abnormally high luminance levels of the FDT were applied. This suggested that the measurement of the contrast sensitivity of a frequency doubled grating stimulus may represent a good indicator of neural damage from raised IOP.[175]

Johnson and Samuels reduced the stimulus size of the FDT (5 degrees for the 24-2 and 30-2 programs and 2 degrees for the 10-2 program) and introduced a larger number of testing locations, more efficient methods to calculate threshold and a slightly longer duration (6 minutes). This was claimed toimprove the sensitivity and specificity for the detection of early field loss and to reduce the test-retest variability.[232] This is commercially available as the FDT matrix (Carl Zeiss Meditec, Dublin, CA).

The FDT has been described as a useful tool for the detection of glaucoma for both full threshold [232, 234] and screening procedures.[228, 235, 236] and has been assessed for test-retest variability.[237, 238] In general, it shows good sensitivity and specificity in the detection of field loss in those with established glaucomatous change.[228, 230, 233-237,239] Johnson and Samuels demonstrate a sensitivity of 93% and a specificity of 100% in those with early to moderate glaucoma using the full threshold FDT.[232] Sample et al state that the FDT parameters have higher diagnostic accuracy when compared to other functional tests such as SAP and SWAP.[228] Trible, investigated those with early, moderate and severe glaucoma and found a sensitivity of 35, 88 and 100 % and a specificity of 91%.[240] Delgado et al reviewed a number of studies and detected a sensitivity of 85% and specificity of 90% for

early glaucoma, and a higher sensitivity and specificity of 97% for moderate and advanced glaucoma.[241]

The diagnosis of early glaucomatous defects has been more controversial, with studies resulting in different sensitivities. Some authors have found similar results between SAP and FDT, using a morphological "gold standard"[242, 243] where as others resulted in a sensitivity of 20-54% in those with pre-perimetric glaucoma and normal SAP.[231, 243, 244]

FDT Matrix provides a new testing pattern with smaller targets, spatial frequency of 0.5 cycles/degree and 18 Hz and up to 54 or 69 locations. Average testing time is 5-6 minutes. Medeiros et al compared the abilities of the FDT Matrix and SITA-SAP to diagnose glaucoma, taking into account disease severity. They found that the FDT Matrix performed considerably better than SITA SAP for the detection of early glaucoma. In those with more severe disease there was no significant difference.[244] Other studies, such as Sakata et al found that the FDT Matrix detected more abnormal field defects in glaucoma than SITA SAP, although the difference was (not???)statistically significant.[245] Burgansky-Eliash did not find any difference in the tests, glaucoma patients were defined according to optic disc photographs or OCT.[243] The FDT Matrix is seen as a promising technique to provide early diagnosis of glaucomatous visual field loss; further longitudinal studies are needed for assessment of its utility in detecting progression.

FDT has been known to detect functional loss before SAP. Medeiros et al followed 105 glaucoma suspects for 3.5 years. All patients had normal fields at onset as assessed by SAP, with suspicious optic disc appearances and raised IOP. At baseline, 24% had abnormal FDT results, 16% developed SAP abnormalities throughout the duration of the study.[246] Therefore an abnormal FDT result at baseline predicted the onset and location of future SAP

abnormalities. Another 3.5 year longitudinal comparison between FDT and SAP detected progression in the same number of patients, 49% although only 25% were in the same patients,[247] suggesting that the 2 methods identified patients with differing patterns of disease.

There is evidence that FDT may detect field loss earlier than SAP. Bayer and Erb found that FDT identified progression of existing SAP in 74% of eyes and was able to detect progression 12-24 months prior to SAP.[248] Haymes et al followed 65 glaucoma patients every 6 months; they found that FDT detected 31-49% progressions, SAP detected 35- 49% of progression. Only 15-25% was detected by FDT and SAP at the same time.[247] They used different criteria to detect progression, including several scores using glaucoma change probability analysis and linear regression analysis. The FDT was able to detect progression in more patients than SAP for most of the criteria used. When patients progressed in both FDT and SAP the abnormalities were seen prior to SAP in most cases. (Figure 8)

Figure 8: Example FDT Matrix report of a patient with early glaucoma

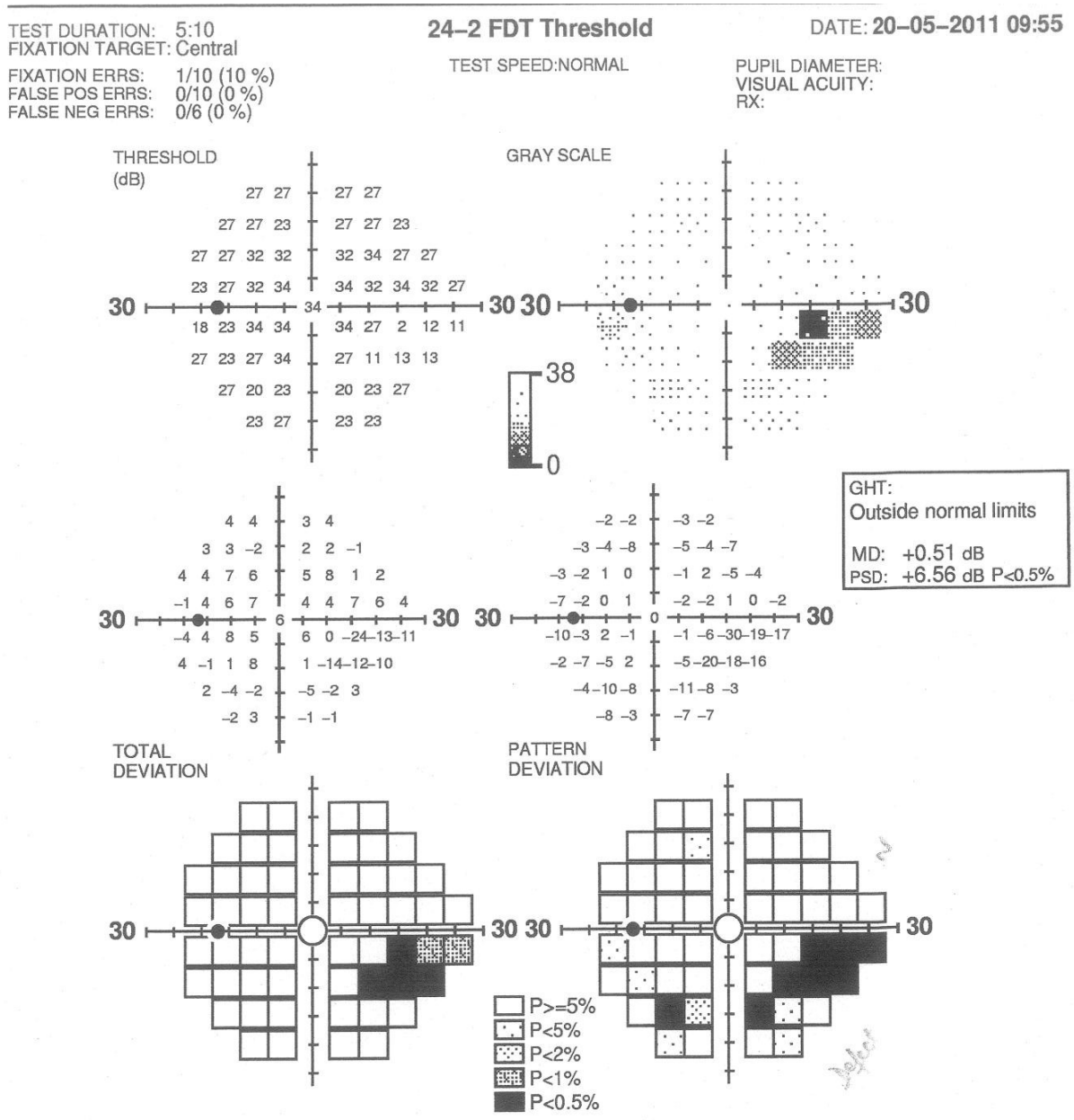

As a result of its diagnostic performance, shorter test time, probability, lower expense and ease of use,[232] it is a cost effective screening tool in glaucoma. In normal subjects the intra and inter test variability of the FDT is similar to SAP. In patients with glaucomatous eyes, the variability of the FDT remains stable,[249] in contrast, SAP variability increases dramatically as the defects severity increases.[250] The smaller influence of media opacities, pupil diameter and refractive error on the results is consistent with reduced variability with lower test retest variability when compared to both SAP and SWAP.[237] There is a more precise discrimination between normal and abnormal responses as the hill of vision is flatter in comparison to SAP and SWAP and allows lower point to point confidence intervals.[251]

The learning effect is absent in a large number of subjects. For those whose performance improves, it is only the first examination that is affected.[252] It can be used in children,[253] and it has been suggested that it is unaffected by defocus and uncorrected refractive errors up to 6 diopters,[254] although some findings have found the contrary.[249] Measurements are resistant to pupil size differences, unless the difference in pupil diameter between the two eyes is more than 2mm.[232]

The disadvantage of the FDT is the suboptimal spatial resolution due to the large stimulus size and low number of targets presented. The low target number makes the ability to monitor progression more difficult and limits its clinical use in glaucoma follow up.[255, 256] Cataracts also affect the threshold sensitivities, although probably to a lesser extent than short wave automated perimetry. Sensitivity values are improved in both normal and glaucoma patients post cataract surgery.[257]

d. Electroretinogrm (ERG)

The ERG is the summed transient electrical response produced from the entire retina after it has been exposed to a single flash of diffuse bright light, delivered from a full field dome. It is recorded indirectly by various electrodes in contact with the eye, for example, Burian Allen, DTL and gold foil. The signal from the active recording electrode is compared with the signal from a reference electrode placed remotely from the eye, either on the forehead or on the lateral orbital rim. This response depends on the state of retinal adaptation (dark or light adapted) as well as the intensity of the flash, it consists of 3 components, a-, b- and c-waves.[258]

Electrical potentials arise because of localised conductance changes in the membranes of active cells, which give rise to inward or outward currents that flow into the extracellular space and produce potential gradients. In the dark adapted state, scotopic ERGs are recorded after at least 20 minutes dark adaptation, dim flashes produce the b wave which represents current produced from membrane depolarisation of rod bipolar cells. A current loop occurs as the increase in extracellular potassium enters and depolarises the Muller cells causing a current flow towards the inner retina.[259, 260] As the flash intensity increases, a faster initial negative deflection is produced, the a-wave, which predominantly reflects hyperpolarisation of the rod photoreceptors secondary to a reduction in sodium conductance of the plasma membrane. This is then truncated by the rise in the b-wave (Figure 9).[258]

Figure 9: Responses of a dissociated Müller cell (penetrated near the nucleus) to K+ ejections from an extracellular pipette

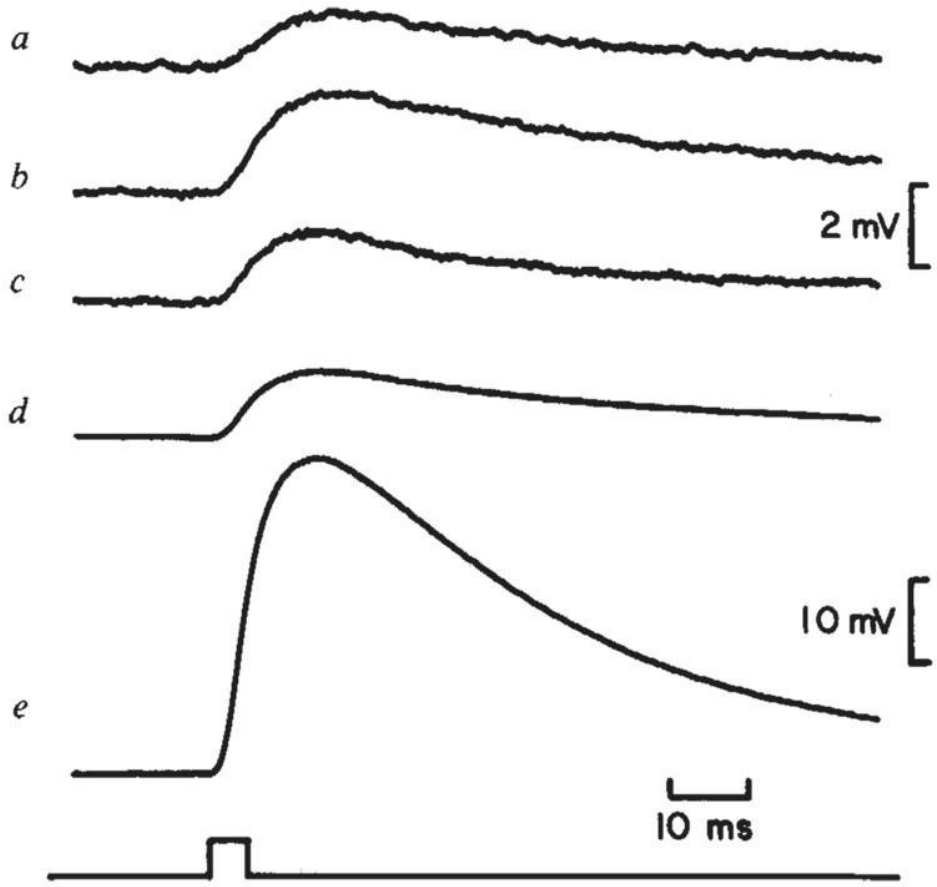

The c-wave is a slower positive wave that follows after the relatively fast a- and b-wave. The origin of the c-wave is the decrease in extracellular potassium around photoreceptor cell outer segments in the sub retinal space and the high resistance of tight junctions of the RPE. This results in an electrical potential between the apical and basal surface of the RPE. The wave represents the summation of the corneal positive sub component generated at the RPE and a corneal negative sub component generated by the hyperpolarisation at the distal portion of the Muller cells.[261]

Once photopic adaptation occurs, the response becomes cone driven as the background light saturates the rod contribution to the ERG. A smaller response is produced from the flashes, the light adapted a-wave represents the cone photoreceptors and 'off' bipolar cells. The b-wave is from the depolarising 'on' and 'off' bipolar cells.[262]

Many studies have shown that the full field ERG is essential for the diagnosis of numerous disorders such as retinitis pigmentosa, cone dystrophy, retinoschisis and congenital stationary night blindness. However, it is not clinically useful in the detection of glaucoma as there are only minimal reductions in amplitude or latency delays in comparison to the normal population,[263-266] perhaps this is because there is little retinal ganglion input into the response. It is also a gross potential that reflects all the cells of the retina, the full field ERG shows poor sensitivity in comparison to the pattern ERG in the detection of early to moderate glaucomatous loss.[264] It provides no topographical information and the patients need to be fully dilated because small pupils decrease retinal illuminance and hence ERG responses.

i.<u>Oscillatory potentials in glaucoma</u>

Cobb and Moreton in 1954 first described rhythmic wavelets now known as oscillatory

potentials.[265] They occur in response to a strong stimulus, as a series of high frequency (100-160 Hz), low amplitude oscillatory wavelets that are superimposed along the ascending limb of the b-wave. They are contributed to by both rod and cone systems and are present in both scotopic and photopic recording conditions. Their cellular origin is uncertain, they are said to be post-receptoral in origin. Two components are thought to be involved: neuronal interaction and inhibitory feedback circuitry responses from the IPL, which account for the oscillatory nature of the response.[267-269] It has been suggested that they are generated by both amacrine and bipolar cells, the early potentials are related to the 'on' pathway the latter ones to the 'off' pathway.[266]

Differing results have been found with OPs ability to detect glaucoma: one study indicated that they have poor sensitivity in detecting glaucoma.[264] Conversely, others demonstrated a reduction in OP responses in glaucoma.[270, 271] When compared to the pattern ERG which showed a reduction in unilateral glaucoma, the OPs were normal.[272]

ii. Photopic negative response (PhNR) in glaucoma

The PhNR is a slow negative response that occurs in response to a long flash, in the dark adapted ERG, immediately after the b-wave. It has been suggested that this response is generated in the inner retina, that it originates from ganglion cell spiking activity and is therefore likely to be affected in optic neuropathies such as glaucoma.[273, 274] Viswanathan et al[269] induced experimental glaucoma in macaque monkeys and determined the effects of tetrodotoxin (TTX) on blocking spiking activity in the PhNR and pattern ERG. They found similar results, indicating common retinal origins.[267]

The PhNR is reduced in patients with POAG,[268, 269, 275] with a good correlation with pattern ERG reductions.[268] The s-cone PhNR was found to be more sensitive in detecting glaucoma

than the pattern ERG.[275] It also has the advantages of being a larger response not requiring refractive correction.

iii. Scotopic threshold response (STR) in glaucoma

The STR occurs below the b-wave threshold, it is a negative response to a very dim light during dark adaptation and has a latency 100-140 msec. With progressively brighter stimuli the STR amplitude increases until it is buried by the emerging b-wave. It is a reflection of the inner retinal function.[276, 277] It is believed to reflect the activity of amacrine and ganglion cells.[278]

Selective STR abnormalities have not yet been reported in human glaucoma.[279] However, it has shown promise as being sensitive in experimental glaucoma,[280, 281] and acutely elevated IOPs.[282, 283] One study found that the STR was only mildly affected in glaucoma whereas the P2 was significantly reduced.[273]

iv. Pattern ERG (PERG) in glaucoma

The PERG is the most common minimally-invasive measure of perimacular ganglion cell function and inner retinal activity[284-289] and has been proposed as a parameter to indicate early glaucoma. It is recorded using ISO-luminant reversing black and white checkerboard or grating, which reverses its local luminance whilst keeping the average luminance constant throughout the recording. The ganglion cells and the inner retinal cellular components generate a response to changes in the light-dark edges of a pattern stimulus.

There are two types of responses: the transient PERG and the steady state PERG. The transient PERG is recorded using a reversal rate less than 6 reversals per sec (3 Hz) and is ideal for identification of specific waveform components. It has an initial small negative response (N1 or

N35) at 35 ms, followed by a large positive component (P1 or P50) at 50 ms, followed by a further negative wave at 95 ms (N2 or N95) (Figure 10)

Figure 10: Normal transient PERG response

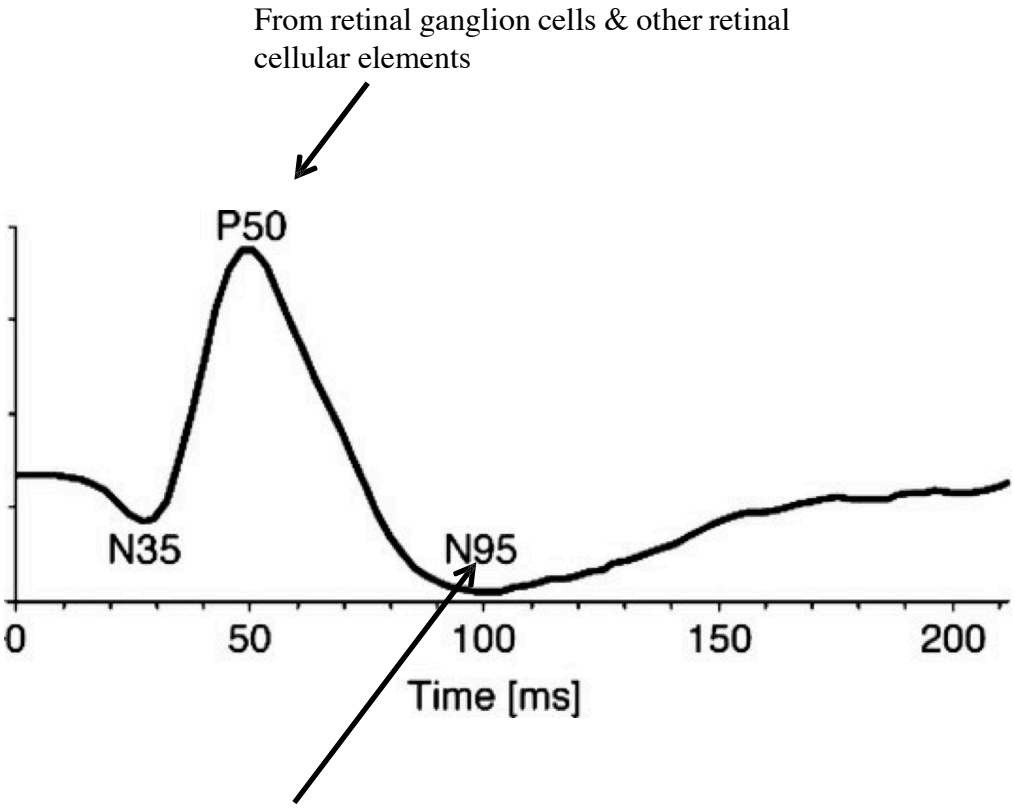

These latter two components are the focus for the clinical diagnostic work. The N95 becomes obscured by the next P50, producing the second type of response, the steady state response if the frequency of stimulation is fast (>10 reversals per second). The response is a sinusoidal wave, which does not allow for component analysis, limiting its clinical application. The technique is minimally invasive requiring a gold foil, thread or fibre as an electrode as a contact lens degrades the image quality.[274, 290]

Since the original suggestion by Maffei and Fiorentini in 1981 that the PERG could be used to monitor the electrical response of the ganglion cell, there have been a large number of studies on patients with glaucoma.[264, 284,291-300] These studies had different aims. Firstly, to test the hypothesis that the PERG has a ganglion cell origin by studying conditions that directly affect the ganglion cell response. The P50 was found partly reduced, and the N95 severely reduced in monkeys treated with TTX which abolishes the action potentials generated from ganglion cells.[267] This is consistent with PERG recordings after optic nerve transection.[285]

Secondly, the PERG was tested in subjects with known glaucoma to assess its clinical value. There is a consistent consensus that PERG abnormalities are evident in those with diagnosed POAG. Notable changes have been observed: both amplitude reductions and latency delays of P50, N95 are affected in glaucoma.[264, 272, 284, 286, 292-298] Therefore the PERG has been regarded as a clinical indicator of RGC function and is consistently markedly affected in glaucoma. The PERG has been suggested as method of measuring the RGC function dysfunction in patients with OHT prior to the development of glaucoma. The results are more variable in those with OHT than in glaucoma: some reporting a latency delay or reduction in amplitude, others reporting no change.[301-307] Porciatti et[287] reported 11 of 12 (91.6%) ocular hypertensives had amplitude reductions, while Wanger and Perrson,[300] showed only 4 of 7

(57.1%) had amplitude reductions in those with unilateral hypertension. Trick et al[288] investigated a larger number of ocular hypertensives, but only a smaller number (15 of 130 (11.5%) had amplitude reductions. A recent study shows a very high rate of glaucoma detection (100%) and a very high sensitivity in OHT, 85% had a delayed P50 and 69% had a reduced P50-N95.[289]

Studies suggest that steady state PERG with higher temporal frequency (10-20 reversals) compared with transient stimulation (<4 cycles) improves the sensitivity of glaucoma detection by increasing the magnitude of the deficit.[308, 309] Bach et al also reduced the variability by using check size specific PERG. They introduced a PERG ratio between the amplitudes of small 0.8 degree checks and the 16 degree checks.[294, 310] The PERG with a smaller check size tend to be reduced in early and late glaucoma, whereas the PERG to large check sizes are reduced only in advanced glaucoma. They reported predictive abnormalities in small numbers of those with OHT that subsequently developed glaucoma. ROC specificity was 85%.[292]

Longitudinal studies are few. In a recent study of ocular hypertensives, the PERG (ratio of small versus large check response amplitudes) was able to predict the conversion to early glaucoma (defined as a reliable new field defect). Over a 1-3 year period, in 95 ocular hypertensive eyes 8 eyes developed glaucoma. The sensitivity was 80% and specificity 71%, 1 year prior to conversion. The predictive value of PERG measurements acquired at longer durations was poor in the group of patients prior to conversion to glaucoma. These results suggest that the PERG ratio becomes abnormal prior to standard automated perimetry.[311]

The PERG optimised for glaucoma screening (PERGLA) paradigm[312] is another method to help refine the technique, it has a smaller amplitude, uses skin electrodes, which avoids contact with

the cornea and a grating rather than a checkerboard. The recording procedure is standardised which helps minimise variability. The value of this approach has been demonstrated by large amplitude reductions in glaucoma of up to 90% and delays in latency of up to 15 ms compared with age matched controls.[313-315] Other studies found the repeatability of PERG recordings was good and similar within and between tests for both healthy and diseased groups (glaucoma and OHT). They suggested that this test is promising for monitoring progression.[250] Inter-session coefficient of variation is approximately 10-12%.[302, 303] There has also been developed a frequency doubled PERG stimulus with 9 test regions within thefield. This was able to detect 100% of moderate to advanced glaucoma and found abnormalities in 67% of high-risk subjects.

The strengths of PERG are that it is clinically easy to perform and no light adaptation is required. The limitation of PERG is that it is acuity dependent: therefore optical blur, media opacities and pupil size confound the results.[274, 290] Dilation and contact lens electrodes are not recommended as they blur the image, hence it requires an electrode that is in contact with the lower eyelid. The small response amplitude (<10uV) results in a low signal to noise ratio, computer averaging of multiple recordings or sweeps is necessary to isolate this response. Blink and eye movement artifacts can be a problem increasing noise and variability. Both the inter and intra variability of the response are also limitations,[253] therefore care must be taken to ensure optimal recording conditions. The standardisation of the recording technique had minimised this variability, allowing the technique to be more clinically viable. Another limitation is if there is retinal pathology distal to the ganglion cells, this will also affect the PERG. The technique also only provides a cumulative signal from the central visual field, so it cannot topographically localise abnormalities.

v. Multifocal ERG (mfERG)

The standard mfERG is a measure of the function of the outer retinal cells, largely shaped from the bipolar cells with smaller contributions from the photoreceptors and inner retinal, amacrine and ganglion cells[316-318] and the optic nerve head.[319, 320] The inner retina makes a relatively small contribution to the waveform.[321]

The mfERG is a valuable tool in detecting pathology of the outer retinal layers and photopic retinal function.[322, 323] However, there are only slight differences detected in the responses of those with moderate and advanced glaucoma compared with normal subjects and topographical correspondence has not been establishes with the RNFL loss or visual field defects.[321, 324-326]

There has been development of new protocols to try to isolate response components from ganglion cell activity, such as the optic nerve head component (ONHC).[319] The ONHC is thought to originate from the beginning of the axonal myelination near the ONH and reflects the activity of the RGCs. A delay in the ONHC is thought to relate to the length of the unmyelinated nerve fibres that action potentials must travel between the focal stimulation and the ONH.

Alternative modes of mfERG stimulation were developed, designed to produce larger ONHC in normal eyes[327, 328] in an effort to detect any losses secondary to glaucoma. Initial studies of human[327-329] and glaucomatous eyes,[329, 330] supported this theory. However, this has been limited by variability in the responses,[331] as well as the necessity of a contact lens electrode to isolate the ONHC, thus limiting its clinical application.

The stimulus for the mfERG was modified to present patterns within each of the hexagonal areas

recorded so that a pattern ERG could be recorded from each area of the retina. Because the pattern signal was much smaller, generally the stimulus area of the individual hexagons needed to be increased and their number reduced to produce a reasonable signal. The first order kernel of these recordings was flat, the second order kernel represented the non liner component generated by the pattern and showed a consistent signal.[332]

Unfortunately the mfERG pattern stimuli did not improve diagnostic capability to a significant amount, although moderate loss has been demonstrated for glaucoma population averages, there is substantial overlap with control populations and no relationship to disease measured perimetrically.[333-335]

vi. Visual Evoked Potential (VEP)

The VEP is a gross electroencephalographic (EEG) recording generated by the cells in the occipital cortex. It is easily recorded with scalp electrodes and provides an objective and reproducible clinical measure of the function of the visual pathways up to and including the visual cortex.[306] For over 40 years, the VEP has been used to diagnose and study diseases of the visual system detecting any abnormalities along the chain of the visual pathway from the retina to the occipital cortex.[307]

The commonest visual stimulus used is a high contrast pattern reversal black and white checkerboard. Thirty years ago Regan established that a temporally reversing chromatic checkerboard pattern could generate robust VEPs.[336] The cells of the retina and LGN respond well to a change in the luminance in their receptive field, the cortical neurons of the striate cortex respond more actively to light-dark edges and orientation.[337] A checkerboard stimulus is thought

to activate many components of the visual system and has the advantage of generating large cortical responses whilst minimising variability.

The stimulus is a checkerboard consisting of black and white squares that alternate in a regular phase frequency every 1-2 seconds with a certain fixation point. A spatial frequency of 10-20 minutes of arc with a temporal frequency of 8Hz gives an optimal response.[338, 339] With standard electrode positioning of about 2 cm above and below the inion, the resulting waveform is a large biphasic response, consisting of components which reflect the activity of the striate cells in area 17 (the first positive component N75, occurs at 50-75 ms) and possibly extrastriate cortex (deflected wave P100, occurring at 95-110 ms) (Figure 11).[340, 341] More recently, the technique has allowed changes in contrast, spatial and temporal frequency as well as chromatic gratings we varied to be studied. Chromatic contrast stimuli, however, usually elicits small cortical responses that can be difficult to detect.[342]

The stimulus for a flash or full field VEP is a diffuse flash presented in the Ganzfeld bowl under photopic adapted conditions. The flash VEP displays large inter individual variation and are thus primarily used as a gross test of cortical response in uncooperative patients or in those with poor fixation. The response is a series of positive and negative components; the most prominent is the P2.

Figure 11: Normal Standard VEP response

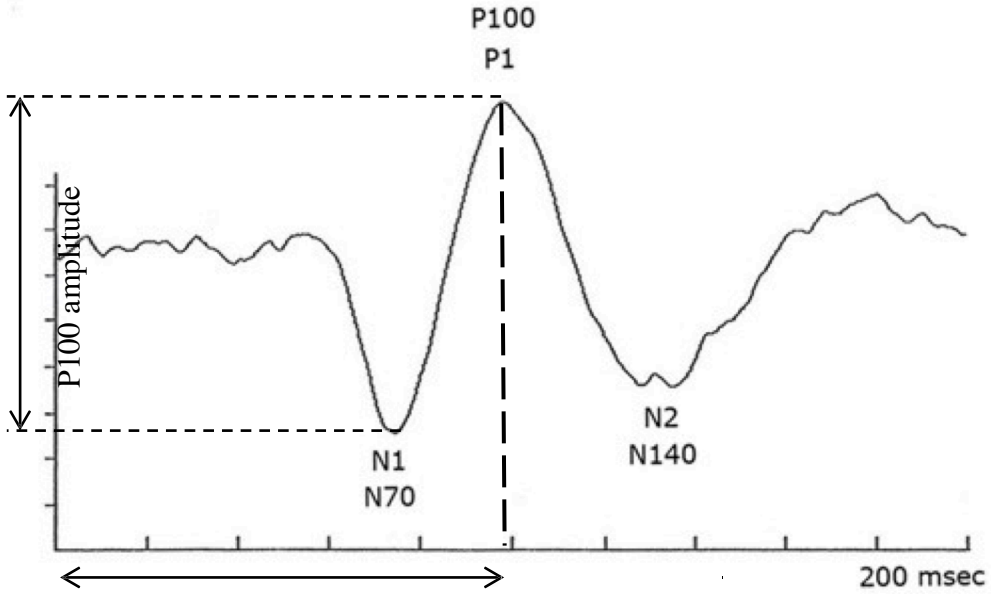

P 100 Latency

Both the standard flash and the pattern VEP responses are of limited value in the study of glaucoma. While they have been shown to be abnormal in some cases the sensitivity in early glaucoma is very poor and consequently many cases are missed.[314, 315, 343] The major limitation of this technique in detecting glaucoma is that evoked responses are dominated by foveal input, which has cortical overrepresentation and is unable to detect abnormalities in the peripheral field.[344-346] The fovea is represented disproportionately as a large cortical area occupying the posterior portion of the striate cortex where the scalp VEP electrodes are placed. The peripheral visual field is represented by a smaller cortical area located more anteriorly in the striate cortex and provides a limited contribution to the VEP. It has been estimated that the central 2 degrees of the visual field produces 65% of the response, compared to the ERG where the fovea is thought to represent less than 2% of the total response.[332]

The technique does not provide a topographical measure and hence is unable to determine the location of pathology. This is important especially in glaucomawhere damage often involves localised regions of the retina and foveal involvement only late in the disease. The pattern VEP is also easily affected by refractive error,[347] and is best corrected for near vision, the small check size also tends towards central bias.[308, 309] To avoid this variability in amplitude, most studies focused on delay in latency. Up to 50% of the POAG patients and 25% of OHT patients have a delay in latency compared to normal subjects. This was found to correlate with morphological change in the optic discs and severity of field defects.[313]

Topographic correlations have also been studied, hemifield defects in glaucoma patients were observed to cause a decrease in amplitude and were topographically correlated in quadrantic analysis.[348] Also the pattern VEP generated by stimulating the mid peripheral visual field (central

5 degrees blocked) detected 44% of POAG and 15.4% of OHT had a latency delay ranging from 3-20 ms.

Overall, the conventional VEP shows variable results in glaucoma and cannot be reliably used to diagnose glaucoma. To obtain multiple VEPs at different retinal locations would be too time consuming. Therefore a topographic method of VEP recordings,[349] based upon Sutter's multifocal technology was developed to circumvent these problems.

It has been shown that the topographic organisation of the RGCs is projected and maintained along the visual pathway to the visual cortex and thus discrete VEPs can be recorded from each representative area of the retina that is stimulated. The visual cortex is located on either side of the calcarine fissure in the occipital lobe. The cortical cells that receive responses from the peripheral fields lie anteriorly, with those from macula at the tip. The upper fields are represented in the lower half of the visual cortex and the lower in the upper half.[350] It is due to the spatial maintenance of the retinal projections to the cortex that the multifocal technique is possible.

The multifocal stimulation technique has been a major advancement in the field of electrophysiology. The technique was developed by Sutter and Tran[351, 352] and applied to VEP recordings by Baseler and colleagues.[349, 353] It has allowed the presentation of a multifocal stimulus and enabled the recording of evoked responses simultaneously in many locations, topographically mapping spatially localised damage in the visual pathway. This technique evolved as sequential recordings from multiple areas of the retina as using focal ERGs were too time consuming. Two concepts are fundamental to the application of this technique, scaling of the stimulus and the use of binary sequence, such as the m- sequence to drive temporal change in the stimulus.

Cortical scaling occurs when each element increases in size from the centre to the periphery, such that they stimulate equal areas of the striate cortex at different eccentricities, thereby avoiding foveal dominance in the evoked responses.[349] The increase in the stimulus size with eccentricity is proportional to cortical magnification and is based on equations derived from histological studies.[354] The original stimulus used by Baseler resembled a series of hexagons with checkerboards comprising 24 equal triangles forming each hexagon.[349] The pattern of the stimulus was controlled by a pseudo random binary exchange of two opposite checkerboard pattern conditions at each of the test sites in the visual field. Each input site modulated with time according to the same pseudorandom binary m sequence.[349]

This m sequence was the original binary sequence to be employed in VEP recordings.[349] This property was utilised by Sutter who employed 56 such sequences shifted by an integer number of stimulus frames to 56 locations in the visual field. The responses generated for each location are different and therefore do not contaminate the responses for other locations. The responses were correlated with the stimulus element and averaged, resulting in an effective method of mapping evoked responses.[355] Thus, the individual signals may be extracted from the EEG by cross correlation of the response evoked and the stimulus sequence. To maintain isoluminance about half the total elements are white and half are black.

The stimulus paradigm however, has provided greater insight into temporal interaction of neural elements. In order to decrease the test time the binary sequence is presented at the maximum refresh rate of the cathode ray tube of 75 Hz. At this high speed the effect of a stimulus on the response of the subsequent stimulus can be studies using the Weiner kernel analysis technique.[356, 357] This allows the analysis of cross correlation kernels which can characterise non linear analysis between visual events that occur in the visual system.[358]

The first order kernel is calculated by adding all recordings following a black frame and then subtracting all recordings from a white frame. The response from the hexagon is summed and the responses from other hexagons diminished. The second order response is used to calculate the response from successive flashes of the white hexagon and is used to determine the short-term adaptation from the preceding flash. The first slice of the second order response represents the visual evoked potential to a reversal between two successive intervals, regardless of the direction of transition (0 to 1 or 1 to 0), summed over all the reversals in the m-sequence cycle, minus all instances in which no reversal occurred. It is analogous but not identical to the conventional pattern reversal VEP.[353] The second slice calculates the effect of a flash in the frame before the immediately preceding frame. The second order response lasts much longer than one frame (13.3 ms at 75 Hz).[359]

Klistorner et al using flash mfVEP found that the first slice of the second order kernel showed response to a low luminance contrast saturating at 40%, while the second slice showed non-saturating linear increase in response with contrast. This behaviour was found to resemble the magnocellular and parvocellular dichotomy and was attributed to these mechanisms.[360] Using pattern mfVEP, Baseler and Sutter showed that 2 components of the evoked potentials showed topographic distribution, one dominated in the central field, while the other occurred more in the periphery. These were also found to vary differently with contrast. This topographic distribution was thought to resemble the parvocellular to magnocellular distribution of neurons between centre and periphery.[353] However, some reports suggest that there is no differential distribution of neurons between the centre and periphery.[363]

Baseler and colleagues found the application of the m sequence very successful in mfERG

monitoring but did not consider it to be useful for clinical mfVEP recordings.[349] The mfVEP was limited by the use of midline electrodes, either fronto-occipital[362] or bipolar electrodes.[353] This resulted in signals being dominated by the inferior hemifield, especially in the flash mfVEP and was only able to detect areas of the striate cortex, which had surface perpendicular to the vertical dipole. The cortical convolutions therefore limited the detection of the stimulus from areas representing the horizontal and vertical meridian of the visual field. The pattern mfVEP although smaller than the central flash mfVEP, produced more uniform responses throughout the visual field. Flash mfVEP was a limited technique as it had limited topographic value, analysing more of the central test zone, the peripheral responses were too small.

The mfVEP was the first multifocal test used to topographically map the visual field loss from a variety of pathologies including glaucoma.[362] Graham et al first examined the use of mfVEP in glaucoma patients using bipolar straddle electrode positions. 42 glaucoma patients with reproducible visual field defects were tested. The mfVEP showed loss of amplitude in the areas corresponding to the scotomas seen on SAP.[363]

Over the last 10 years many advancements in the techniques have occurred, including changes in the electrode positions,[363-366] multiple channel recording,[364, 367] pattern sequence,[367] EEG scaling,[271] dichoptic stimulation,[368, 369] inter-eye asymmetry and analysis of waveforms,[370, 371] as well as improvement in the signal to noise ratio (SNR)[360, 370, 372] and use of alternative stimuli patterns.[373-377]

To date, studies from different centres have confirmed the mfVEP as a tool for the objective assessment of visual field defects, primarily for glaucomatous visual field loss.[370, 378-381] The method has also been applied to other optic neuropathies, ON and multiple sclerosis,[382-394] and

ischaemic optic neuropathy,[395] and has shown promise in the assessment of neurological disorders such a cortical lesions,[396-499] compressive optic neuopathies.[400, 401] The technique has been applied to children,[402, 403] as well as those with non organic field loss.

The new electrode positions were developed, using four bipolar electrodes in the form of a cross straddling the inion. This allowed recording from multiple channels rather than a single midline channel. This significantly improved the signal strength as the different recording vectors overcame the problems of cortical convolution obstructing the previous monopolar or single channel recording.[363-366] This was confirmed by Hood et al, who concluded that the addition of 2 lateral electrodes and multiple channel recordings improved the responses from 79% of the SNR exceeding 0.6 for the typical midline channel, to 93% when the best SNR was used.[364] Meigen and Kramer also found that two additional perpendicular electrodes straddling the inion was the most effective recording set up.[365]

The pattern sequence was redesigned in the second commercially available system, Accumap™ (Objectivision Pty Ltd, Sydney) that was developed in Australia. This system uses a 58-segment dartboard configuration, the segments cortically scaled with eccentricity to stimulate approximately equal areas of the striate surface. This system employs a spread spectrum technique using Kasami binary sequences. During a standard recording run of 54 seconds, each of the 58 segments of the visual field are stimulated approximately 2000 times. This technique computes the resulting signal, by cross correlation of the response evoked by a sequence stimulation, with the sequence itself at each of the stimulation sites.[367] This differs from the m sequence based recording systems (such as Veris ™), where the first slice of the second order kernel contained the mfVEP response. With this new technique, simple cross correlation replaced kernel analysis. Real time recording of the

electroencephalographic (EEG) signal was introduced, which allows the quality of the recording to be checked during the acquisition of data. The raw mfVEP data is also scaled according to the patients background EEG and is their own unique condition characteristics. It has been established that this reduces inter individual variability from 42 to 25%. Thus a mfVEP signal normalized with respect to the background EEG reduces the variability.[360] Inter eye asymmetry analysis was developed as the right and left response signals were observed to be almost identical for normal patients, due to the proximity of the signal generating areas in the visual cortex. This has proved useful to detect early defects. (Figure 12) By comparing test points between eyes for an individual 98.6% of patients were identified with field loss. They also found that defects could be identified in some high- risk glaucoma suspects with normal SAP. However, it is less reliable for those with symmetrical field defects or those with bilateral disease when assessing the less affected eye.[370] Hood et al, quantitatively measured the eyes of 6 normal subjects and 4 patients whose pathology included unilateral glaucoma, ischaemic optic neuropathy and optic neuritis. They found that essentially pairs of two eyes of the controls were almost identical except for small naso-temporal differences. This differed from the paired patient responses which were found to be significantly different.[371] It is therefore clinically important to assess both amplitude and asymmetry deviation plots.

Figure 12: Example mfVEP report of a patient with early glaucoma

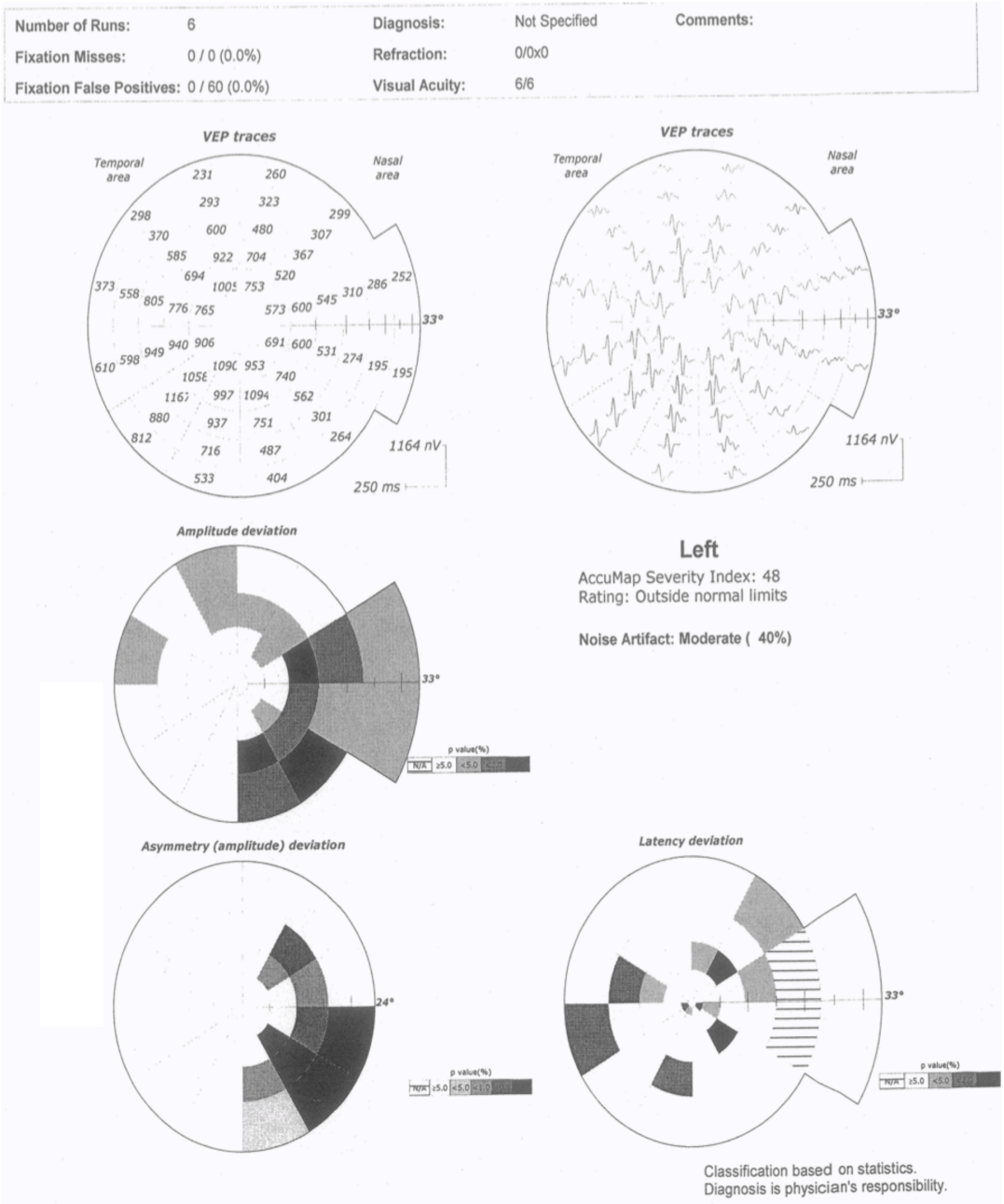

Several investigations have been done to adapt the mfVEP methods into a dichoptic test. This allows simultaneous stimulation of both eyes by independent sequences, thus reducing recording time[369] as well as providing a statistical advantage when comparing the results between the two eyes,[371, 383, 384] with more reliable assessment of inter eye asymmetry.[368, 369]

Arvind et al recorded 28 glaucomatous patients and 30 normals. It was found that the dichoptic mfVEP responses identified early defects in areas unaffected on SAP in addition to field losses detected on SAP and reduced testing time by 30%.[368]

In the past, the intra and inter subject variability of the multifocal technique has limited its clinical application. Inter subject variability is due to the difference between the individuals in the location and convolution of the visual cortex as well as variation in external cranial landmarks.[85, 385-387] It results in large standard deviations of normal values and minimizes the ability of the technique to detect early cases. Intra-subject variability leads to difficulty in monitoring progression of the disease. It is caused from the responses being of opposite polarity between the upper and lower fields[353] and the nasal responses being slightly faster than the temporal,[385] due to the differing distance in the ganglion cells from the optic nerve. Just above the horizontal meridian, responses from the temporal retina are slightly larger than the nasal,[370] as well as responses just above being larger than the below.[385, 388] It has been suggested that this is caused by the horizontal meridian falling below the bend in the calcarine fissure. The responses from the vertical meridian differ from the other responses, as extra striate cortex may contribute more to the responses near the vertical meridian.[327, 395, 396]

Responses from the same subject on different days have been found to be very similar[349, 362] with a coefficient of variation on average being 16% across the whole field[367, 389] and the repeatability of the mfVEP was found to be slightly more than that of the SAP.[390-392] In the

study by Chen et al, the repeat reliability of the mfVEP was evaluated within a day and across weeks (2-12 weeks) in both normal and glaucomatous eyes.[391] Fortune et al, similarly reported findings after repeat testing on normal subjects after a year.[390] This suggests that progression in the early stages should be more easily detected by mfVEP than by SAP.

Wangusupadilok et al[393] recently described a method that can be used to distinguish between inter-test variability and progression of glaucoma. They used 87 patients with POAG, underwent repeat mfVEP testing within 50 days (group 1) and a second group of 44 patients that underwent repeat mfVEP testing within 6 months (group 2). They calculated test scores (the total number of test points with p values exceeding 5%) and cluster sizes (the number of abnormal test points within a cluster). Group 1 did not show a significant difference in either total score or cluster size. Group 2 showed a significant difference in the interocular and monocular comparison between tests ($p<0.05$) as well as the interocular comparison of cluster size ($p<0.05$). This may therefore be a possible method of monitoring the progression of functional deficits using mfVEP.

There was a need to improve this variability and reproducibility by enhancing the SNR by either minimizing noise artifacts or increasing the signal amplitude, to improve diagnostic accuracy. Several studies have used alternative stimuli that were developed to evoke larger responses. The use of the pattern pulse stimulus rather than a pattern reversal[377] and a slowed stimulation rate 280 significantly improves the signal to noise ratio (SNR) on average 1.9 times. James[377] suggested that this is due to contrast gain control mechanisms. When stimulated by pattern reversal, spatial contrast is present at all times resulting in adaptation of the visual system and hence smaller response amplitudes. Pattern pulse stimulus reduced the adaptation by having an interval of no contrast, allowing full recovery of contrast sensitivity, and hence larger amplitudes.[377]

This has been supported by further studies that suggest there is an increase in the SNR of 60-90% using temporally sparse stimuli instead of pattern reversal.[373, 374, 375] The benefit is dependent on eccentricity, as the use of this alternative stimuli has been shown to be advantageous for the central field (up to 9.5 degrees) displaying larger mfVEP responses although in the periphery (up to 23 degrees) there was no demonstrated difference in amplitudes.[376] Pattern onset stimuli has also been seen to enhance SNR but only in the central field with a decrease in the periphery.[397]

Fortune et al[373] compared a number of stimuli – pattern reversal, pattern onset and sparse pulse stimuli to study the effect of spatial sparseness. Spatial isolation increased the SNR by 62% for temporally sparse pulses and 22% for reversal responses. Temporally sparse pattern pulses were also 3.5 times larger although there was no gain in the SNR.[373] Therefore spatial isolation had a greater effect. Onset responses were 3.5 times larger than conventional reversal stimuli and twice as large as those for offset. This supports James findings that larger SNR occur when brief contrast stimuli are sparsely distributed in space and time.

The advantages of this technique are that it is an objective, topographic, non invasive means of mapping the visual fields to a wide eccentricity. It is tolerated well by patients. A recent study on patient opinions of 7 different clinical tests used in the assessment of glaucoma ranked the mfVEP (median rank, 4.0) better than the SAP (median rank, 4.8) although not as high as Goldmann applanation tonometry, which ranked significantly better than the others (median rank 2.5, $p<0.01$).[398]

However, the mfVEP is limited by the fact that both refractive error and cataracts blur the stimulus. The effect of optical defocus on the response is dependent on eccentricity. Greater

than +2.0D defocus caused central amplitudes to be reduced to approximately 60% while there was no effect on eccentricities greater than 7 degrees.[378, 379] Patients with cataract are usually excluded from mfVEPstudies as they cause apparent field defects in the mfVEP as well as SAP.[379, 380]

The mfVEP is now established as an objective tool that compliments subjective testing as a method of visual field examination.[362, 389] In spite of the advantages of the mfVEP being objective and the possibility of detecting defects earlier than the SAP, there remains a concern as the detection of subtle changes in the early stages still remains a continuing challenge. To date, this technique has used a black and white stimulus to demonstrate visual field defects in glaucoma patients. Our design was to use a Low Luminance Achromatic (LLA) stimulus and a blue yellow stimulus in an attempt to detect glaucoma at an earlier stage.

In addition to glaucoma detection, the mfVEP is a sensitive and specific test for detecting optic neuritis.[399-403] The mfVEP has been reported to be superior to full field VEPs in ON patients, by topographically analysing the conductivity of the optic nerve[315, 371, 399] and recovery of the optic nerve function.[404, 405]

In a study of 64 eyes with confirmed optic neuritis, 97.3% were abnormal on VEP testing.[406] Both amplitudes were reduced and latencies delayed, the latency z score had 100% sensitivity and specificity for detecting ON when compared to normal patients,[406] in a recent study of patients with MS and a history of ON. Cluster criteria of both amplitude and latency resulted in an ROC of 0.96, 91% sensitivity and 95% specificity.[401] The mfVEP detects more abnormalities in patients with ON than SAP.[407] There is a significant delay in latency in 80% of eyes and also 57% of the unaffected eyes. Amplitudes were also reduced when analysed in quadrants (50.3%) compared with SAP (30.5%).[407] Studies on the fellow eyes of patients with unilateral ON have also shown reduced amplitudes and delays in latencies, indicating widespread sub-clinical inflammatory changes in the CNS.[399,408] The magnitude of the

electrophysiological changes in the fellow eye were related to the risk of multiple sclerosis.[399]

The mfVEP may aid in monitoring the progression of patients with optic neuritis. In a prospective case series, 36.4% of patients with ON and delayed latencies on mfVEP progressed clinically to MS over a 1 year period, compared to 0% of patients with normal latencies.[409] It can also be used to monitor improvement in conduction velocity over time after the acute episode of optic neuritis.[400]

CHAPTER 2: STRUCTURAL AND FUNCTIONAL IDENTIFICATION OF EARLY GLAUCOMA

(The results of this chapter will be submitted for publication in IOVS.)

2.1 INTRODUCTION

Glaucoma is a progressive optic neuropathy characterized by a specific pattern of optic nerve head and visual field damage due to the death of RGCs Typically, the diagnosis is based on characteristic changes in the optic nerve head combined with a visual field defect determined with static automated, achromatic perimetry (SAP). However, substantial ganglion cell damage can take place before SAP detects functional deficits.[182, 410]

Structural measurements of the optic nerve head (ONH) and functional measurements of the visual field represent two main pillars of glaucoma diagnosis and management.[404] A number of diagnostic tests have been developed and attempt to diagnose glaucoma before its appearance on subjective standard automated perimetry (SAP) testing.[77, 405-409] The structural measures are less patient dependent and therefore more objective, demonstration of functional loss that corresponds to observed structural changes lends more confidence to the diagnosis.

Early detection of glaucoma is very important, because the earlier and more reliable detection will enable preservation of a significant proportion of the subject's ganglion cells normally lost prior to disease recognition, and ultimately thereby preserve vision. The current study utilizes several new concepts in early glaucoma diagnosis and applies principles proven to be helpful in subjective strategies to new objective measures. These alone could provide an even more sensitive tool for diagnosis, and when combined with other tests known as early markers, may produce a new diagnostic model to detect the

earliest signs of damage in glaucoma.

2.2 AIM OF THE STUDY

The aim of the current study was to determine the optimal combination of tests for detecting early glaucoma using new and diverse strategies for selective testing of specific visual pathways, in combination with structural analysis for nerve fibre loss.

2.3 METHODS

70 glaucoma patients from a specialist eye clinic and 18 normal subjects who volunteered to be normal controls were recruited for the study. All patients had a glaucomatous disc in at least one eye and had reliable visual fields previously. The patients had previously undergone a comprehensive eye examination by the referring ophthalmologist including visual acuity testing, IOP and stereo biomicroscopic optic disc examination. In addition, as part of the study, they underwent visual acuity testing and refraction, standard white on white perimetry, short wavelength automated perimetry, FDT Matrix, LLA mfVEP, BonY mfVEP, Spectralis OCT, HRT and stereoscopic disc photographs. The controls were included into the study based on having a normal eye examination with no previous history of any ocular problems and no family history of any ocular diseases. Approval was obtained from the institutional review board. Written informed consent was obtained from all participants, and the study was conducted in accordance with the tenets of the Declaration of Helsinki. The order of tests was randomized.

The white-on-white standard automated perimetry (SAP) and short wavelength automated perimetry (SWAP) tests were performed with the Humphrey Field Analyzer model 745,

(Zeiss Humphrey Systems, Dublin, Ca), using the SITA –Std 24-2 program. Near addition was added to the subject's refractive correction. If fixation losses were more than 20% or false positive or false negative rates were more than 33% (rates of reliability fixed by the perimeter software), the test was repeated. Abnormal SAP and SWAP was defined by the presence of a cluster of 3 or more abnormal points at $p<5\%$ with at least one point lower than $p<1\%$ on the pattern deviation plot, and Glaucoma Hemifield Test outside normal limits.

FDT perimetry was performed with the FDT Humphrey Matrix (Carl Zeiss Meditec) using the 24-2 full-threshold strategy with 5° stimuli and a spatial frequency of 0.5 cycles per degree, counterphase flickered at 18 Hz. Reliability and abnormality criteria was similar to the other perimetry tests.

The Spectralis SD-OCT (software v. 5.3.3.0) was used to obtain RNFL thickness measurements. The high-resolution protocol was used, obtaining 1536 A-scans from a 3.45-mm circle centered at the optic disc, providing an axial resolution of 3.9 μm and a lateral resolution of 6 μm. The examiner was required to manually place the scan around the optic disc. To improve the image quality, the Spectralis SD-OCT includes an automatic real-time function that gathers multiple frames (B-scans). The images were then averaged for noise reduction. The standard deviation of the signal-to-noise ratio was available to the examiner, enabling the assessment of the signal's acceptability. The quality scores ranges from 0 dB (poor) to 40 dB (excellent). For each parameter, the Spectralis SD-OCT software provides a classification (within normal limits, borderline, and outside normal limits) based on the comparison with an internal normative database of 201 healthy eyes of Caucasian patients. The parameter is classified as within normal limits if its value falls within the 95% confidence interval (CI) of the healthy, age-matched population. A borderline result

indicates that the value is between the 99% and 95% CI, and an outside normal limits result indicates that the value is less than the 99% CI. In this study all borderline values were considered as normal for analysis.

The HRT-III (Heidelberg Explorer Software v. 1.5.10.0, Heidelberg Engineering) was used to acquire CSLO images in the study. It uses confocal scanning laser principles to obtain a 3-dimensional topographic image of the optic nerve. The nerve margin on the mean topographic image was outlined by the examiner. Good images required a focused reflectance image with a standard deviation not greater than 50 μm.

The software for the HRT-III also incorporates the Moorefield's Regression Analysis (MRA), which compares the patient's rim area with a predicted rim area for a given disc area and age, based on confidence limits of a regression analysis derived from 627 normal patients (452 Caucasians, 111 of African origin, and 64 Indians). Each sector and the global rim area are classified as within normal limits if the measurement is within the 95% CI, borderline if the measurements are between the 99.9% and 95% CI, and outside normal limits if the measurements is lower than the 99.9% CI. Only the MRA was used for the purpose of analysis in this study. Similar to the OCT, all borderline values were considered as normal.

The mfVEP was performed using Accumap version 2.0 (ObjectiVision Pty. Ltd., Sydney, Australia). Two different pattern onset stimulus presentations were used. Both stimuli consisted of a cortically scaled dartboard pattern of 58 segments; 56 segments were arranged in five concentric rings (eccentricities 1–2.5°, 2.5–5°, 5–10°, 10–16°, and 16– 24°), and 2 segments straddled the horizontal nasally (24°–33°). A fixation target occupied the central 1°. For the BonY mfVEP, each segment contained a 4x4 grid of blue checks scaled proportional to segment size (luminance 20 cd/m^2 that appeared briefly on a bright yellow background

(luminance 125 cd/m^2 according to a pseudorandom binary sequence). Briefly, the sequence had a total length of 440 elements and consisted of two types of elements (elements 0 and 1) distributed pseudorandomly. Each element of the sequence lasted nine frames of the monitor. Element 1 of the binary sequence was represented by two consecutive states: a blue pattern-on (checker-board blue-and-yellow pattern) state,which lasted two frames, and a pattern- off (diffuse, bright yellow illumination of the entire segment) state, which lasted seven frames. For the element 0 of stimulating sequence, the pattern-off state (diffuse yellow illumination) was active for all nine frames of the element. The LLA stimulus was similar to the BonY one, but was its equivalent in gray scale. The yellow background was replaced by light gray of the same luminance as the yellow, and the blue color of the checkerboard was replaced by a darker gray of the same luminance as the blue. A scotoma on mfVEP was considered to be present if on the amplitude deviation plot, there were 3 or more contiguous non-rim points of amplitude less than p<2% of the normal database, with at least 1 point, p<1%; or on the asymmetry plot, at least 3 contiguous points with p<1% or 2 contiguous points p<0.5%.

Abnormal discs were identified based on one or more of the following criteria: (1) definite focal rim notching, (2) cup-to-disc asymmetry of 0.2 or more with no disc size asymmetry plus rim irregularity, and (3) relative thinning of the neuroretinal rim with no abnormal disc configuration as explanation (e.g., tilting). The disc photographs were examined by two masked observers, assessed for confirmation of glaucoma, and graded for the presence or absence of a defect in the superior or inferior rim. The visual fields of all patients were analysed and those with no field defects were termed to have preperimetric glaucoma and those with field defects but MD>-6 dB were termed to have early glaucoma. All tests (imaging and visual field tests) were considered to have a positive hemifield defect if a defect identified by that test corresponded topographically to the disc damage identified on

photographs. Combinations of two and three tests were performed to identify the best combination of tests that detected early glaucomatous damage.

2.4 RESULTS

101 eyes of 64 patients had a glaucomatous disc appearance confirmed. There were 32 females and 32 males. The mean age of the patients was 64.89 ±8.15 years. 16 eyes of 15 patients were found to have early glaucoma and 85 eyes of 59 patients had preperimetric glaucoma based on white on white perimetry.

OCT was found to have 100% specificity, while HRT was found to have the best sensitivity in identifying patients with preperimetric glaucoma. Low contrast mfVEP also had a high sensitivity of 50.6% for preperimetric glaucoma. The sensitivity of each of the tests was calculated for patients with early glaucoma and pre perimetric glaucoma.
(Table 1)

Table 1: Sensitivity of all the tests

		Controls (n=36)	Preperimetric (n=85)		Early glaucoma (n=16)		Total group (n=101)	
		Specificity	Sensitivity	p value*	Sensitivity	p value*	Sensitivity	p value*
VF	SAP	35 (97.22%)	-NA	-NA	15 (93.75%)	0.69	15 (14.85%)	<0.0001
	SWAP	31 (86.11%)	18 (21.18%)	<0.0001	12 (75.0%)	1.00	30 (29.70%)	<0.0001
	FDT Matrix	35 (97.22%)	16 (18.82%)	<0.0001	13 (81.25%)	1.00	29 (28.71%)	<0.0001
VEP	LLA	32 (88.89%)	43 (50.59%)		12 (75.0%)		55 (54.46%)	
	BonY	32 (88.89%)	33 (38.82%)	0.06	12 (75.0%)	1.00	45 (44.45%)	0.05
HRT		31 (86.11%)	44 (51.76%)	1.00	12 (75.0%)	1.00	56 (55.45%)	1.00
OCT		36 (100%)	21 (24.71%)	<0.0001	8 (50.0%)	0.18	29 (28.71%)	<0.0001

* p value calculated using Mcnemar test comparing the sensitivity of LLA (since it had the highest sensitivity) with other tests.

The sensitivities were also calculated for a combination of two tests (Table 2). The combination of LLA and HRT (any one test positive) was found to have the best sensitivity, identifying 77.65% of patients with preperimetric glaucoma.

Table 2: Sensitivities for combination of two tests

	Preperimetric (n=85)		Early glaucoma (n=16)		Total group (n=101)	
	Sensitivity	p value*	Sensitivity	p value*	Sensitivity	p value*
SAP-SWAP	18 (21.18%)	<0.0001	15 (93.75%)	1.00	33 (32.67%)	<0.0001
SAP-Matrix	16 (18.82%)	<0.0001	15 (93.75%)	1.00	31 (30.69%)	<0.0001
SAP-LLA	43 (50.59%)	<0.0001	16 (100.00%)	0.48	59 (58.42%)	<0.0001
SAP-BonY	33 (38.82%)	<0.0001	16 (100.00%)	0.48	49 (48.51%)	<0.0001
SAP-HRT	49 (57.65%)	<0.0001	16 (100.00%)	0.48	65 (64.36%)	0.0005
SAP-OCT	21 (24.71%)	<0.0001	15 (93.75%)	1.00	36 (35.64%)	<0.0001
SWAP-Matrix	25 (29.41%)	<0.0001	14 (87.50%)	0.48	39 (38.61%)	<0.0001
SWAP-LLA	48 (56.47%)	<0.0001	14 (87.50%)	0.48	62 (61.39%)	0.0002
SWAP-BonY	44 (51.76%)	<0.0001	15 (93.75%)	1.00	59 (58.42%)	<0.0001
SWAP-HRT	54 (63.53%)	0.0022	15 (93.75%)	1.00	69 (68.32%)	0.0059
SWAP-OCT	33 (38.82%)	<0.0001	15 (93.75%)	1.00	48 (47.52%)	0.0059
Matrix-LLA	46 (54.12%)	<0.0001	15 (93.75%)	1.00	61 (60.40%)	<0.0001
Matrix-BonY	46 (54.12%)	<0.0001	15 (93.75%)	1.00	61 (60.40%)	<0.0001
Matrix-HRT	55 (64.71%)	0.0036	14 (87.50%)	0.48	69 (68.32%)	0.0059
Matrix-OCT	28 (32.94%)	<0.0001	14 (87.50%)	0.62	42 (41.58%)	<0.0001
LLA-BonY	48 (56.47%)	<0.0001	13 (81.25%)	1.00	61 (60.40%)	<0.0001
LLA-HRT	66 (77.65%)		14 (87.50%)		80 (79.21%)	
LLA-OCT	49 (57.65%)	0.0002	14 (87.50%)	0.48	63 (62.38%)	0.0003
BonY-HRT	61 (71.76%)	0.0455	14 (87.50%)	1.00	75 (74.26%)	0.0455
BonY-OCT	45 (52.94%)	<0.0001	13 (81.25%)	1.00	58 (57.43%)	<0.0001
HRT-OCT	54 (63.53%)	0.0008	14 (87.50%)	0.48	68 (67.33%)	0.0037

* p value calculated using Mcnemar test comparing the sensitivity of LLA-HRT combination of tests (since it had the highest sensitivity) with other tests combination.

2.5 DISCUSSION

There are several tests performed in the clinic to diagnose glaucoma. This study was conducted to understand which single test or a combination of two tests would help identify patients with early ganglion cell loss and treat them early to prevent further extensive damage to the optic nerve. In this study, we found that the LLA mfVEP identified a field damage corresponding to disc damage in 50.6% of patients with preperimetric glaucoma. In the entire group of patients, which included patients with preperimetric and early glaucoma, HRT was found to correspond with optic disc damage in 55.45%, followed by LLA mfVEP in 54.46%. These two tests were found to be more sensitive in identifying patients with very early glaucomatous changes.

The structure-function relationship in glaucoma is well known and recognized.[411, 412] A number of tests that target this relationship and attempt to diagnose glaucoma prior to its appearance on subjective white-on-white visual field testing have been developed, with varying degrees of success.[413-417] While structural measures are less patient- dependent and therefore more objective, demonstration of functional loss that corresponds to observed structural changes lends much more confidence and credibility to the diagnosis.

SWAP and FDP are visual function tests that target different RGC subsets. SWAP isolates and tests the function of blue-on axons in the koniocellular pathway,[413] whereas FDP targets cells of the magnocellular pathway,[414] although a recent study suggests a cortical mechanism may underlie the doubling perception.[418] Both cell types are relatively sparse

within the retina, which may allow functional loss to be detected sooner than with SAP.[419] Both tests attempt to improve detection of field loss in glaucoma by selectively stimulating visual pathways with low functional redundancy, and both techniques have shown success, with about 20% success in identifying preperimetric glaucoma.[417] Arend and Plange reported that SWAP and FDT showed that progression in early glaucoma could be detected before SAP damage occurs. However, SWAP seems to have a considerable learning curve, which counteracts its effective usage for detecting progression early. Leeprechanon et al[420] reported that the diagnostic precision of FDP was similar to that of SWAP in early detection of glaucoma before it becomes visible on SAP perimetry.

Structural changes are generally proposed to precede functional changes and hence one would expect a higher sensitivity on structural tests then the functional tests. However, Jeoung et al reported that the sensitivity of the OCT ranged from 18.9% to 83.8% in patients with preperimetric glaucoma depending on the parameters used to define an abnormal OCT.[412] In this study we found the sensitivity of OCT to be low (24.71%). This could probably be because most of the study patients had very early RNFL loss and all borderline defects were termed as normal.

The HRT variables have reported higher detection rates of 42% for preperimetric glaucoma and between 74-87% for early glaucoma.[413] This study reports a similar sensitivity of 51.76% in preperimetric glaucoma and 75% in early glaucomas. The mild discrepency could be due to the difference in criteria used to define abnormal HRT in the two studies. However, it was found to be the single best test in identifying preperimetric glaucoma. Since all our patients included in the study were selected based on the appearance of a glaucomatous disc, this could have biased the results. However the disc area as measured by HRT on the patients in this study was 2.13 ± 0.47 mm^2 which is significantly larger than the disc area reported by Blue Mountains eye study. This could probably explain why HRT was

found to show high sensitivity in this study.

Objective perimetry using multifocal stimulation is a relatively new psychophysical test. Since it provides a topographical measure of damage, its results can be compared with SAP. Objective perimetry has been reported to have several advantages over subjective perimetry.[414] Patients prefer performing this test to automated perimetry because of the removal of any decision-making and performance pressure. It has no learning curve. Objective perimetry is also useful in patients with unreliable fields that cannot be interpreted, where it can be used to confirm or exclude field loss. It has the potential to detect malingerers and may be useful in children. Different stimuli presentations on mfVEP have showed different sensitivities. The conventional black-and-white pattern reversal stimulus demonstrated 80% to 92% sensitivity in early glaucoma.[417, 418] Its sensitivity in preperimetric glaucoma has been reported to be 21% of perimetrically normal fellow eyes of glaucomatous patients[418] and in 20% of glaucoma suspects.[419] The LLA and the BonY are two different stimuli used in mfVEP. They differ from the regular pattern reversal stimulus in the contrast stimulation and colour and using the pattern onset stimulus. The novel LLA[102] and BonY[419] mfVEP have been reported to identify functional loss in nearly 40-50% of patients with preperimetric glaucoma. This variability in sensitivities could probably be due to different pathways being stimulated by different pathways being affected.

In this study the LLA was found to be the best functional test in identifying preperimetric glaucoma. The sensitivity of LLA mfVEP was also as good as that of the HRT, though traditionally structural tests have been thought to have higher sensitivities than functional tests. The sensitivity of LLA was higher, but not found significantly so from that of BonY. This is very similar to the finding reported by Arvind et al.[102] The mfVEP responses to achromatic stimulation saturate at approximately 40% to 50% contrast, which is similar to what has been used in this study for LLA and BonY.

Response at this level of luminance contrast has been described to have predominant magnocellular contributions, which may be the reason for the excellent performance of LLA in this group of patients.

The sensitivities of the other perimetric tests-SWAP and Matrix were about 20% for preperimetric glaucoma, in keeping with previously published data. In perimetric glaucoma, the sensitivities increased to 75-80% for almost all tests, however in the realm of preperimetric glaucoma, where clinical decisions are hardest to make, and where demonstration of functional loss makes the greatest difference to clinical management, LLA mfVEP outperformed the other functional tests significantly.

The HRT-LLA mfVEP combination of tests identified losses corresponding to disc changes in 78% of subjects (66 eyes) with preperimetric glaucoma. This is an extremely encouraging result, considering that this combination of tests would take about 20-30 minutes to perform, and provides topographically corresponding structural and/or functional evidence of damage in this group of patients with very early glaucoma. They offer an excellent opportunity for early intervention, and significantly limiting irreversible NFL loss.

In conclusion, we found that the LLA, HRT and their combination had the best sensitivity in identifying preperimetric glaucoma, together identifying corresponding losses in nearly 80% of eyes with preperimetric glaucoma.

CHAPTER 3: REPRODUCIBILITY OF MULTIFOCAL VEP LATENCY USING DIFFERENT STIMULUS PRESENTATIONS

Latency is used to identify and monitor demyelination in optic nerve disease. We need to identify the optimal stimulus and the signal peak that provides the best reproducibility to monitor latency in a longitudinal study. Hence, this chapter was done as a sub study since we will use latency of mfVEP as a measure of inflammatory demyelination along the visual pathway. This study has been published in Documenta Ophthalmologica ***(Doc Ophthalmol. 2012 Aug;125(1):43-9).***

3.1 ABSTRACT

Purpose

To study the reproducibility of latency of mfVEP recorded using different stimulus presentations, and to identify the peak with least variability.

Methods

Ten normal subjects, aged between 22 and 52 years (mean age 32 ± 8.37 yrs) participated in the study. All subjects underwent mfVEP testing with Pattern-reversal and Pattern-pulse stimulus presentations. The stimulus subtends 26 degrees from fixation and includes 24 segments. Only the vertical channel was recorded on all subjects. Testing was repeated after 1-2 weeks. Only the right eye of all subjects was analysed. Segments with low signal to noise ratios (SNR<1.5) were excluded from analysis. The latencies were analysed to confirm values from the same peak for the two tests. The latency values were then analysed for the start of the response, the 1st peak and the 2nd peak.

Results

The waveforms were reproducible throughout the field. Reproducibility of latency at the "start of the response" was significantly lesser than the first and the second peaks studied, while the reproducibility of latency at the first peak was not statistically different from the second peak for both pattern reversal and pattern pulse stimulation. The latency values were not different between the 1st and the 2nd session for either pattern reversal or pattern pulse stimulation for any of the peaks.

Conclusion

The pattern reversal stimulus presentation produced less variability in latency. The 1st peak is the most reproducible among the three measures in both the stimulus presentation.

INTRODUCTION

Visual evoked potentials (VEP) are used as an objective means for measuring function of the visual pathway and are understood to be generated at the level of striate cortex by the combined activity of postsynaptic potentials.[421, 422] The mfVEP allows recording of local VEP responses, provides a measure of these local losses and is a reliable and objective method of assessing neural damage to the optic pathways.[422, 423] The possibility of topographical study of optic nerve function with measurement of amplitude and latency from locally derived VEP responses, in numerous small areas of the visual field, has proven to be an advantage of the mfVEP over the conventional VEP since diseases of the RGCs and the optic nerve cause spatially localized losses in visual function.[424-426] The disease can affect the latency as well as the amplitude of the VEP, and hence, it is important to measure both.[421, 427]

Delayed conduction of VEP has been found in a high proportion of patients with ON and is

thought to reflect demyelination of the optic nerve fibres, with the subsequent shortening of latency thought to represent the process of remyelination. There have been studies suggesting that the mfVEP is more effective in identifying demyelinating events.[428, 429] With new treatments for remyelination being introduced, latency measurement can be used as a marker for de-/remyelination. However, variability of the mfVEP latency and difficulty defining the appropriate method for determining latency has been a problem for its clinical application. This is often due to the wide variety of waveforms within the field and changes in waveform between tests. Rendering a template has been one approach. [430, 431]

Relatively little is known about the repeat reliability of latency of the mfVEP. The purpose of this study is to assess the reproducibility of latency of the mfVEP under two different test conditions in the same individual. With the possibility that pattern reversal and pattern pulse stimulus presentations stimulate different subsets of neurons and may therefore both be diagnostically useful in the clinical setting, we examined reproducibility of both stimulation methods.

3.2 METHODS

The mfVEP was performed on 10 normal subjects, aged between 22 and 52 years. All subjects had a best corrected visual acuity of 6/6 in both eyes and normal anterior and posterior segment on evaluation. The subjects underwent mfVEP recording on the pattern reversal and the pattern pulse stimulus presentation. The test was repeated on all subjects, 1–2 weeks later to study reproducibility. Procedures followed the tenets of the Declaration of Helsinki, and informed consent was obtained from all participants.

The mfVEP testing was performed using the AccumapTM (Objectivision Pty Ltd., Sydney, Australia). The display consisted of a cortically scaled dartboard with 24 segments arranged

in three concentric rings, with an eccentricity up to 26° and a central fixation target extending up to 1°. The stimulus in any segment consisted of a 6 x 5 black and white check pattern. The segment size was scaled according to the cortical magnification factor. Corresponding to the size of the segments, the size of the individual checks also increased with eccentricity. Luminance of the white check was 146 cd/m2, and luminance of the black check was 1.1 cd/m2 producing a Michaelson constant of 99 %. The mean background luminance of the computer screen was 73.5 cd/m^2, and a dim room light was always on. The system used a spread spectrum technique with families of binary sequences to drive the visual stimulus (see previous publications).[432-435] For pattern reversal stimulation, two opposite checkerboard pattern conditions underwent pseudorandom binary exchange at each of the 24 sites, with the probability of reversal being 50% at each frame of the monitor (Figure 13a).

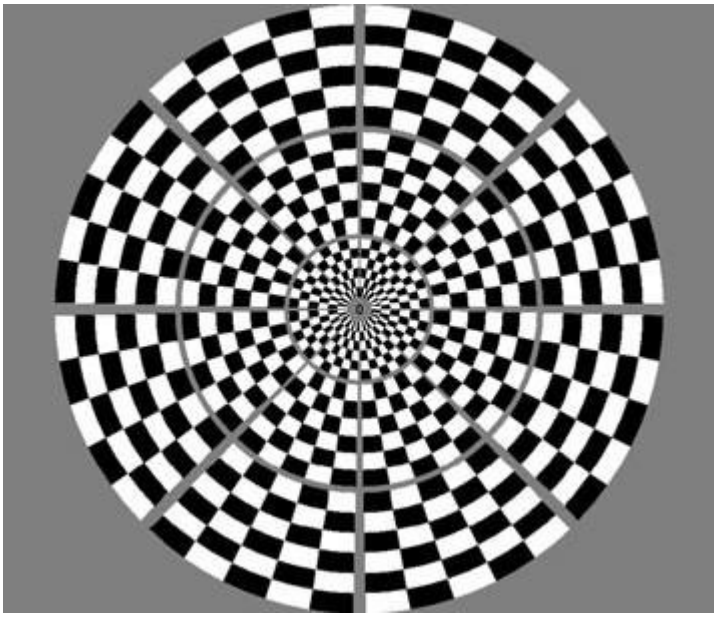

Figure 13a: Pattern reversal stimulus

For each segment of the visual field the pattern reversed each time, the binary pseudorandom sequence assigned to the segment has an element 1 and remained unchanged when the sequence

had element 0.[432] For pattern pulse stimulation, each element 1 of the binary sequence is represented by two consecutive states: state ‘‘pattern-on’’ checkerboard pattern (duration 2 frames) and state ‘‘pattern-off’’ diffuse illumination (duration 7 frames) of the whole segment with an intensity of a mean luminance between the black and white check (73.5 cd/m2)[432] (Figure 13b).

Figure 13b: Pattern pulse stimulus

The duration of each run is 56 s on both pattern reversal and pattern pulse stimulations. The runs were repeated till good trace improvement was achieved. An average of 8–10 on pattern reversal and 6–7 runs on pattern pulse stimulation were required. Subjects were seated 30 cm from the screen with refractive correction for near vision. They were asked to fixate on the small, randomly changing number at the centre of the stimulus pattern, which was used to monitor fixation. Pupils were not dilated, and all recordings were performed monocularly. Two gold cup electrodes (Grass, RI, USA), one electrode 2.5 cm above and one 4.5 cm below the inion in the midline were used for bipolar recording. Visual evoked responses were amplified 1 x 10^5 times and band-pass filtered 1–20 Hz. Data were analysed using Opera

V1.3 software. The largest peak-trough amplitude within the interval of 70–200 ms was determined. The wave of maximum amplitude for each segment in the visual field was selected, and a combined topographical map was created by the software.[432-435] The signals were then analysed to confirm values from the same peaks for the two tests and also to identify waveforms with reversed polarity. The raw data were exported into Microsoft excel format for analysis. Difference between minimum and maximum amplitude within interval of analysis (70–200 ms) was calculated. Noise level was calculated as the standard deviation of amplitudes between 400 and 800 ms. Signal-to- noise ratio (SNR) was calculated by dividing amplitude of signal by noise. SNR was calculated for all segments. Segments with SNR>1.5 were excluded from analysis. Figure 14a–c shows examples of a few waveforms with poor, moderate and good SNR.

Figure 14 a Poor signal-to-noise ratio (SNR = 0.9). b Moderate signal-to-noise ratio (SNR = 1.4). c Good signal-to-noise ratio (SNR = 3.5)

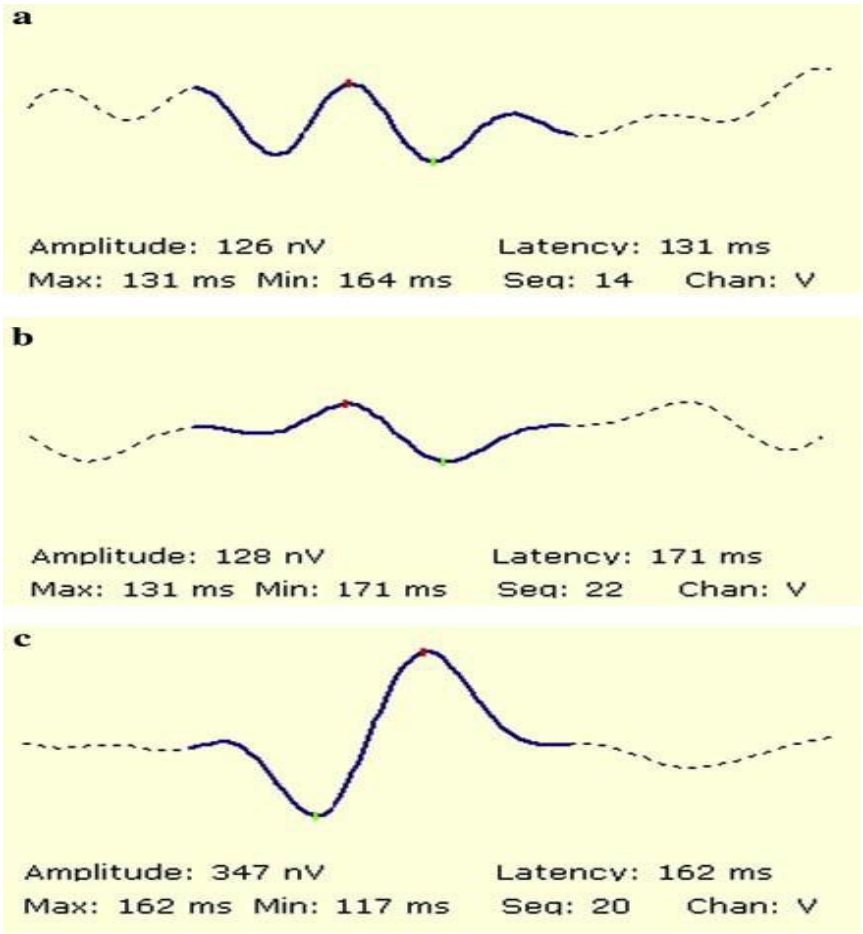

Traces with reversed polarity between the two sessions were also excluded. Three various latency definitions were tested: start of the response, first and second major peaks (Figure 15).

Figure 15: Waveform showing the three different locations studied

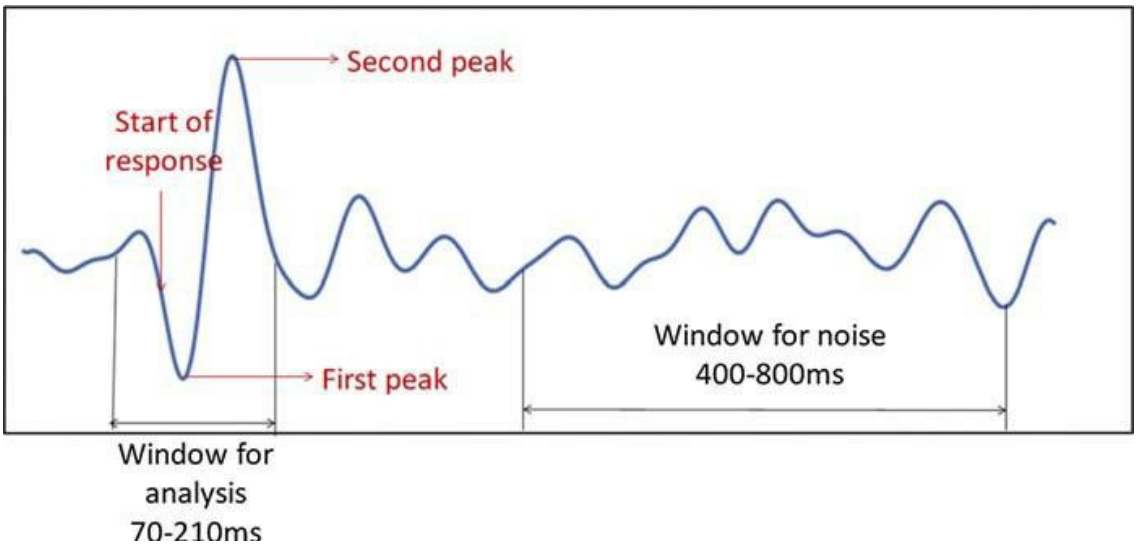

The first point to cross the 95th percentile of noise was considered as the start of the response. The mean difference of latencies between the two sessions was calculated to assess the test retest variability. Data analysis Paired t test was performed to calculate the difference between two sessions. Intra Class Coefficient (ICC) and Coefficient of Reliability (CR) were performed to calculate repeatability. Statistical significance was defined as $p<0.05$. A repeated measure ANOVA was performed to examine differences between the rings.

3.4 RESULTS

The tests were performed on 10 normal subjects (mean age 32 ± 8.4 years). The recordings were obtained from both eyes, but only the results from right eye were used for analysis. Twenty per cent of the sectors on pattern reversal stimulus and 12.1 % of sectors on pattern pulse stimulus presentations had to be excluded due to either low SNR in any one session or reversed polarity between two sessions. Most of the signals excluded due to poor SNR were in the superior rim area. The average value of latencies on both stimulus presentations is shown in Table 3.

Table 3: Average latencies on pattern reversal and pattern onset stimulations at the 3 peaks studied

	Start of response (mean±SD) (in ms)			1st peak (mean±SD) (in ms)			2nd peak (mean±SD) (in ms)		
	PR	PO	p value	PR	PO	p value	PR	PO	p value
1st session	99.67± 9.16	96.55± 10.14	0.046	118.54± 6.91	121.79± 6.45	0.010	161.70 ±6.88	176.31± 9.06	<0.0001
2nd session	97.57± 6.81	94.75± 5.76	0.090	119.13± 6.38	121.85± 5.65	0.002	162.65± 4.56	174.37± 2.97	<0.0001
p value	0.217	0.263		0.437	0.961		0.289	0.132	

* paired t test was performed to obtain the p values

The latency values were not different between the first and the second sessions for either pattern reversal or pattern pulse stimulation for any of the peaks. The latencies were significantly longer on the pattern pulse presentation for both first and second peaks for both sessions. The average values for the inter visit difference in latency was 11.9, 3.2 and 4.6 ms for the start of response, first peak and second peak on the pattern reversal and 9.6, 3.9 and 6.5 ms on the pattern pulse stimulation, respectively. Tukey's multiple comparison tests revealed significantly lower variability for the first and second peaks compared to start of the response for pattern reversal stimulation, with no significant differences between the first and second peaks. For pattern pulse stimulation, the first peak was the least variable, significantly lower than the second peak, which was significantly lower than the response onset. The test– retest variability was obtained by calculating the ICC and CR between the two sessions (Table 4).

Table 4: Intra class coefficients and average CR for PR and PO stimulus presentations

	Start of		1^{st} peak		2^{nd} peak	
	ICC	CR	ICC	CR	ICC	CR
Pattern Reversal (PR)	0.817	38.82	0.974	9.61	0.976	11.69
Pattern Onset (PO)	0.766	24.47	0.816	11.12	0.865	18.77
p value		0.0006		0.347		0.060

The variability of latency within the field did not vary significantly between pattern reversal and pattern pulse stimulations for any of the three locations studied (p values 0.11, 0.63 and 0.14, respectively, for the start of response, first peak and second peak). The CR was calculated for each sector and then averaged for the three rings to analyse the effect of eccentricity (Table 5).

Table 5: Coefficient of repeatability across the 3 rings

	1^{st} ring			2^{nd} ring			3^{rd} ring		
	PR	PO	p value	PR	PO	p value	PR	PO	p value
Start	37.68	19.65	<0.001	38.14	22.73	0.09	40.64	31.03	0.33
1^{st} peak	9.50	9.22	0.9	8.36	9.61	0.59	10.98	14.53	0.001
2^{nd} peak	8.58	14.83	0.04	11.78	15.45	0.26	14.72	26.04	0.34

While there was a general trend towards increased variability from centre to periphery, it did not reach significance for any of the peaks studied.

3.5 DISCUSSION

For the full-field VEP, the timing of the P100 peak is the internationally accepted measure of latency.[436] With the mfVEP, however, no such internationally accepted measure exists. Previous studies have shown variability of the mfVEP latency, and it has been difficult to define the appropriate technique for determining latency, due to waveform changes within field and between tests. Therefore, in the current paper, we analyse the three locations along the generated waveform that lend themselves to analysis as possible indicators of latency— the start of the response, the first peak (analogous to P100) and the second peak (Figure 15), using both pattern reversal and pattern pulse types of stimulation.

In the current study, we found that reproducibility of the first and second peaks demonstrated similar latency variability, which was significantly better compared to the start of response. This was true for either pattern reversal or pattern pulse stimulation. When pattern reversal and pattern pulse stimulations were compared, the former demonstrated better reproducibility for both peaks.

The start of the response produced least reproducibility and a high CR for both stimulus presentations. Identification of the start of the response depends, to a large extent, on noise levels; hence, even small differences in noise levels (and therefore SNR) between the two sessions can affect the timing of beginning of the response more than it affects the peaks.

We also noted that the latencies of both peaks were significantly longer on pattern pulse presentation when compared to pattern reversal stimulus (for both sessions, Table 3). Pattern pulse stimulus, due to its low frequency, is believed to mainly stimulate the parvocellular neurons.[432, 437, 438] The parvocellular neurons, in turn, display slow and sustained responses to light, which may result in longer latency. Pattern reversal stimulation, on the other hand,

which has a much faster stimulus rate, may recruit more of the magnocellular neurons, which display faster responses, resulting in relatively shorter latencies.

While this longer latency was a consistent feature, pattern pulse stimulation also displayed more variability in the timing compared to pattern reversal stimulation particularly for the second peak, where it reached significance. One possible explanation is a greater extra striate contribution to the second peak in pattern pulse, which could render it more prone to the effects of visual attention and may therefore result in greater variability.[439]

Delayed conduction of VEPs has been found in a high proportion of patients with optic neuritis. It is thought to reflect demyelination of the optic nerve fibres (or elsewhere along the optic pathway) with the delay caused by a shift from saltatory to continuous conduction along the nerve.[440] This hypothesis has been supported by recent animal studies.[441] Subsequent shortening of latency over the following weeks or months is thought to represent remyelination of the lesion.[429, 442] The finding of persistent delayed latency at 1 year has been reported to be associated with increased risk of conversion to MS.[443, 444] Therefore, latency of the VEP is a crucial diagnostic and prognostic marker, which is especially relevant when patients are followed up longitudinally.

The clinical usefulness of the full-field VEP is, however, limited by the fact that it provides a summed response of a large number of neuronal elements and is greatly dominated by the macular region due to its cortical over- representation.[426] Being the vector sum of numerous differently oriented dipoles, the waveform of the full-field VEP is prone to cancellation and distortion, leading sometimes to apparent, rather than real, latency delay.[445] The mfVEP, on the other hand, allows independent stimulation of small areas of the visual field, resulting in detailed topographical assessment of small groups of axons within the optic nerve and visual cortex, and therefore is resistant to waveform distortion.[436, 446-449] However, it is still

subject to changes in waveform shape between recording sessions probably due to subtle changes in electrode positioning. This often leads to a reversal of polarity of the signal. In addition, the upper rim field locations often show low SNRs, so reliable latency at these points cannot be determined. Such polarity changes and low SNRs need to be identified and excluded before analysing focal latency changes. This does represent a limitation of the technique with 12– 20% test locations excluded, but overall the mfVEP technique still represents a vast improvement over full-field techniques, which only provide one latency value that is dominated by the lower central field. As the greatest clinical utility of mfVEP latency is on longitudinal follow-up, good reproducibility is important for meaningful interpretation. However, there have been very limited reports on reproducibility of the latency of mfVEP.[450]

In conclusion, we noted that the pattern reversal stimulus presentation produced less variability in latency. We also note that the first peak is the most reproducible among the three measures in both the stimulus presentations. Hence, if mapping defects using latencies, for example in monitoring de-/re-myelination in optic nerve disease, latency plots obtained from pattern reversal stimulus using the first peak would provide better results when longitudinally studying remyelination.

CHAPTER 4: OPTIC NEURPATHY IN MULTIPLE SCLEROSIS

(The results of this chapter will be submitted for publication in the journal Multiple Sclerosis.)

4.1 INTRODUCTION

MS is an inflammatory and degenerative disease of the CNS with predominant involvement of white matter. Although the concept that inflammation and demyelination are major pathological substrates of neurological deficit prevailed for a long time, it has recently become clear that permanent neurological disability in MS is associated with axonal loss.[451] It is now believed that axonal injury is an early event in disease pathogenesis and is not restricted to long-standing lesions.[92, 93]

ON is a frequent initial manifestation of MS.[98] In contrast with most brain lesions, the effects of disease on the optic nerve are clinically apparent and potentially measurable, and therefore present an opportunity to examine the processes of myelin destruction, repair, and axonal degeneration.[500]

It is understood that transection of axons along the visual pathway leads to retrograde degeneration, which ultimately reaches the RNFL and RGCs. The RNFL is the only part of the CNS where unmyelinated axons can be visualized and axonal degeneration can be quantified in vivo.[501] Therefore, RNFL thickness as measured by OCT has been recently suggested as a structural marker of axonal loss in the optic nerve.[131,502]

The visual-evoked potentials (VEPs), in contrast, were developed as a means of functional assessment of the integrity of the visual pathway in ON (for review see Nuver)[503]. The amplitude of the VEPs is believed to reflect the number of functional optic nerve fibres,

which is determined by combination of two factors: the severity of the inflammation (acute or chronic) along the visual pathway and axonal degeneration.[429] Therefore, diminished amplitude indicates either inflammatory conduction block or axonal atrophy, or both. Delayed conduction of VEPs has also been found in a high proportion of patients with ON and is thought to reflect demyelination of the optic nerve fibres[443] with the subsequent shortening of latency thought to represent the process of remyelination.[429,442]

While various aspects of RGC axonal damage in MS have been addressed before, none of the studies undertook comprehensive functional and structural assessment of the entire visual pathway to evaluated possible association of both proximate (outer retinal) and distal (optic tract and optic radiation) pathology along the visual pathway with loss of RGC axons, which is an aim of the current investigation.

4.2 METHODS

Sixty-two patients with RRMS with no previous history of ON in at least one eye were enrolled. All subjects underwent a complete eye examination including OCT, ERG and mfVEP. Procedures followed the tenets of the Declaration of Helsinki and written informed consent was obtained from all participants.

The OCT was performed on a Spectralis scanner (Heidelberg Engineering) using the RNFL protocol. Total RNFL thickness and temporal quadrant RNFL thickness were assessed. In addition, a radial protocol using a star-like pattern of line scans centred on the macula with resolution of 1536 pixels was used. Analysis was performed on vertical scan only. One hundred scans were averaged for each line scan. Thirty degrees of visual angle (15 degrees of eccentricity) were scanned, but only the central 14 degrees (7 degrees of eccentricity) were

used for analysis, since the definition of layers becomes much less distinct beyond that. Retinal layers were segmented automatically using a custom designed algorithm which applied vessel detection and removal, multiple size median filtering, and Canny edge detection to identify borders of retinal layers.

The GCL and IPL were combined together (GCL/IPL) as well as OPL, ONL and Photoreceptor Inner Segment layer since the border between them was indistinguishable in several subjects. Inner nuclear layer (INL) was analysed on its own (Figure 16). The thickness of each layer was measured at seven points for each hemifield, which were equally distributed between 1.75 and 7 degrees of eccentricity. OCT measurements were compared to values of 50 age and gender matched controls.

Figure 16: OCT scanning pattern (left) and segmentation of retinal layers (right)

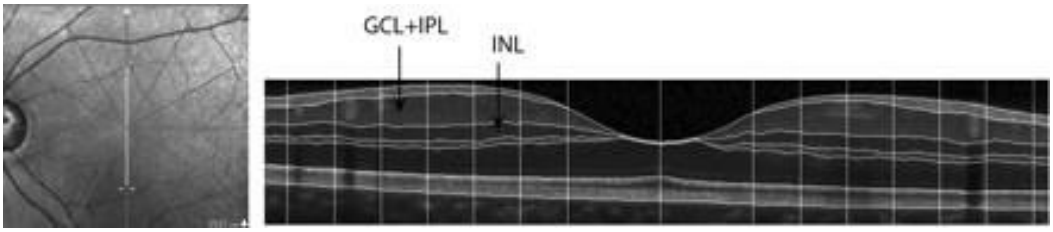

The mfVEP testing was performed using the Accumap™ (ObjectiVision Pty. Ltd., Sydney, Australia) employing standard stimulus conditions. A multi-channel mfVEP was recorded using 4 channels with an occipital cross electrode configuration. Latency analysis was performed as described in previous chapter. Full-field ERG was performed according to ISCEV standard using ESPION system (Diagnosys LLC, Lowell, MA, USA).

4.3 RESULTS

We recruited 62 RRMS patients. Four patients had high myopia and had to be excluded from analysis. One patient had a large optic disc and hence his temporal RNFL was not included for analysis. Therefore, data from 58 patients (39.9±11.3 years, 18 Males / 40 Females) were analysed. Average time from diagnosis of MS was 4.7±2.9years (1-14 years). Twenty five patients had a previous history of ON in at least one eye. The ON eyes were analysed as a separate group. Thirty-three patients did not have a history of ON. One eye of these patients were randomly selected and analysed together with the fellow eyes of ON patients (MS-NON eyes).

Table 6: Comparison of functional and structural measurements in controls, MS-NON and ON eyes

Controls		MS-NON eyes		ON eyes	
	Mean±SD	Mean±SD	p value*	Mean±SD	p value*
Total RNFL (μ)	99.2±7.5	93.6±9.9	0.002	74.1±11.8	<0.0001
Temp RNFL (μ)	70.8±7.8	64.2±9.3	0.0002	45.2±15.1	<0.0001
GCL (μ)	86.5±5.5	81.4±7.1	<0.0001	64.9±10.1	<0.0001
INL (μ)	37.3±2.8	37.6±3.1	0.59	40.9±5.1	0.0001
ORL (μ)	178.9±8.6	176.4±8.7	0.12	179.9±9.7	0.65
mfVEP amplitude (μV)	238.1±36.1	151.6±42.9	<0.0001	123.5±40.5	<0.0001
mfVEP latency (ms)	149.3±5.1	161.5±9.2	<0.0001	172.3±13.2	<0.0001
Dim white b-wave Amplitude (μv)	354.4±134.8	353.7±90.7	0.92	355.3±75.8	0.98
Dim white b-wave latency (ms)	97.7±8.9	97.32±7.9	0.89	97.1±8.5	0.8

Dark max 3 a-wave amplitude (μv)	-268.3±48.4	-287.0±58.8	0.11	-282.2±70.5	0.41
Dark max 3 a-wave latency (ms)	16.6±1.4	16.8±0.6	0.37	16.8±0.9	0.58
Dark max 3 b-wave amplitude (μv)	490.9±103.8	524.5±104.6	0.10	533.6±89.0	0.13
Dark max 3 b-wave latency (ms)	53.1±3.6	53.9±4.0	0.26	53.9±4.2	0.43
Dark max 12 a-wave amplitude (μv)	-325.5±52.4	-342.5±64.6	0.20	-337.7±71.0	0.49
Dark max 12 a-wave latency (ms)	13.5±1.1	13.7±0.9	0.43	13.4±1.1	0.84
Dark max 12 b-wave amplitude (μv)	511.9±109.2	537.0±111.1	0.27	537.7±97.8	0.39
Dark max 12 b-wave latency (ms)	52.9±1.9	53.4±1.5	0.17	52.9±4.7	0.9
Photopic a-wave amplitude (μv)	-41.4±18.1	-46.3±10.9	0.15	-45.1±12.7	0.42
Photopic a-wave latency (ms)	15.1±0.8	15.4±0.6	0.06	15.4±0.6	0.12
Photopic b-wave amplitude (μv)	174.7±35.5	185.3±41.4	0.21	183.3±42.8	0.44
Photopic b-wave latency (ms)	29.8±0.8	30.4±0.8	0.004	30.4±1.1	0.04

* p value calculated using student t-test

4.3.1 MS-NON eyes

There was a significant reduction of GCL ($p<0.0001$) in the NON-eyes of MS patients. The total and temporal RNFL also showed significant reduction ($p=0.002$ and 0.0002 respectively). However, temporal RNFL demonstrated by far the largest thinning as compared to normal controls (9.98%, 5.95% and 6.28% for temporal RNFL, total RNFL and

GCL thickness respectively).

In patients without ON in either eye RGC axonal and neuronal loss, where present, was binocular (Figure 17, oval includes points below 5th percentile (1.96 SD) of RNFL thickness in normal controls).

Figure 17: Correlation of temporal RNFL thickness between right and left eyes

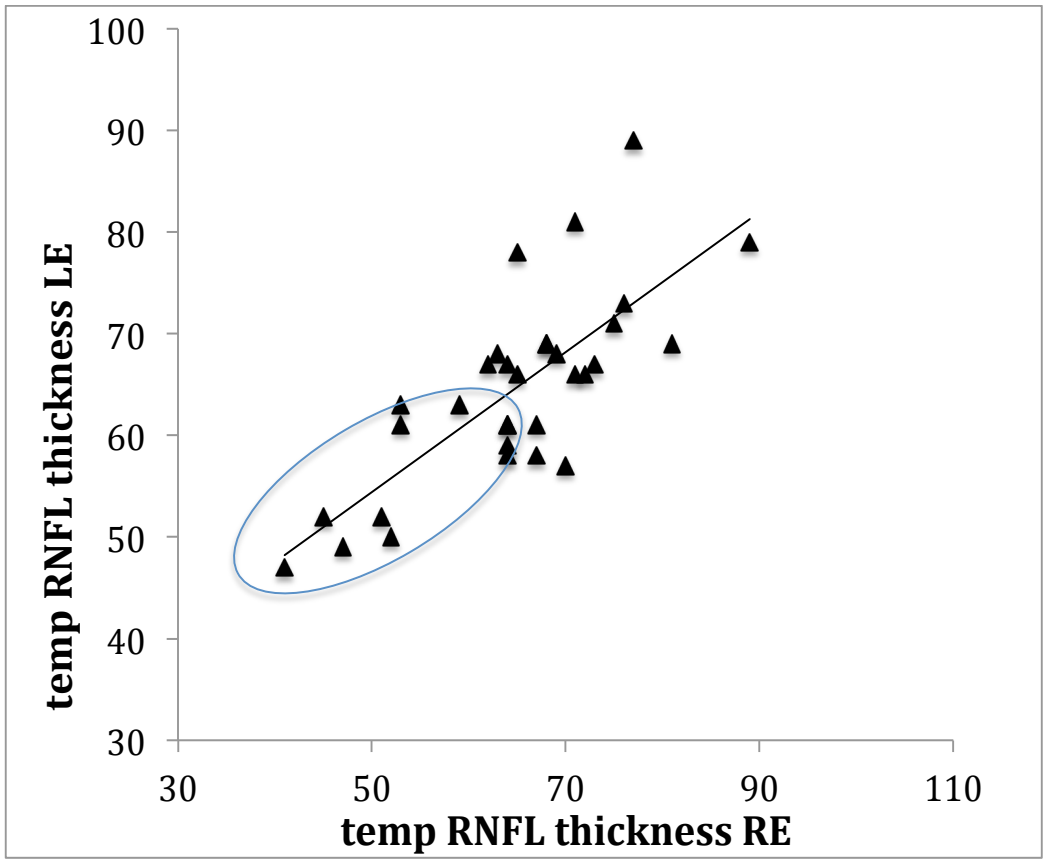

Outer retina and its correlation with GCL and RNFL

1. Structural measures: There was no significant reduction in the thickness in the outer retinal layers (ORL) (p=0.12) and INL (p=0.59). There was also no correlation of INL or ORL with total RNFL thickness, temp RNFL thickness or GCL thickness (Table 7)

Table 7: Correlation of RNFL and GCL thickness with INL AND ORL

	INL thickness	ORL thickness
Temp RNFL thickness	r^2=-0.04 p=0.6	r^2=-0.06 p=0.06
Total RNFL thickness	r^2=0.01 p=0.47	r^2=-0.003 p=0.7
GCL thickness	r^2=0.03 p=0.2	r^2=0.008 p=0.5

2. Functional measures. Of all ERG parameters, the photopic b- wave latency was significantly delayed compared to the normal controls (p=0.001). No other ERG parameters were affected. The photopic b-wave latency significantly correlated with GCL thickness, total and temporal RNFL thickness (r^2=0.12, p=0.01; r^2=0.11, p=0.025; r^2=0.13, p=0.008 respectively) (Figure18 a-c)

Figure18a: Correlation of temp RNFL thickness with Photopic ERG b-wave latency.

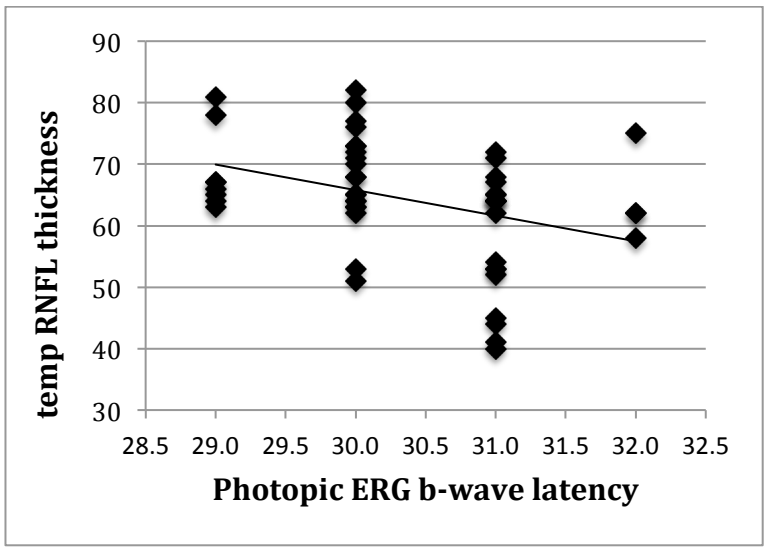

Figure18b: Correlation of total RNFL thickness with Photopic ERG b-wave latency.

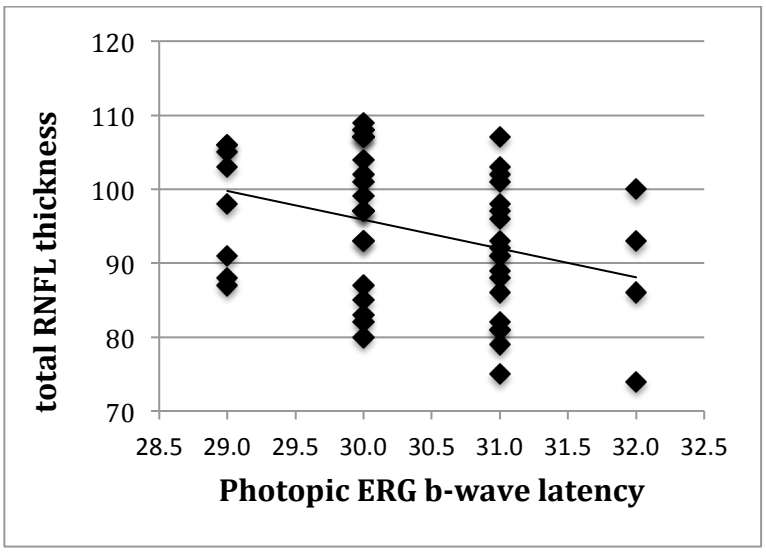

Figure18c: Correlation of GCL thickness with Photpic ERG b-wave latency.

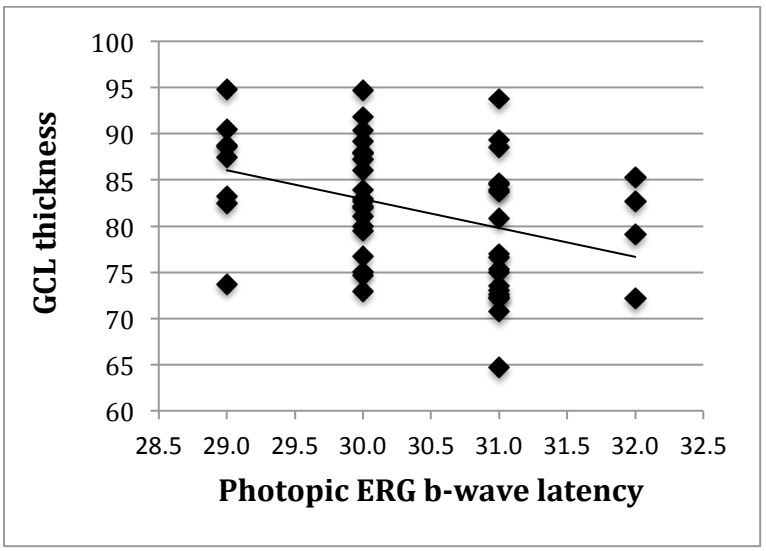

Posterior visual pathway markers and its correlation with GCL and RNFL

There was significant reduction of the mfVEP amplitude and delay in latency in the MS NON eyes as compared to normal controls ($p<0.0001$ for both) (see Table 6). Amplitude of mfVEP

correlated with temp RNFL and GCL thickness (r^2=0.19, p=0.002 and r^2=0.1, p=0.026) and displayed tendency for association with total RNFL (r^2=0.07, p=0.057) (Figure 19 a- c).

Figure 19a: Correlation of temp RNFL thickness with mfVEP amplitude.

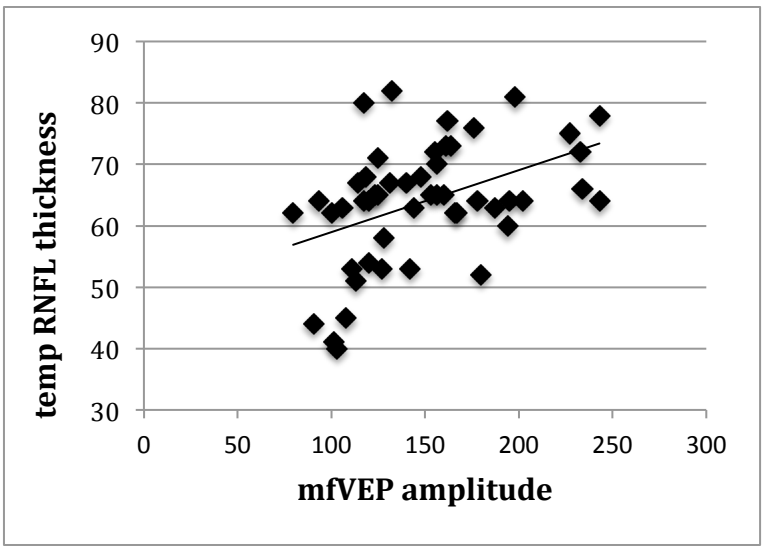

Figure 19b: Correlation of total RNFL thickness with mfVEP amplitude.

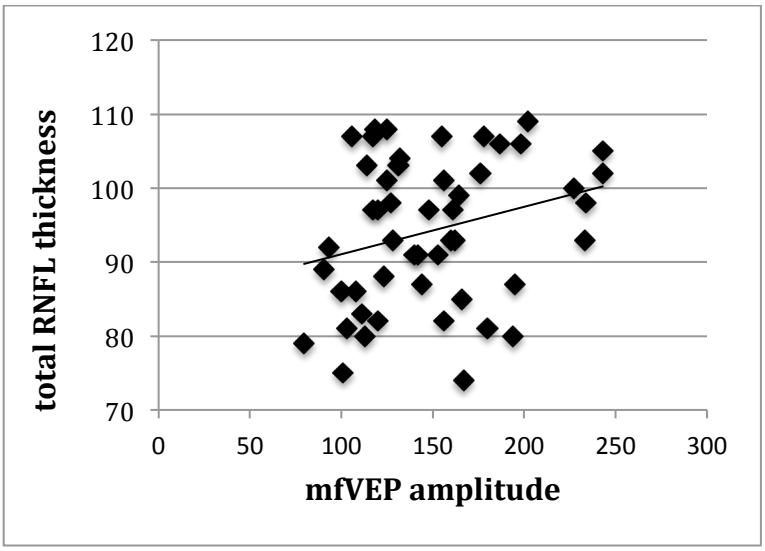

Figure 19c: Correlation of GCL thickness with mfVEP amplitude.

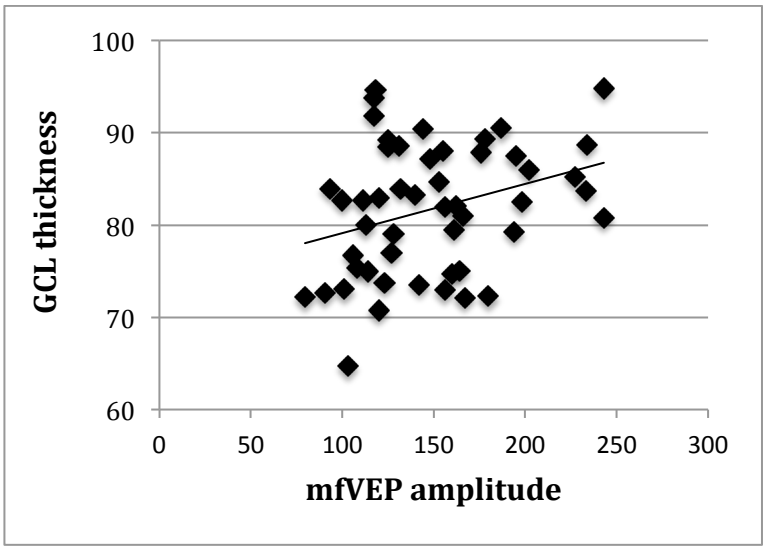

The latency of mfVEP was found to significantly correlate with temporal RNFL, total RNFL and GCL thickness (r^2=0.35, p<0.0001; r^2=0.28, p<0.0001 and r^2=0.23, p<0.0001 respectively) (Figure 20 a-c)

Figure 20a: Correlation of temp RNFL thickness with mfVEP latency.

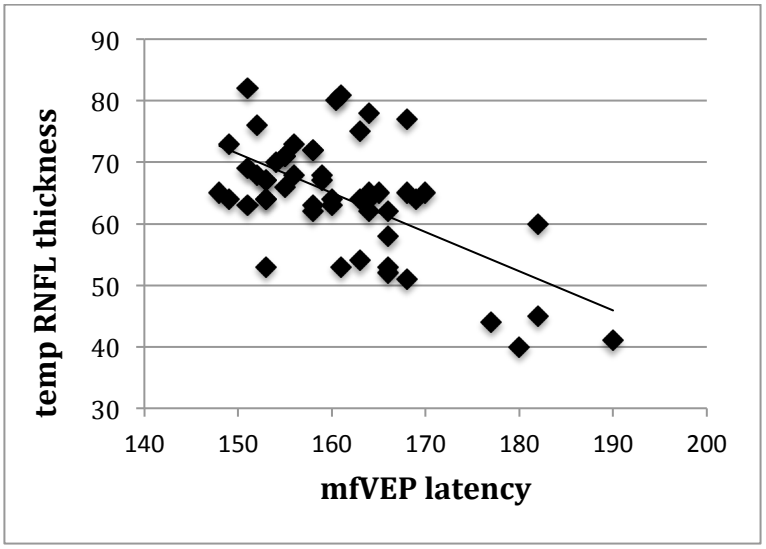

Figure 20b: Correlation of total RNFL thickness with mfVEP latency.

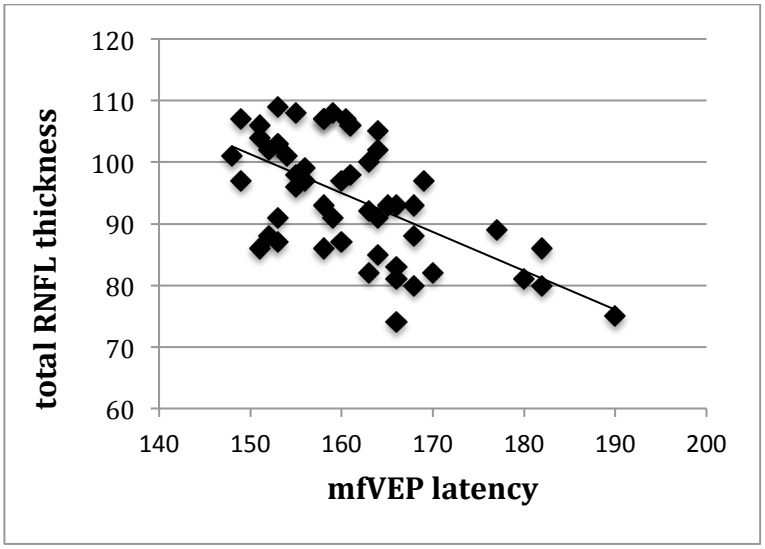

Figure 20c: Correlation of GCL thickness with mfVEP latency

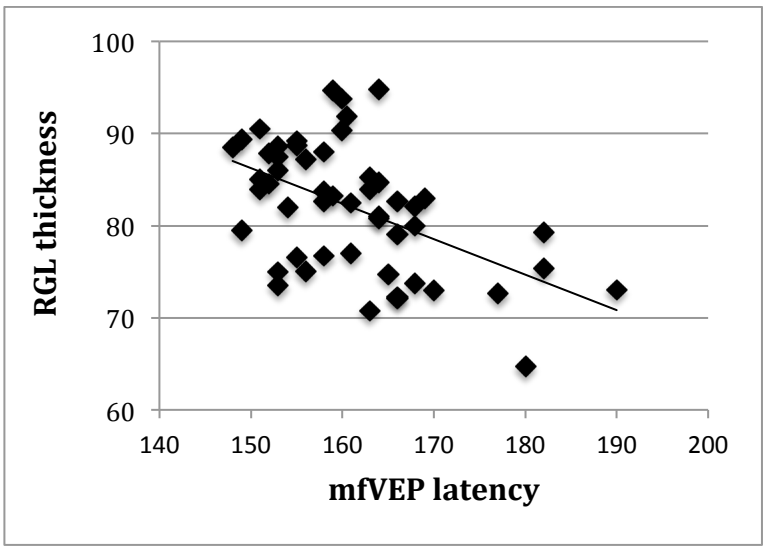

In patients without ON in either eye the mfVEP latency delay, where present, was binocular (Figure 21, oval indicates points above 5% (1.96 SD) of mfVEP latency in normal controls).

Figure 21: Correlation of mfVEP latency between the right and left eyes.

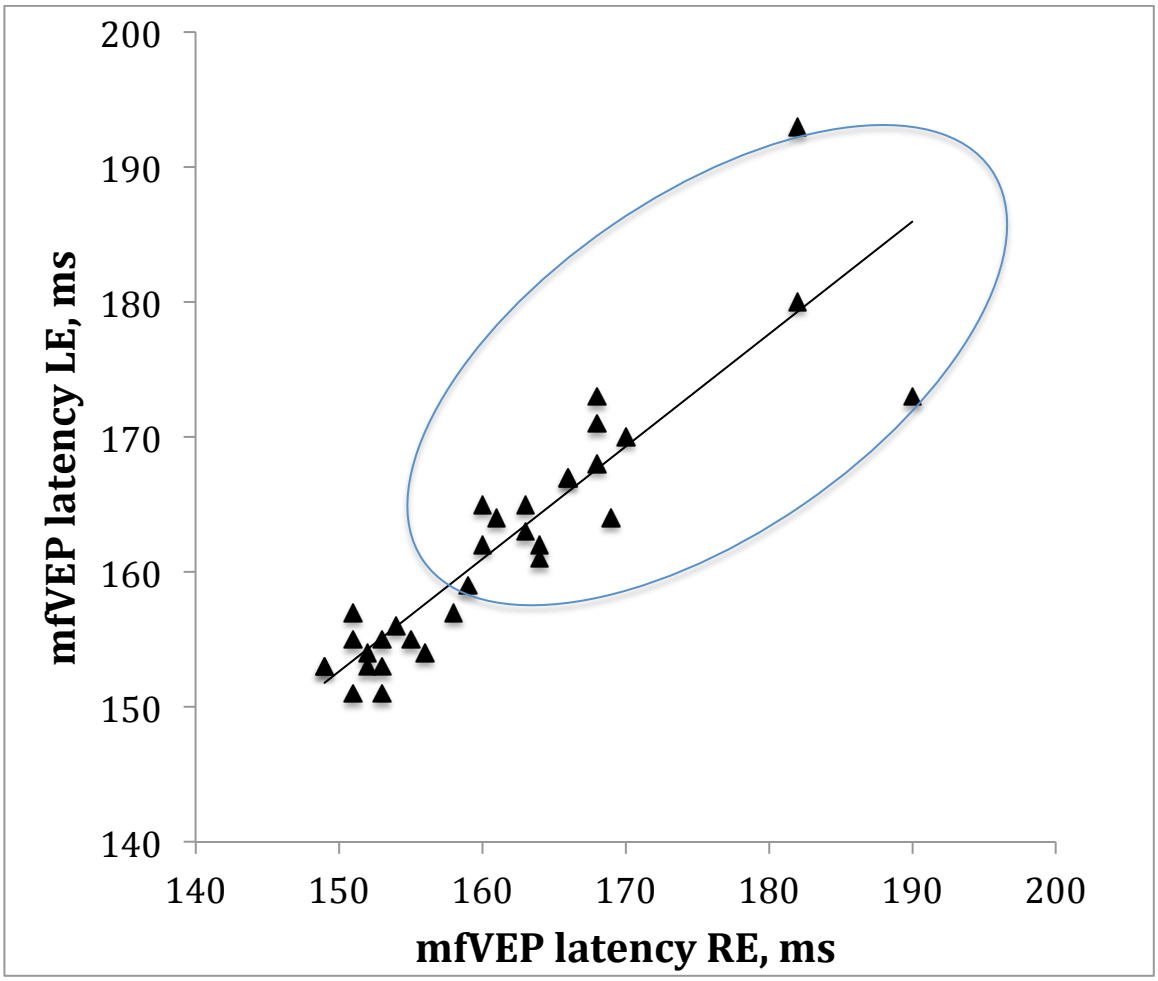

Group analysis

The patients were separated into two groups based on normal/delay latency of mfVEP latency. Latency threshold was set up at mean+1.96 SD (95% probability) of latency in normal controls.

There were 25 patients with normal latency. Since the duration of MS was found to be significantly longer in the group with latency delay (3.4 vs 6.0 years, p=0.001) Univariate General Linear Model (ANCOVA) adjusted for disease duration, age and gender was used to analyse difference between the groups. Bonferroni correction was

used for multiple comparisons. For temporal RNFL significant reduction was detected in the group with delayed latency as compared to normal controls (p=0.03). Temporal RNFL in delayed latency group was also significantly thinner than in patients with non-delay latency (p=0.04).

There was significant difference between delayed and non-delayed groups for total RNFL (p=0.006). Difference between delayed latency group and normal controls, while highly significant by itself (t-test p<0.001), did not survived Bonferonni correction (p=0.2). GCL thickness was also significantly reduced in the delayed latency group compared to the normal controls (p=0.015). Difference between delayed and non-delayed groups, while significant by itself (p=0.01), again did not survive correction for multiple comparisons (p=0.06). There was no significant difference between non-delayed latency group and normal controls for all measures (total RNFL, temp RNFL and GCL)

Linear regression model for GCL axonal and neuronal loss

To assess the contribution of various factors to GCL and RNFL loss, multivariate linear regression models were performed. GCL thickness, total RNFL and temporal RNFL were used as dependent variables in individual models. The latency of mfVEP was used as marker for posterior visual pathway. The photopic b-wave latency on ERG, the thickness of INL and ORL were used as indicators of outer retinal involvement. Also age, gender and disease duration were entered into the model. Backward elimination variable selection procedure in which all variables are entered into the equation and then sequentially removed based on removal criteria was used. We used 0.05 probability of F as entry and 0.1 as removal criteria.

Models explained 46.8% of temp RNFL thickness variability, 35.9% of total RNFL thickness variability and 30.3% of GCL thickness variability. mfVEP latency was a major contributor

in all models. Photopic b-wave latency contributed significantly to temp RNFL and GCL models, while ORL thickness was significant in temp RNFL model only (Table 8). According to Standardized Beta coefficient, mfVEP latency was by far the strongest predictor of axonal RNFL and GCL thinning.

Table 8: Linear regression model for GCL, temporal and total RNFL thickness

Model						
	GCL		Total RNFL		Temporal RNFL	
Variables	Stand. Beta	Sig	Stand. Beta	Sig	Stand. Beta	Sig
mfVEP latency	-0.46	<0.001	-0.61	<0.001	-0.56	<0.001
Photopic b-wave ERG latency	-0.25	0.04			-0.24	0.03
ORL					-0.26	0.02

4.3.2 Optic Neuritis eyes

As expected, there was a severe reduction in mfVEP amplitude and latency delay in ON eyes ($p<0.0001$ for both) (Table 6). There was also a severe loss of total and temporal RNFL and the GCL as compared to both MS-NON eyes and normal controls ($p<0.0001$ for all). However, contrary to MS-NON eyes, the INL showed a significant increase in thickness compared to the controls ($p=0.0008$). It was also negatively correlated with total and temporal RNFL ($r^2=0.26$, $p=0.007$; $r^2=0.38$, $p=0.001$ respectively) (Figure 22 a, b) and with GCL thickness ($r^2=0.26$, $p=0.006$) (Figure 22c).

Figure 22a: Correlation of total RNFL thickness with INL thickness.

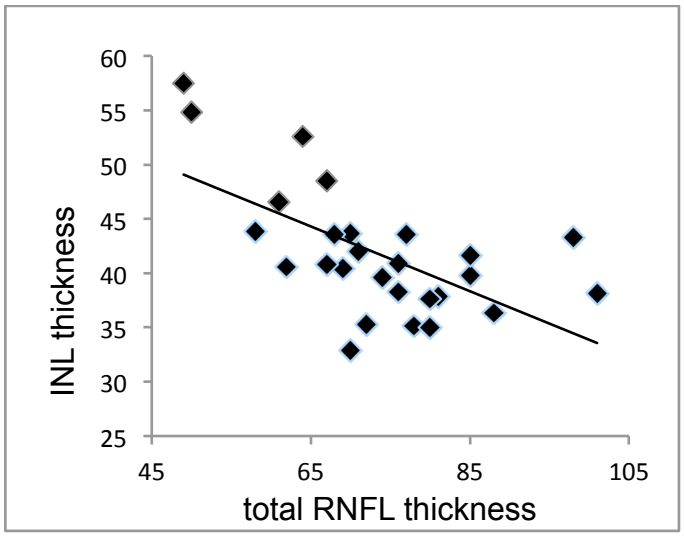

Figure 22b: Correlation of temp RNFL thickness with INL thickness.

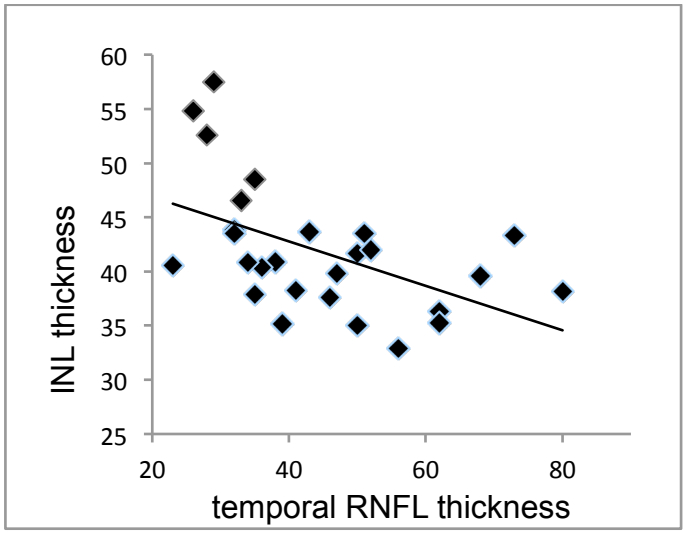

Figure 22c: Correlation of GCL thickness with INL thickness.

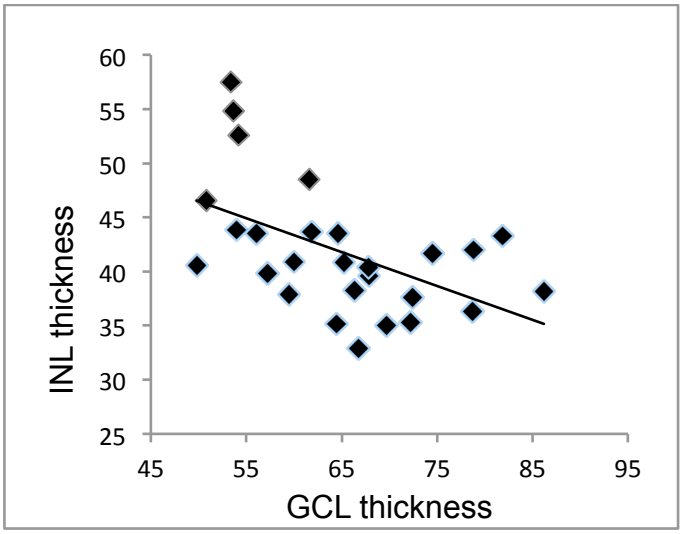

Thickness of ORL was not significantly different from normal controls (p=0.65) and did not correlate with GCL thickness (r^2=0.04, p=0.34) and also temporal and total RNFL (r^2=0.02, p=0.48; r^2 <0.001, p=0.97 respectively).

The photopic b-wave latency was also significantly delayed in the ON eyes of MS patients (p=0.036). Degree of delay was similar to MS-NON eyes.

4.4 DISCUSSION

Our result confirms previous reports of GCL and RNFL thinning in NON eyes of MS patients. By far the largest loss was detected in temporal RNFL, which again is consistent with earlier studies.[118, 119 176, 456, 457] Preferential loss of temporal RNFL may be related to the fact that it supplies the central retina including the macula and is represented by small diameter fibres, which may be more susceptible to damage in MS.[458, 459] In patients without ON in either eye RGC axonal and neuronal loss, where present, was binocular, which suggest a retro-chiasmal origin.

The goal of this study was to determine any relationship of this loss with neighbouring elements of the visual pathway. We used structural (OCT) and functional (ERG) measures of outer-retina and assessed posterior visual pathway using mfVEP latency as the marker. The major finding of the study is a strong association found between mfVEP parameters (latency delay and, to a lesser extent, amplitude reduction) and thinning of RGC layer and RNFL. Group analysis confirms this funding demonstrating significant loss of RGC and their axons only in patients with evidence of previous inflammatory demyelination within the visual pathway. Since, similar to neuronal and axonal loss of GCL, latency delay is binocular (where present) and, therefore, is likely to be a result of retro-chiasmal demyelination, this association suggests possible causal relationship between acute MS-related retro-chiasmal inflammation (lesions) and RGC axonal and neuronal loss.

Due to the fact that optic tract lesions are very rare in MS, optic radiation is the most likely site of such lesions. The transmission of damage from LGN neurons (which form optic radiation) to RGC axons, however, requires trans-neuronal degeneration. The phenomenon of trans-neuronal degeneration in the optic pathway was described by Matthew and colleagues as early as 1960.[460] It can be retrograde i.e. from posterior visual pathway to anterior visual pathway (for instance, from optic radiation to retina) or anterograde, i.e. from anterior visual pathway to posterior visual pathway (for instance, from retina to visual cortex).

The compelling evidence of retrograde trans-neuronal degeneration has emerged from animal and human studies recently.[461, 462] Mehta and Plant[463] reported topographically accurate reduction of RNFL thickness in patients with long-standing occipital lesions, while Cowey et al demonstrated transneuronal RGC degeneration following cortical

lesions in both primate species and humans using MRI.[464] Jindahra et al recently demonstrated trans-synaptic

retrograde degeneration in the visual system not only in congenital homonymous hemianopia, but also in acquired lesions of occipital cortex[465] and Bridge et al showed that RNFL thinning presents after post-striate lesions.[466]

Anterograde trans-neuronal dystrophy in human was suggested by Ciccarelli[467] in a study of optic radiation changes following optic neuritis. There is also some evidence that trans-neuronal degeneration may cause axonal loss in MS. Trans-neuronal changes were found by Evangelou[458] in post-mortem studies of the anterior visual pathway of MS patients. Moreover, there is a recent report demonstrating moderate, but significant correlation of MRI indexes along the optic radiation with RNFL thickness in MS patients[110] also advocating trans- neuronal degeneration as a possible mechanism of axonal loss. Last year evidence was presented for trans-neuronal degeneration in the visual system of MS patients using Diffusion Tensor Imaging (G. Inigo, ECTRIMS, 2012).

It is, therefore, tempting to speculate that mechanism of trans-neuronal degeneration may indeed play some role in axonal and neuronal loss in MS. However, since this study is cross- sectional, question of causality cannot be answered with certainty. Longitudinal studies are required to address the issue by analysing the relationship between GCL loss and posterior visual pathway damage in chronological order.

Second major finding is related to outer-retina. We found significant delay of photopic ERG b-wave, which indicates functional impairment of cone bipolar cells in NON eyes of MS patients. Association of bipolar cells damage and axonal and neuronal loss of RGC is supported by the significant correlation found between ERG delay and structural markers of GCL integrity (total and temporal RNFL thickness and RGL thickness). However, structurally INL (where bipolar cells are located) seems to be unaffected, as the thickness of INL was found to be comparable to normal controls.

This structure/function paradox may be better understood by examining ON eyes. A recently published report by Saidha et al[137] demonstrated a significant increase of INL thickness in eyes of RRMS patients, a considerable proportion of whom previously had ON. Our study confirmed this finding. In addition, we demonstrated that thickening of INL correlates with loss of temp RNFL. In other words, the greater the loss of RNFL following ON, the wider the INL. A similar mechanism, but on a lesser scale, may operate in NON eyes. Therefore, whatever the underlying mechanism of INL widening is (and there have been suggestions of its autoimmune, inflammatory or mechanical origin, which may even be not MS-specific[137, 468-471]), it may mask any potential thinning of the layer caused by loss of its neuronal elements. Another possible reason for this could be the multiplication of the Muller cell bodies in the INL, which could multiple under stressful conditions. The possibility that functional changes of bipolar cells (reflected by ERG

change) precede structural damage also cannot be excluded.

Regardless of the structural data, however, the ERG result demonstrated dysfunction of bipolar cells in MS patients,[136] which is linked to the loss GCL axons. A retrograde degeneration spreading from GCL to bipolar cells is unlikely since ERG changes in ON eyes (which have considerably larger RNFL loss) was of similar magnitude to that found in NON eyes. This is also in line with studies of experimental optic nerve axotomy, which failed to show damage of outer-retina.[472, 473] However, whether primary damage of bipolar cells initiates anterograde degeneration of GCL, or a primary retinal process affects both neuronal layers simultaneously, remains an open question.

Taken together, the result of our study suggests a dual nature of GCL axonal and neuronal damage in NON eyes of MS patients. While mfVEP delay suggests lesions in the posterior visual pathway as a major factor, significant association of RNFL and GCL thickness with photopic ERG latency delay also implicates primary retinal pathology. The Multiple linear regression models supported a dual nature of GCL axonal and neuronal loss by demonstrating a significant contribution of both retinal dysfunction and posterior visual pathway damage to 2 out of 3 models. The combined effect of all included variables explained 46.8% of temp RNFL thickness variability, 35.9% of total RNFL thickness variability and 30.3% of GCL thickness variability. While the contribution of retinal dysfunction was significant in GCL and temp RNFL models, estimated predictive power of

the posterior visual pathway damage was by far the largest.

There is no reason to believe that the mechanisms of axonal damage described in the current study are unique to the visual system. The results, therefore, may (at least to some extent) be extrapolated to the entire CNS, suggesting that in addition to the direct effect of acute inflammation, trans-neuronal degeneration and primary neuronal pathology may also contribute to progressive neurodegeneration in MS.

CHAPTER 5: TRANSSYNAPTIC RETINAL DEGENERATION IN OPTIC NEUROPATHIES: OPTICAL COHERENCE TOMOGRAPHY STUDY

Visual Neurophysiology

This study was performed to determine if there was any loss of INL secondary to the loss of GCL and thereby prove the presence or absence of transsynaptic degeneration in MS. The results of this study have been published in IOVS (**Invest Ophthalmol Vis Sci. 2012 Mar 9;53(3):1271-5).**

5.1 ABSTRACT

Purpose. Recently demonstrated neuronal loss in the inner nuclear layer of the retina in MS and glaucoma raises the question of a primary (possibly immune-mediated) or secondary (transsynaptic) mechanism of retinal damage in these diseases. In the present study we used OCT to investigate retrograde retinal transsynaptic degeneration in patients with long- standing and severe loss of ganglion cells due to optic neuropathy.

Methods. Fifteen eyes of glaucoma patients with visual field defect limited to upper hemifield and 15 eyes of MS patients with previous episode of ON and extensive loss of ganglion cells were imaged using SDOCT and compared with two groups of age- matched controls. Combined retinal GCL/IPL thickness and inner nuclear layer (INL) thickness were analyzed.

Results. In the glaucoma group there was a significant (p=0.0005) reduction of GCL/IPL

thickness in the lower (affected) retina compared with normal controls; however INL thickness was not statistically reduced (p=0.49). In the MS group reduction of GCL/IPL thickness in both hemifields of ON eyes was also significant (p=0.0001 and p<0.0001 for inferior and superior retina respectively). However, similar to the glaucomatous eyes, there was no significant reduction of INL thickness in both hemifields (p=0.25 and p=0.45).

Conclusions. This study demonstrates no significant loss of INL thickness in parts of the retina with long-standing and severe loss of RGCs.

5.2 INTRODUCTION

Transsynaptic degeneration has recently attracted considerable interest as one of the possible mechanisms of neuro- degeneration in MS and glaucoma.[476, 477] The visual system represents an ideal model to study transsynaptic degeneration because it comprises relatively independent pathways of hierarchically linked neurons and can be studied not only morphologically, but in vivo. The process of transsynaptic degeneration has been documented in the visual system from the GCL extending proximally[472-475] but this still remains unproven within the retina. Neuronal loss in layers of the retina outside of the GCL has been demonstrated pathologically and electrophysiologically in human glaucoma and multiple sclerosis[476-478,] and raises the question of whether the mechanism for this cell loss is a primary degeneration (possibly immune-mediated) or secondary on the basis of transsynaptic degeneration.[479]

An experimental way to study retinal transneuronal degeneration is using optic nerve axotomy. While few animal studies failed to find pathologic changes distal to GCL after optic nerve axotomy[471, 480] a reduction of the inner nuclear layer after long survival times has been demonstrated by Hollander et al.[470]

Optic neuropathies such as glaucoma and ON damage axons of RGCs that cause retrograde axonal degeneration and finally results in neuronal death. One should not, however, expect to find changes in inner nuclear layer compared with healthy individuals unless it caused by retinal transsynaptic degeneration.

The OCT permits segmentation and measurement of retinal layers in vivo by using selective reflectivity of backscattered near-infrared light by different retinal layers.[134, 481] The spectral- domain OCT technique demonstrates axial resolution in the range of few microns and allows clear visualization of individual retinal layers,[136, 482, 483] allowing evaluation of retinal transsynaptic degeneration in vivo.

The aim of the present study, therefore, was to employ such high-resolution spectral-domain OCT imaging to identify evidence of possible inner nuclear layer (INL) degeneration in post optic neuritis MS and primary open angle glaucoma (POAG) patients with long-standing severe loss of retinal GCL.

5.1 MATERIALS AND METHODS

Two groups of patients were enrolled in the study. The first group comprised of 15 POAG patients with dense visual field defects (Humphrey 10-2 program) limited to superior hemifield. All patients had at least 20 points in the superior hemifield with $p < 0.005$ and not >2 non-rim points with $p< 0.02$ in the inferior hemifield on pattern deviation plot. The diagnosis of glaucoma was based on the finding of a typical excavation of the optic disc with neural rim loss corresponding with visual field loss in that hemifield. The visual fields were reproducible (same defect >3 fields) and reliable (fixation losses, false negatives, and false positives all < 30%). Raised IOP was not a criterion for diagnosis.

The second group was comprised of 15 patients who had Clinically Definite Multiple Sclerosis (CDMS) and a unilateral episode of ON at least 3 years before the study. Average time since onset of ON was 3.7 ± 0.8 years (range 3 to 6 years). The diagnosis of CDMS was based on the criteria of McDonald et al.[484] ON was diagnosed by a neuro-ophthalmologist based on clinical findings. Exclusion criteria were an atypical presentation, recurrent ON, and a history of other ocular or neurologic disease.

Thirty-two age- and sex-matched controls were examined with the OCT, 17 for the MS group and 15 for the POAG group. The eligibility criteria for control subjects included 6/6 vision in both eyes and normal ophthalmic examination. All normal subjects

underwent complete ophthalmic examination and were found normal on the slit lamp biomicroscope, and dilated fundus examination. They also had normal visual fields on the Humphrey 24-2 SITA (Swedish interactive thresholding algorithm) standard program. One eye of each normal subject was selected randomly.

The study was approved by the Institutional review board. Procedures followed the tenets of the Declaration of Helsinki and informed consent was obtained from all participants.

OCT Recording and Analysis

The OCT was performed using Spectralis HRA+OCT (Heidelberg Engineering, Heidelberg, Germany). A radial protocol using a star-like pattern of line scans centered on the macula with resolution of 1536 pixels was used (Figure 16). The criteria for a good quality scan included signal strength greater than 25, good centration of the scan, and uniform brightness. Scans that satisfied these criteria were taken for analysis. Analysis was performed on vertical scan only. One hundred scans were averaged for each line scan. Thirty degrees of visual angle (15° of eccentricity) were scanned, but only the central 14° (7° of eccentricity) were used for analysis, because the definition of layers becomes much less distinct beyond that. Retinal layers were segmented automatically using a custom designed algorithm, which applied vessel detection and removal, multiple size median filtering, and Canny edge detection to identify borders of retinal layers.

The GCL and IPL were combined together because the border between them was indistinguishable in several subjects, while the inner nuclear layer (INL) was analyzed on its own (see example in Figure 23). The thickness of each layer was measured at seven points for each hemifield, which were equally distributed between 1.75° and 7° of eccentricity.

Statistics

Statistical analysis was performed using statistical software (SPSS 11.0 for Windows; SPSS, Chicago, IL). Mean values of GCL/IPL and INL thickness were compared between an aged- matched control, affected and nonaffected hemifields of glaucomatous eye, or affected and fellow eyes (hemifield-based) of MS patients using Student's t-test. Significance was assessed at the $p < 0.05$ level.

5.4 RESULTS

All subjects achieved good quality scans (dB > 20). The demographic data for each group are presented in Table 9.

Table 9: Demographic Data for Each Group

	Age (y)	Male/Female Ratio	Visual Acuity ≥6/9 (*n*)
Glaucoma group (*n* = 15)	64.1 ± 9.8	7/8	15
Glaucoma control group (*n* = 15)	63.8 ± 10.3	6/9	15
MS group (*n* = 15)	37.1 ± 8.5	6/9	9
MS control group (*n*= 17)	36.4 ± 9.6	7/10	17

5.4.1 Glaucoma Group

Averaged Humphrey mean deviation (MD) of affected (superior) hemifield was -23.7 ± 4.9 dB and of nonaffected (lower) hemifield -1.75 dB ($p < 0.0001$). There was a significant (29.0%, $p = 0.00037$, paired t-test) reduction of GCL/IPL thickness in the lower retina compared with normal controls (Table 10). Reduction was significant at all eccentricities studied for the affected hemifield ($p < 0.02$ for all points) (Figure 24A). Figure 23 represents an example of Humphrey visual field and OCT scan of an affected eye of one of the glaucoma patients.

Figure 23: A typical example of Humphrey visual field (upper row) and retinal thickness profile (lower row) of a glaucoma patient. Note absence of RNFL and significant thinning of GCL/IPL in the upper retina (left side).

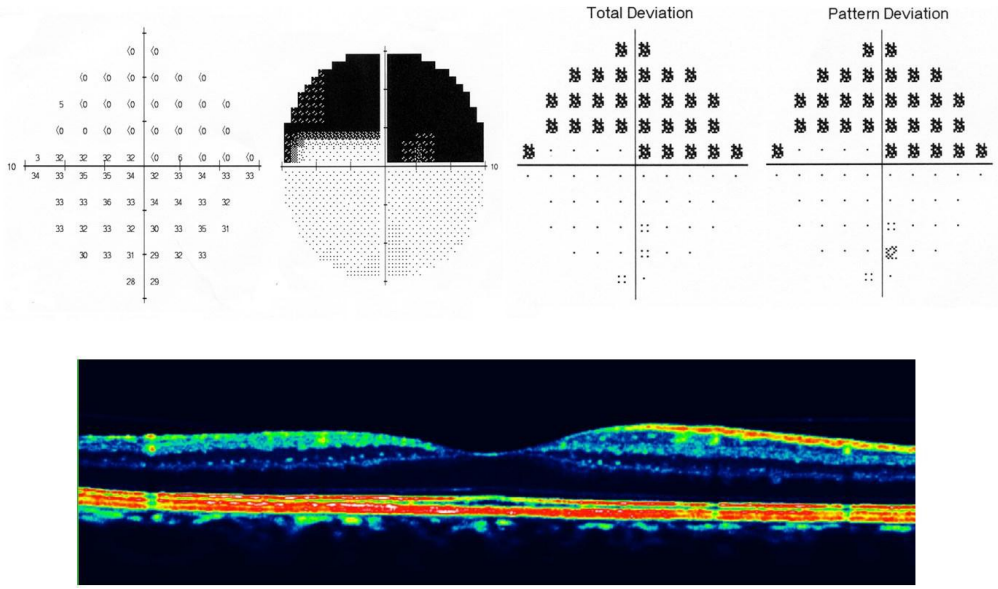

While the thickness of GCL/IPL in the upper retina was also significantly reduced ($p = 0.005$), reduction was of considerably smaller magnitude (11.7%) and was non significant for the first, second, third, and seventh points (Table 10).

Contrary to GCL/IPL, the thickness of INL in the affected hemifield (lower retina) of the glaucomatous eye was not significantly different from controls ($p = 0.32$) (Table 10).

There was no difference for any of the points tested ($p > 0.2$, for all points) (Figure 24 B). INL thickness in the non affected hemifield (upper retina) was similarly not reduced for both averaged ($p = 0.94$), as well as the individual points ($p = 0.1$ for all points) (Table 10).

Figure 24: Averaged thickness of GCL/IPL (A) and INL (B) in affected (left) and non affected (right) hemifield of glaucoma patients (black columns) and corresponding hemifield of age-matched controls (gray columns).

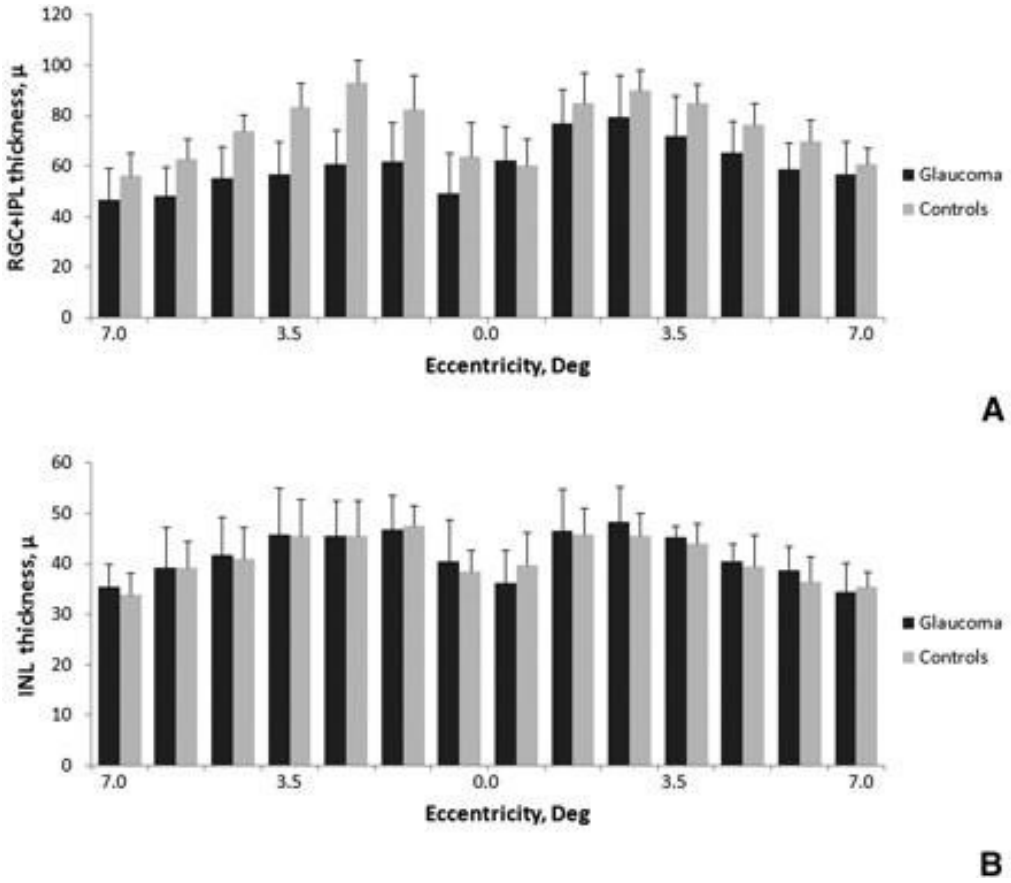

5.4.2 Multiple Sclerosis Group

Because ON predominantly affects central fibres of the optic nerve without upper or lower field preponderance, both hemifields of the affected eye were considered

abnormal.[485] There was a significant reduction of GCL/IPL thickness in both hemifields of ON eye (28.5% and 30.5% reduction, $p = 0.0001$ and $p < 0.0001$ for inferior and superior retina, respectively) (Table 10).

Table 10. Hemifield GCL/IPL and INL Thickness in Glaucoma and ON Patients and Normal Controls

	GCL/IPL Thickness (μ)	INL Thickness (μ)
Glaucoma Group		
Glaucomatous eye		
Affected (upper) hemifield	52.4 ± 12.0*	41.9 ± 7.3
Fellow (lower) hemifield	66.6 ± 14.9*	41.5 ± 5.3
Age-matched normal controls		
Upper hemifield	73.7 ± 13.4	42.1 ± 5.1
Lower hemifield	75.4 ± 12.1	41.3 ± 4.1
MS Group		
ON eye		
Upper hemifield	57.4 ± 7.6*	43.8 ± 4.5
Lower hemifield	60.0 ± 7.2*	43.2 ± 4.1
Fellow eye		
Upper hemifield	71.4 ± 11.2*	44.0 ± 5.2
Lower hemifield	73.8 ± 11.5*	42.4 ± 4.7

Age-matched normal controls		
Upper hemifield	80.2 ± 13.5	42.4 ± 5.2
Lower hemifield	83.4 ± 11.4	43.0 ± 4.1

* Statistically significant difference between patients and normal controls

Reduction was significant at all eccentricities for both affected hemifields ($p < 0.02$ for all points) (Figure 25A)

Non-ON eyes also demonstrated a significant reduction of GCL/IPL thickness in both hemifields, albeit on a lesser scale (9.7% and 10.6% reduction, $p = 0.0003$ and $p < 0.0001$ for inferior and superior retinas respectively).

The thickness of INL, however, did not differ significantly from the normal controls in both hemifields of ON eyes ($p = 0.1$ and $p = 0.12$ for inferior and superior retina respectively) (Figure 25B). Non-ON eyes also had normal INL thickness ($p = 0.1$ and $p = 0.12$ for inferior and superior retina respectively).

Figure 25.Averaged thickness of GCL/IPL (A) and INL (B) in inferior (left) and superior (right) hemifield of MS patients (black columns) and corresponding hemifield of age-matched controls (gray columns).

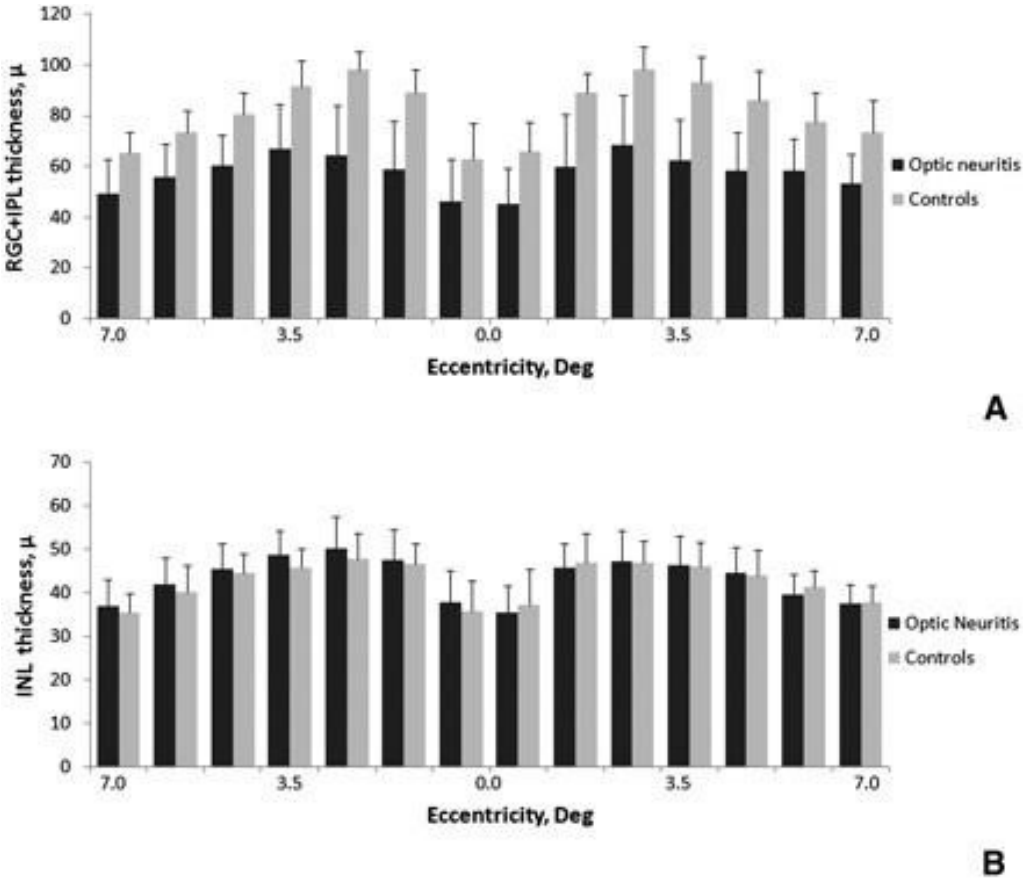

5.5 DISCUSSION

The presence of transsynaptic degeneration in the visual system is well documented.[472-475, 486- 489] There is strong evidence of anterograde and retrograde degeneration between RGCs and target neurons in higher visual areas. Anterograde degeneration of LGN cells, optic radiation, and cortical neurons after loss of RGC was demonstrated in human and

experimental glaucoma[472-475] and in multiple sclerosis.[486, 487] Similarly, retrograde transsynaptic changes in RGC after cortical lesions were found in animals and human studies.[488, 489]Expansion of transsynaptic changes into the retina, however, remains controversial. Recently a deficit of bipolar cells in the retina of MS patients (identified pathophysiologically) has been suggested as possible evidence of transsynaptic retinal degeneration.[476] However, a similar abnormality in outer nuclear layer reported in the same study makes this explanation less likely.[479]

An OCT study of the retina in MS patients recently published by Saidha et al[136] demonstrated that reduction of RNFL and GCL/IPL thickness after an episode of ON was not accompanied by INL thinning. However, the follow-up period was probably not long enough to verify the existence of transsynaptic degeneration because patients as early as 3 months after acute ON may have been included. This study, on the other hand, demonstrated that there is a subgroup of MS patients (approximately 10%) in whom the thickness of all retinal layers is reduced with RGC layer producing largest degree of reduction (16%) compared with INL (6.6%) and ONL (6.7%). Whether this is a result of transsynaptic (anterograde or retrograde) retinal degeneration or a con- sequence of primary retinal pathology in MS or simply an artificially selected group representing the

low end of the spectrum of the retinal thickness[490] is not clear.

Similar results were demonstrated by Wang et al[491] in glaucoma patients. Authors

concluded that RNFL and GCL/IPL thickness is reduced while INL thickness remains unchanged. However, spectrum of the visual field loss in the study patients varied widely and the topographic relationship between visual field sensitivity and GCL/IPL loss was examined only in one patient.

Therefore, in the present study we used clear-cut cases of optic neuropathies with substantial and long-standing RGL loss. We specifically selected glaucoma patients with severe perimetrical field loss confined to one (upper) hemifield, which indicates extensive, but relatively localized loss of RGC. While normal result of standard perimetry in lower hemifield does not preclude loss of ganglion cells (and, in fact, we did find moderate reduction of GCL/IPL thickness in perimetrically normal upper retina), it is not likely to exceed 20%.[492]

Similarly, in the MS group we selected subjects with severe unilateral post-ON loss of RGC (of similar magnitude to glaucomatous eyes), which was a result of inflammatory transection of optic nerve fibres and subsequent retrograde degeneration. While there was significant reduction of GCL in fellow eyes, the degree of thinning was modest compared with the ON eye. The thinning of RNFL in fellow eyes is most likely a result of subclinical inflammation in a visual pathway of the fellow eye, which is not uncommon in MS.[493, 494]

In our subjects the loss of RGC was relatively long-standing because glaucoma is a slowly- progressing disease, while all MS patients had an episode of ON at least 3 years

before the study. Despite the severity of RGC loss and its duration we did not find evidence of INL thinning in either of the groups. While the most likely explanation of the result observed is an absence of transsynaptic degeneration in studied conditions, other possibilities must be considered. The INL includes not only nuclei of bipolar cells, but also horizontal cells, amacrine cells, interplexiform cells, and supportive Muller cells. Even though the percentage of bipolar cells in INL is by far the largest,[495, 496] the presence of other cell types may obscure detection of bipolar cell decline. Transsynaptic degeneration can be an extremely slow process, which may take many years to manifest. For example, the duration of disease in a postmortem study, which demonstrated INL abnormalities in MS patients was > 20 years.[476] A recent study, however, suggested that retrograde transsynaptic degeneration in human optic tract is functionally apparent as early as 18 months after cortical damage.[497] Additionally, a long delay of structurally visible changes compared with more subtle functional alteration is another possibility. In fact, functional impediment of INL has been reported in both conditions.[478, 498-500] Finally, changes in cellular composition of the overlying retinal layers (extensive loss of RNFL and ganglion cells) can potentially alter light reflectivity of INL structures and therefore influence the measurement of INL thickness. Our study is also limited by relatively small sample size and cross-sectional study design.

In summary, our study demonstrated no significant loss of INL thickness in parts of the

retina with long-standing and severe loss of RGC in patients with optic neuropathies.

CHAPTER 6: CONCLUSIONS

Visual field assessment and several other tests are being used in the clinical diagnosis of optic neuropathies, which is accompanied by damage of ganglion cell bodies and their axons. The mfVEP, in the past, has proven to provide both perimetric and electrophysiological assessment of the visual system and hence has expanded its role from glaucoma to the field of neuro-opthalmology.

In the discussion of results in Chapter 2, the sensitivities of several regularly performed glaucoma diagnostic tests were compared among patients with preperimetric glaucoma and early glaucoma. Current methods of glaucoma diagnosis use standard automated perimetry and disc evaluation as gold standard. SAP depends on subjective responses to detect visual field defects due to ganglion cell loss. Many patients perform poorly on subjective tests and there is also a learning curve associated with it, which makes interpretation complicated in patients with early glaucoma. Objective perimetry using mfVEP is a relatively new psychophysical test. Since it provides a topographical measure of damage, its results can be compared with SAP.

Also, there has been no learning curve reported for mfVEP. We have established in our study that mfVEP detects field defects even in patients with preperimetric glaucoma, which is indicative of ganglion cell damage. Two different stimulus presentations were

used in the study. The difference in sensitivities could probably be due to testing two different pathways. Although almost similar in sensivities, the performance of LLA was slightly better than the BonY. This variability could be due to different pathways being stimulated with different sensitivity to glaucoma damage.

HRT was found to be the single best test in identifying preperimetric glaucoma. However, since all our patients included in the study were selected based on the appearance of a glaucomatous disc, this could have biased the results. When combining two tests to give better results the HRT-LLA mfVEP combination identified losses corresponding to disc changes in majority of patients with preperimetric glaucoma. This combination could be regularly performed in the clinic as it is easy to perform and also does not take much more of the patient's time.

Future work on this study would involve a longitudinal follow up of these patients to see if they progress to have further optic nerve damage and ganglion cell loss. This would help identify which of the diagnostic tests would help detect the defects earlier than the other. These tests can then be performed regularly in the clinic to monitor patients with a high risk of progression. This would help prevent damage to the optic nerve at an early stage.

In Chapter 3, two different stimulus presentations were compared to analyse which had better reproducibility of latency. The pattern reversal stimulus presentation produced less

variability in latency. This stimulus was then used in the following study on patients with MS where latency was used as a marker of demyelination in the visual pathway.

In Chapter 4, ganglion cell loss in MS was studied. The results from this study confirmed the loss of GCL and their axons even in MS patients without previous history of multiple sclerosis. The goal of this study was also to see if there was any relation of this loss with other parts of the visual pathway. The mfVEP latency was found to significantly correlate with the thinning of the GCL and RNFL, indicating a strong association between loss of ganglion cells and visual pathway demyelination. However, since the latency delay was binocular, the demyelination is presumed to be retrochiasmal. This correlation indicated the presence of a trans neuronal degeneration, which could be retrograde (from optic radiation to retina) or anterograde (from retina to visual cortex). The study also found significant delay in photopic ERG b-wave in the NON eyes of ON patients indicative of functional impairment of the cone bipolar cells located in the INL of the retina. However structurally this layer seemed to be unaffected in the NON eyes, although the ON eyes showed a significant thickening of the INL.

The presence of a retrograde degeneration from the GCL to bipolar cells was also studied in patients with ON and glaucoma and discussed in Chapter 5. This study proved the absence of retrograde degeneration since the ERG changes were of similar magnitude in

both ON and NON eyes of MS patients. This suggests a dual nature of GCL and their axons in NON eyes of MS patients. Though lesions in the posterior visual pathway was a major factor, primary retinal pathology also played a role in ganglion cell loss.

Future work in this study would involve a longitudinal follow up of these patients with mfVEP and OCT with additional MRI to document the effect of new lesions and acute ON on ganglion cell loss. The could shed some light into the effect of lesions in optic radiations on the GCL and their axons to prove the occurrence of retrograde trans synaptic degeneration.

REFERENCES

1. Bach, L., Seefelder, R. Atlas zur Entwicklungsgeschichte des menschlichen Auges. Verlag von Wilhelm Engelmann, Leipzig. 1914
2. Dejean, C.H., Hervouët, F.R., Leplat, G. L'embryologie de l'oeil et sa tératologie. Société Française d'Ophtalmologie. Paris: Masson. Libraire de l'Académie de Médicine, pp. 1–728. 1958
3. Mann, I. The Development of the Human Eye, 3rd edn. British Medical Association, Tavistock Square, London. 1964
4. Duke-Elder, S., Cook, C. Normal and abnormal develop- ment. Part 1. Embryology. In: Duke-Elder, S. (ed.) System of Ophthalmology, vol 3, pp. 190–201. Henry Kimpton, London. 1963
5. Cook, C., Sulik, K.K., Wright, K.W. Embryology. In: Wright, K.W., Spiegel, P.H. (eds.) Pediatric Ophthalmology and Strabismus, 2nd edn, pp. 3–38. Springer, Berlin. 2003
6. Sharma, R.K., Ehinger, B.E.J. Development and structure of the retina. In: Kaufman, P.L., Alm, A. (eds.) Adler's Physiology of the Eye, 10th edn, pp. 319–347. Mosby, St Louis. 2003
7. Seefelder R: Die Entwicklungdes menschlichen Auges. In: Schieck, F., Bruckner, A. (eds) Kurzes Hanbuch der Ophthalmologie. Pp.476-518. Springer, Berlin (1930)
8. Burke, J.M. Determinants of retinal pigment epithelial cell phenotype and polarity.

In: Marmor, M.F., Wolfensberger, T.J. (eds.) The Retinal Pigment Epithelium, pp. 86–102. Oxford University, Oxford. 1998

9. Panda-Jonas, S., Jonas, J.B., Jakobczk-Zmija, M. Retinal pigment epithelial cell count, distribution and correlations in normal human eyes. American Journal of Ophthalmology. 1996; 121: 181–189
10. Boulton, M., Dayhaw-Barker, P. The role of the retinal epithelium: topographical variation and ageing changes. Eye. 2001 ; 15: 384–389
11. La Cour, M. The retinal pigment epithelium. In: Kaufman, P.L., Alm, A. (eds.) Adler's Physiology of the Eye, 10th edn, pp. 348–357. Mosby, St Louis. 2003
12. Schnaudigel, O. Die Vitalfärbung mit Trypanblau am Auge. Albrecht von Graefes Archives of Ophthalmology. 1913; 86: 93–97
13. Cunha-Vaz, J.G. The blood-ocular barriers. Survey of Ophthalmology. 1979; 23: 279–296
14. Cunha-Vaz, J.G. The blood-retinal barriers system. Basic concepts and clinical evaluation. Review. Experimental Eye Research. 2004; 78: 715–721
15. Davson, H. The aqueous humour and the intraocular pressure (chapter 1). In: Davson, H. (ed.) Physiology of the Eye, 5th edn, pp. 3–95. MacMillan, London. 1990
16. Thumann, G., Hoffmann, S., Hinton, D.R. Cell biology of the retinal pigment epithelium. In: Ryan, S.J. (ed). Retina, 4th (ed), pp. 137–152. Elsevier-Mosby, St.

Louis. 2006

17. Strauss, O. The retinal pigment epithelium in visual function. Physiology Review. 2005; 85: 845–881
18. Kanski, J.J., Milewski, S.A. Introduction. In: Kanski, J.J., Milewski, S.A. (eds.) Diseases of the Macula, pp. 1–18. Mosby, St Louis. 2002
19. Levin, L.A. Optic Nerve. In: Kaufman,P.L., Alm, A. (eds). Adler's physiology of the eye, 10th edn. Pp.603-638. Morsby, ST Louis. 2003
20. Hughes, B.A., Gallemore, R.P., Miller, S.S. Transport mechanisms in the retinal pigment epithelium. In: Marmor, M.F., Wolfensberger, T.J. (eds.) The Retinal Pigment Epithelium, pp. 103–134. Oxford University, Oxford. 1998
21. Wurtz, R.H., Kandel, E.R. Central visual pathways. In: Kandel, E.R., Schwartz, J.H., Jessell, T.M. (eds.) Principles of Neural Science, 4th edn, pp. 523–547. McGraw-Hill, New York. 2000
22. Oyster, C. Retinal III: regional variation and spatial organization (Chapter 15). In: Oyster, C. (ed.) The Human Eye – Structure and Function, pp. 649– 700. Sinauer Associates, Sunderland, Massachusetts. 1999
23. Roof, D.J., Makino, C.L. The structure and function of retinal photoreceptors. In: Albert, D.A., Jakobiec, F.A. (eds.) Principles and Practice of Ophthalmology, 2nd edn, pp. 1624– 1673. Saunders, Philadelphia. 2000
24. Sharma, R.K., Ehinger, B.E.J. Development and structure of the retina. In: Kaufman,

P.L., Alm, A. (eds.) Adler's Physiology of the Eye, 10th edn, pp. 319–347. Mosby, St Louis. 2003

25. Radius, R.H., Anderson, D.R.: The histology of retinal nerve fiber layer bundles and bundle defects. Archives of Ophthalmology. 1979; 97: 948–950
26. Minckler, D.S. The organization of nerve fiber bundles in the primate optic nerve head. Archives of Ophthalmology. 1980; 98: 1630– 1636
27. Ogden, T.E. Nerve fiber layer of the macaque retina: retinotopic organization. Investigative Ophthalmology and Vision Science. 1983; 24: 85–98
28. Fitzgibbon, T., Taylor, S.F. Retinotopy of the human retinal nerve fibre layer and optic nerve head. Journal of Comp. Neurology. 1996; 375: 238–251
29. Fitzgibbon, T. The human fetal retinal nerve fiber layer and optic nerve head: a DiI and DiA tracing study. Vision Neuroscience. 1997; 14: 433–447
30. Provis, J.M., Penfold, P.L., Cornish, E.E., Sandercoe, T.M., Madigan, M.C. Anatomy and development of the macula: specialisation and the vulnerability to macular degeneration. Clinical and Experimental Optometry. 2005; 88: 269–281
31. Callaway, E.M. Structure and function of parallel pathways in the primate early visual system. Journal of Physiology. 2005; 566: 13–19
32. Davson, H. Retinal structure and organization (chapter 5). In: Davson, H. (ed.) Physiology of the Eye, 5th edn, pp. 205–218. MacMillan, London. 1990

33. Kincaid, M.C. Pathology of the retina. In: Sassani, J.W. (ed.) Ophthalmic Pathology with Clinical Correlations, pp. 269–291. Lippincott-Raven, Philadelphia. 1997

34. Oyster, C. Blood supply and drainage (Chapter 6). In: Oyster, C. (ed.) The Human Eye – Structure and Function, pp. 247–289. Sinauer Associates, Sunderland, Massachusetts. 1999

35. Harris, A., Gingaman, D.P., Ciulla, T.A., Martin, B.J. Retinal and choroidal blood flow in health and disease. In: Ryan, S.J. (ed.) The Retina, 3rd edn, pp. 68–88. Mosby, St Louis. 2001

36. Saint-Geniez, M., D'Amore, P.A. Development and pathology of the hyaloid, choroidal and retinal vasculature. International Journal of Developmental Biology. 2004; 48: 1045– 1058

37. Cioffi, G.A., Granstam, E., Alm, A. Ocular circulation (Chapter 33). In: Kaufman, P.L., Alm, A. (eds.) Adler's Physiology of the Eye, 10th edn, pp. 747–784. Mosby, St Louis. 2003

38. Provis, J.M. Development of the primate retinal vasculature. Progress in Retina and Eye Research. 2001; 20: 799–821

39. Curcio, C.A., Sloan, K.R., Packer, O., Hendrickson, A.E., Kalina, R.E. Distribution of cones in human and monkey retina: individual variability and radial asymmetry. Science. 1987; 236: 579–582

40. Olver, J.M., McCartney, A.C.E. Orbital and ocular microvascular corrosion casting in

man. Eye. 1989; 3: 588–596

41. Olver, J.M., Spalton, D.J., McCartney, A.C.E. Microvascular study of the retrolaminar optic nerve in man: The possible significance on anterior ischaemic optic neuropathy. Eye. 1990; 4: 7–24
42. Alm, A., Bill, A., Young, F.A. The effects of pilocarpine and neostigmine on the blood flow through the anterior uvea in monkeys: a study with radioactively labelled microspheres. Experimental Eye Research. 1973; 15: 31
43. Alm, A., Bill, A. Ocular and optic nerve blood flow at normal and increased intraocular pressures in monkeys (Macaca irus): a study with radioactively labelled microspheres including flow determinations in brain and some other tissues. Experimental Eye Research. 1973; 15: 15
44. Levin, L.A. Optic nerve. In: Kaufman, P.L., Alm, A. (eds.) Adler's Physiology of the Eye, 10th edn, pp. 603–638. Mosby, St Louis. 2003
45. Zhu, M., Madigan, M.C., Van Driel, D., Maslim, J., Billson, F., Provis, J.M., Penfold, P.L. The human hyaloid system: cell death and vascular regression. Experimental Eye Research. 2000; 70: 767–776
46. Anderson, D.R., Quigley, H.A. The optic nerve. In: Hart Jr.,W.M. (ed.) Adler's Physiology of the Eye, 9th edn, pp. 616–639. Mosby, St. Louis. 1992
47. Kincaid, M.C., Green, W.R. Anatomy of the vitrous, retina and choroid. In: Regillo, C.D., Brown, G.C., Flynn, H.W. (eds.) Vitreoretinal Disease, pp. 11–24. Thieme,

New York, Stuttgart. 1999

48. Hogan, M.J., Alvarado, J.A., Weddell, J.E. Retina. In: Histology of the Human Eye. An Atlas and Textbook, pp. 393–521. Saunders: Philadelphia. 1971
49. Wilson, C., Theodorou, M., Cocker, K.D., Fielder, A. The temporal retinal blood vessels and preterm birth. British Journal of Ophthalmology. 2006; 90: 702–704
50. Tsai, C.S., Zangwill, L., Gonzalez, C., Irak, I., Garden, V., Hoffman, R., Weinreb, R.N. Ethnic differences in optic nerve head topography. Journal of Glaucoma. 1995; 4: 248– 257
51. Kanski, J.J., Nischal, K.K. The optic disc. In: Ophthalmology. Clinical Signs and Differential Diagnosis, pp. 247–285. Mosby: St Louis. 1999
52. Brown, G.C. Arterial occlusive disease. In: Regillo, C.D., Brown, G.C., Flynn, H.W. (eds.) Vitreoretinal Disease, pp. 97–115. Thieme, New York, Stuttgart. 1999
53. Rimmer, S., Keating, C., Chou, T., Farb, M.D., Christenson, P.D., Foos, R.Y., Bateman, J.B. Growth of the human optic disk and nerve during gestation, childhood, and early adulthood. American Journal of Ophthalmology. 1993; 116: 748–753
54. Fekrat, S., Finkelstein, D. Venous occlusive disease. In: Regillo, C.D., Brown, G.C., Flynn, H.W. (eds.) Vitreoretinal Disease, pp. 117–132. Thieme, New York, Stuttgart. 1999
55. Anderson, D.R., Patella, V.M. Automated Static Perimetry, 2nd edn. Mosby, St. Louis.

1999

56. Kline, L.B., Bajandas, F.J. Visual fields. In: Kline, L.B., Bajandas, F.J. (eds.) Neurophthalmology. Review Manual, 5th edn, pp. 1–45. Slack, Thorofare. 2004
57. Miller, N.R., Newman, N.J. Anatomy and physiology of the retina and optic nerve: Distinguishing retinal from optic nerve disease (chapter 2). Anomalies of the optic disc (chapter 3). Topical diagnosis of acquired optic nerve dis- orders (chapter 4). In: Miller, N.R., Newman, N.J. (eds.) Walsh and Hoyt's Clinical Neuro- Ophthalmology. The essentials, 5th edn, pp. 59–166. Williams & Wilkins, Baltimore. 1999
58. Glaser, J.S. Topical diagnosis: prechiasmal visual pathways. In: Glaser, J.S. (ed.) Neuro- Ophthalmology, 3rd edn, pp. 95–198. Lippincott Williams&Wilkins, Philadelphia. 1999
59. Liu, G.T., Volpe, N.J., Galetta, S.L. Vision loss: retinal disorders of neuro-ophthalmic interest. In: Liu, G.T., Volpe, N.J., Galetta, S.L. (eds.) Neuro- Opthalmology. Diagnosis and Management, pp. 58–102. Saunders, Philadelphia. 2001
60. Ali Yoonessi, Ahmad Yoonessi. Functional assessment of magno, parvo and konio cellular pathways; current state and future clinical applications. Journal of Ophthalmic and Vision Research. 2011; 119-212
61. Callaway EM. Structure and function of parallel pathways in the primate early visual system. Journal of Physiology. 2005; 566: 13-19
62. Glickman G, Byrne B, Pineda C, Hauck WW, Brainard GC. Light therapy for

seasonal affective disorder with blue narrow-band light-emitting diodes (LEDs). Biological Psychiatry. 2006; 59: 502-507

63. Zaidi Q, Spehar B, DeBonet J. Color constancy in variegated scenes: role of low-level mechanisms in discounting illumination changes. Journal of Optometric Society and American Academy of Optometry Image Science and Vision. 1997; 14: 2608-2621

64. Yoonessi A, Kingdom FA. Comparison of sensitivity to color changes in natural and phase-scrambled scenes. Journal of Optometric Society and American Academy of Optometry Image Science and Vision. 2008; 25: 676- 684

65. Paul KN, Saafir TB, Tosini G. The role of retinal photoreceptors in the regulation of circadian rhythms. Review of Endocrine Metabolic Disorders. 2009; 10: 271-278

66. Murav'eva SV, Deshkovich AA, Shelepin YE. The human magno and parvo systems and selective impairments of their functions. Neuroscience Behavioral Physiology.2009; 39: 535-543

67. Thurtell MJ, Bala E, Yaniglos SS, Rucker JC, Peachey NS, Leigh RJ. Evaluation of optic neuropathy in multiple sclerosis using low-contrast visual evoked potentials. Neurology. 2009; 73: 1849-1857

68. Silva MF, Faria P, Regateiro FS, Forjaz V, Januário C, Freire A, et al. Independent patterns of damage within magno-, parvo- and koniocellular pathways in Parkinson's disease. Brain. 2005; 128: 2260-2271

69. Guo L, Duggan J, Cordeiro MF. Alzheimer's disease and retinal neurodegeneration. Current Alzheimer Research. 2010; 7: 3-14

70. Sartucci F, Borghetti D, Bocci T, Murri L, Orsini P, Porciatti V, et al. Dysfunction of the magnocellular stream in Alzheimer's disease evaluated by pattern electroretinograms and visual evoked potentials. Brain Research Bulletin. 2010; 82: 169-176.

71. Wässle H. Parallel processing in the mammalian retina. Nature Review Neuroscience. 2004; 5: 747-757

72. Masland RH. The fundamental plan of the retina. Nature Neuroscience. 2001; 4: 877-886

73. Dacey D, Packer OS, Diller L, Brainard D, Peterson B, Lee B. Center surround receptive field structure of cone bipolar cells in primate retina. Vision Research. 2000; 40: 1801- 1811

74. Rodieck RW. The First Steps in Seeing. Sunderland: Sinauer Associates; 1998

75. Ruderman DL. The statistics of natural images. Network: Computation in Neural Systems. 1994; 5: 517- 548

76. Van Essen DC, Newsome WT, Maunsell JH. The visual field representation in striate cortex of the macaque monkey: asymmetries, anisotropies, and individual variability. Vision Research. 1984; 24: 429-448

77. J.B. Jonas, G.C. Gusek, G.O. Naumann. Optic disc, cup and neuroretinal rim size,

configuration and correlations in normal eyes. Invest Ophthalmol Vis Sci. 1988; 29: 1151–1158

78. Quigley H A. Number of people with glaucoma worldwide. British Journal of
79. Ophthalmology. 1996; 80: 389-393
80. Resnikoff S, Pascolini D, Etya'ale D, Kocur I, Pararajasegaram R, Pokharel G. P et al. Global data on visual impairment in the year 2002. Bulletin of World Health Organisation. 2004; 82: 844–851
81. Hood DC, Greenstein VC, Odel JG, et al. Visual field defects and multifocal visual evoked potentials: evidence for a linear relationship. Arch Ophthalmol. 2002; 120:1672–1681
82. Sample PA, Madrid M, Weinreb RN. Evidence for a variety of functional defects in glaucoma suspect eyes. J Glaucoma. 1994; 3(suppl):S5–S18
83. Sample PA, Bosworth CF, Weinreb RN. Short-wavelength automated perimetry and motion automated perimetry in glaucoma. Arch Ophthalmol. 1997; 115:1129–1133
84. Heron G, Adams AJ, Husted R. Central visual fields for short wavelength sensitive pathways in glaucoma and ocular hypertension. Invest Ophthalmol Vis Sci. 1998; 29:64– 72
85. Sample PA, Boynton RM, Weinreb RN. Isolating the color vision loss in primary open angle glaucoma. Am J Ophthalmol. 1988; 106:686–691
86. Graham SL, Klistorner A. Electrophysiology: a review of signal origin and applications to investigating glaucoma. Australian and New Zealand journal of Ophthalmology. 1998; 26:71-85
87. Hasegawa S, Abe H. Mapping of glaucomatous visual field defects by multifocal

VEPs. Invest Ophthalmol Vis Sci. 2001; 42:3341–3348

88. Trap BD, Nave K. Multiple Sclerosis: an immune or neurodegenerative disorder? Annual Review of Neuroscience. 2008; 31: 247-269
89. Sorensen TL, Frederiksen JL, Bronnum-Hansen H, Peterson HC. Optic neuritis as onset manifestation of multiple sclerosis. Neurology. 1999; 53: 473-478
90. Hornabrook RS, Miller DH, Newton MR, MacManus DG, du Boulay GH, Halliday AM, McDonald WI. Frequent involvement of optic radiation in patients with acute isolated optic neuritis. Neurology. 1992; 42: 77-79
91. Jenkins T, Ciccarelli O, Toosy A et al. Dissecting structure-function interactions in acute optic neuritis to investigate neroplasticity. Human Brain Mapping. 2010; 31: 276-286
92. Waxman, S.G.e., 2005. Multiple sclerosis as a neuronal disease. Elsevier Academic Press, Amsterdam
93. Ferguson, B., Matyszak, M.K., Esiri, M.M., Perry, V.H. Axonal damge in acute multiple sclerosis lesions. Brain. 1997; 120: 393-399
94. Trapp, B.D., Peterson, J., Ransohoff, R.M., Rudick, R., Mork, S., Bo, L. Axonal transection in the lesions of multiple sclerosis. New England Journal of Medicine. 1998; 338: 278-285
95. Kornek, B., and Lassmann, H. Axonal pathology in multiple sclerosis: a historical note. Brain Pathology. 1999; 9: 651–656
96. Bitsch, A., Schuchardt, J., Bunkowski, S., et al. Acute axonal injury in multiple sclerosis. Correlation with demyelination and inflammation. Brain. 2000; 123: 1174-1183

97. Zivadiniv, R., Zorton, M. Is gadolinium enhancement predictive of the development of brain atrophy in multiple sclerosis. Journal of Neuroimaging. 2002; 12: 302-309

98. Patani, R., Balaratnam, M., Vora, A., Reynolds, R. Remyelination can be extensive in multiple sclerosis despite a long disease course. Neuropathology and Applied Neurobiology. 2007; 33: 277-287

99. Beck RW, Trobe JD, Moke PS et al. High- and low-risk profiles for the development of multiple sclerosis within 10 years after optic neuritis: experience of the optic neuritis treatment trial. Archives of Ophthalmology. 2003; 121:944–949

100. Bhatti MT; Group ONS. The final 15-year follow-up report on the neurological outcome of the Optic Neuritis Treatment Trial. 34th Annual Meeting of the North American Neuro- Ophthalmology Society (NANOS), Orlando, USA, 2008

101. Rodriguez M, Siva A, Cross SA et al. Optic neuritis: a population based study in Olmsted County, Minnesota. Neurology. 1995; 45: 244–250

102. Rizzo JF 3rd, Lessell S. Risk of developing multiple sclerosis after uncomplicated optic neuritis: a long-term prospective study. Neurology. 1988; 38: 185–190

103. Sorensen, T.L., et al., Optic neuritis as onset manifestation of multiple sclerosis. Neurology. 1999. 53: p. 473-478

104. Hornabrook, R.S., et al., Frequent involvement of optic radiation in patients with acute isolated optic neuritis. Neurology, 1992. 42: p. 77-79

105. Jenkins, T., et al., Dissecting structure-function interactions in acute optic neuritis to investigate neuroplasticity. Hum Brain Map, 2010. 31: p. 276-286

106. Forooghian, F., et al., Electroretinigraphic abnormalities in multiple sclerosis: possible role for retinal autoantibodies. Doc Ophthalmol, 2006. 113: p. 123-132

107.Green, I.J., et al., Ocular pathology in multiple sclerosis: retinal atrophy and inflammation irrespective of disease duration. Brain, 2010. 133: p. 1591-1601

108.Youl BD, Kermode AG, Thompson AJ et al. Destructive lesions in demyelinating disease. J Neurol Neurosurg Psychiatry. 1991; 54: 288-292

109.Petzold, A., et al., Optical coherence tomography in multiple sclerosis: a systematic review and meta-analysis. The Lancet (Neurol), 2010. 9: p. 921-932

110.Klistorner, A., et al., Remyelination of optic nerve lesions: spatial and temporal factors. Mult Scler, 2010. 16: p. 786-795

111.Reich, D.S., et al., Damage to optic radiation in multiple sclerosis is associated with retinal injury and visual disability. Arch Neurol, 2009. 66: p. 998-1006

112.Dasenbrock, H.H., et al., Diffusion Tensor Imaging of the Optic Tracts in Multiple Sclerosis: Association with Retinal Thinning and Visual Disability. J Neuroim, 2011. 21: p. e41-e49

113.Syc, S., et al., Optical coherence tomography segmentation reveals ganglion cell layer pathology after optic neuritis. Brain, 2011. 135: p. 521-533

114.Beck RW, Gal RL, Bhatti MT et al. Visual function more than 10 years after optic neuritis: experience of the optic neuritis treatment trial. American Journal of Ophthalmology. 2004; 137: 77–83

115.Costello F, Coupland S, Hodge W et al. Quantifying axonal loss after optic neuritis with optical coherence tomography. Annals of Neurology. 2006; 59: 963–969

116.Fisher JB, Jacobs DA, Markowitz CE et al. Relation of visual function to retinal nerve fibre layer thickness in multiple sclerosis. Ophthalmology. 2006; 113: 324– 332

117.Trip SA, Schlottmann PG, Jones SJ et al. Retinal nerve fibre layer axonal loss and

visual dysfunction in optic neuritis. Annals of Neurology 2005; 58: 383–391

118. Henderson AP, Trip SA, Schlottmann PG et al. An investigation of the retinal nerve fibre layer in progressive multiple sclerosis using optical coherence tomography. Brain. 2008; 131: 277–287

119. Klistorner, A., et al., Axonal loss in non-optic neuritis eyes of patients with multiple sclerosis linked to delayed visual evoked potential. Neurol, 2013. 15: p. 242-245

120. Pueyo, V., et al., Axonal loss in the retinal fiber layer in patients with multiple sclerosis. Mult Scer, 2008. 14: p. 609-614

121. Sepulcre, J., et al., Diagnostic accuracy of retinal abnormalities in predicting disease activity in MS. Neurology, 2007. 66: p. 1488-1494

122. Talman, L.S., et al., Longitudinal study of vision and retinal nerve fiber layer thickness in multiple sclerosis. Ann neurol, 2010. 67: p. 749-760

123. Henderson, A.P., et al., An investigation of the retinal nerve fibre layer in progressive multiple sclerosis using optical coherence tomography. Brain, 2008. 131: p. 277-287

124. Henderson, A.P., et al., A preliminary longitudinal study of the retinal nerve fiber layer in progressive multiple sclerosis. J Neurol, 2010; 257:1083-1091

125. Gordon-Lipkin, E., et al., Retinal nerve fiber layer is associated with brain atrophy in multiple sclerosis. Neurol, 2007. 69: p. 1603-1609

126. Fisher, J.B., et al., Relation of visual function to retinal nerve fiber layer thickness in multiple sclerosis. Ophthalmol, 2006. 113: p. 324-332

127. Siger, M., et al., Optical coherence tomography in multiple sclerosis. J Neurol, 2008. 255: p. 1555-1560

128. Costello, F., et al., Differences in retinal nerve fiber layer atrophy between multiple

sclerosis subtypes. J Neurol Sci, 2009. 281: p. 74-79

129.Parisi, V., et al., Correlation between optical coherence tomography, pattern electroretinogram, and visual evoked potentials in open-angle glaucoma patients. Ophthalmology, 2001; 108:905-12

130.Pulicken, M., et al., Optical coherence tomography and disease subtype in multiple sclerosis. Neurol, 2007; 69:2085-2092

131.Bock, M., et al., Pattern of retinal nerve fiber layer loss in multiple sclerosis patients with or without optic neuritis and glaucoma patients. Clin Neurol Neurosurg, 2010; 112:647- 652

132.Kallenbach, K. and J.L. Fredericksen, Optical coherence tomography in optic neuritis and multiple sclerosis: a review. Europ J Neurol, 2007; 14:841-849

133.Frohman, E.M., et al., Relationship of optic nerve and brain conventional and non-conventional MRI measures and RNFL, as assessed by OCT and GDx: a pilot study. J Neurolog Sci, 2009; 15:96-105

134.Grazioli, E., et al., Retinal nerve fiber layer thickness is associated with brain MRI outcomes in multiple sclerosis. J Neurolog Sci, 2008. 268: p. 12-17

135.Frohman, E.M., et al., Optical coherence tomography: a window into the mechanisms of multiple sclerosis. Nature Neurol, 2008. 4: p. 664-675

136.Rosenblatt, M.A., et al., Magnetic resonance imaging of optic tract involvement in multiple sclerosis. Am J Ophthalmol, 1987. 104: p. 74-79

137.Saidha, S., Syc, S., Ibrahim M.A., et al., Primary retinal pathology in multiple sclerosis as detected by optical coherence tomography. Brain, 2011; 134: 518-533

138.Saidha, S., et al., Microcystic macular oedema, thickness of the inner nuclear layer of

the retina, and disease characteristics in multiple sclerosis: a retrospective study. Lancet (Neurol), 2012. 11: p. 963-972

139. Lehoszky, T., Pathologic changes in the optic system in multiple sclerosis. Acta Morphol Acad Sci Hung, 1954. 4: p. 395-408.

140. Fingeret M, Medeiros FA, Susanna R, et al. Five rules to evaluate the optic disc and retinal nerve fiber layer for glaucoma. Optometry. 2005;76:661–668

141. Tielsch JM, Katz J, Quigley HA, et al. Intraobserver and interobserver agreement in measurement of optic disc characteristics. Ophthalmology. 1988;95:350–356

142. Varma R, Steinmann WC, Scott IU. Expert agreement in evaluating the optic disc for glaucoma. Ophthalmology. 1992;99:215–221

143. Gaasterland DE, Blackwell B, Dally LG, et al. The Advanced Glaucoma Intervention Study (AGIS): Variability among academic glaucoma subspecialists in assessing optic disc notching. Trans America Ophthalmology Society. 2001;99:177–185

144. Parrish RK, Schiffman JC, Feuer WJ, et al. Test-retest reproducibility of optic disk deterioration detected from stereophotographs by masked graders. American Journal of Ophthalmology. 2005;140:762–764

145. Zeyen T, Miglior S, Pfeiffer N, et al. Reproducibility of evaluation of optic disc change for glaucoma with stereo optic disc photographs. Ophthalmology. 2003;110:340–344

146. Deleón-Ortega JE, Arthur SN, McGwin G, et al. Discrimination between glaucomatous and nonglaucomatous eyes using quantitative imaging devices and subjective optic nerve head assessment. Investigative Ophthalmology and Visual Science. 2006;47:3374–3380

147.Girkin CA, DeLeon-Ortega JE, Xie A, et al. Comparison of the Moorfields classification using confocal scanning laser ophthalmoscopy and subjective optic disc classification in detecting glaucoma in blacks and whites. Ophthalmology. 2006;113:2144–214

148.Henderer JD, Liu C, Kesen M, et al. Reliability of the disk damage likelihood scale. American Journal of Ophthalmology. 2003;135:44–48

149.Medeiros FA, Zangwill LM, Bowd C, et al. Use of progressive glaucomatous optic disk change as the reference standard for evaluation of diagnostic tests in glaucoma. American Journal of Ophthalmology. 2005;139:1010–1018

150.Lin SC, Singh K, Jampel HD, et al. Optic nerve head and retinal nerve fiber layer analysis: a report by the American Academy of Ophthalmology. Ophthalmology. 2007;114:1937–1949.

151.Stein DM, Wollstein G, Schuman JS. Imaging in glaucoma. Ophthalmology Clinics of North America. 2004;17:33-52.

152.Miglior S, Albe E, Guareschi M, Rossetti L, Orzalesi N. Intraobserver and interobserver reproducibility in the evaluation of optic disc stereometric parameters by Heidelberg Retina Tomograph. Ophthalmology. 2002;109:1072-1077

153.Rohrschneider K, Kruse FE. Reproducibility of the optic nerve head topography with a new laser tomographic scanning device. Ophthalmology 1994; 101: 1044- 1049

154.Garway-Heath DG. Moorfields regression analysis. In: Fingeret M, Flanagan JG, Liebmann JM, eds. The Essential HRT Primer. San Ramon, California: Jocoto Advertising Inc; 2005:31–39.

155.Joseph R. Zelefsky, Noga Harizman, Ricardo Mora et al. Assessment of a Race-

specific Normative HRT-III Database to Differentiate Glaucomatous From Normal Eyes. Journal of Glaucoma 2006;15:548–551.

156. Hatch WV, Flanagan JG, Williams-Lyn DE et al. Interobserver agreement of Heidelberg retina tomograph parameters. Journal of Glaucoma.1999;8:232-237

157. Jonas JB, Mardin CY, Grundler AE. Comparison of measurements of neuroretinal rim area between confocal laser scanning tomography and planimetry of photographs. British Journal of Ophthalmology. 1998;82:362-366

158. Dichtl A, Jonas JB, Mardin CY. Comparison between tomographic scanning evaluation and photographic measurement of the neuroretinal rim. American Journal of Ophthalmology. 1996;121:494-501

159. Vernon SA, Hawker MJ, Gerard Ainsworth G et al. Laser Scanning Tomography of the Optic Nerve Head in a Normal Elderly Population: The Bridlington Eye Assessment Project. Investigative Ophthalmology and Visual Science. 2005;46:2823–2828

160. Uchida H, Yamamoto T, Araie M et al. Topographic characteristics of the optic nerve head measured with scanning laser tomography in normal japanese subjects. Japanese Journal of Ophthalmology. 2005;49:469–476

161. Bigelow CE, Iftimia NV, Feruson RD et al. Compact multimodal adaptive optics spectral domain optical coherence tomography instrument for retinal imaging. Journal of Optical Society of America. A optics, image science and vision. 2007; 24: 1327-1336

162. Iliev ME, Meyenberg A, Garweg JG. Morphometric assessment of normal, suspect and glaucomatous optic disks with Stratus OCT and HRT II. Eye (Lond).

2006;20:1288-1299

163.Drexler W, Morgner U, Ghanta RK, et al. Ultrahigh-resolution ophthalmic optical coherence tomography. Nature Medicine. 2001;7:502–507

164.Gabriele ML, Ishikawa H, Wollstein G, et al. Peripapillary nerve fiber layer thickness profile determined with high speed, ultrahigh resolution optical coherence tomography high-density scanning. Investigative Ophthalmology and Visual Science. 2007;48:3154– 3160

165.Wollstein G, Paunescu LA, Ko TH, et al. Ultrahigh-resolution optical coherence tomography in glaucoma. Ophthalmology. 2005;112:229–237

166.Quigley HA, Katz J, Derick RJ, et al. An evaluation of optic disc and nerve fiber layer examinations in monitoring progression of early glaucoma damage. Ophthalmology. 1992;99:19–28

167.Sehi M, Guaqueta DC, Feuer WJ, et al. Scanning laser polarimetry with variable and enhanced corneal compensation in normal and glaucomatous eyes. American Journal of Ophthalmology. 2007;143:272–279

168.Greenfield DS, Knighton RW, Huang XR, et al. Effect of corneal polarization axis on assessment of retinal nerve fiber layer thickness by scanning laser polarimetry. American Journal of Ophthalmology. 2000;129:715–722

169.Brusini P, Salvetat ML, Parisi L, et al. Discrimination between normal and early glaucomatous eyes with scanning laser polarimeter with fixed and variable corneal compensator settings. European Journal of Ophthalmology. 2005;15:468–476

170.Weinreb RN, Bowd C, Zangwill LM. Glaucoma detection using scanning laser polarimetry with variable corneal polarization compensation. Archives of

Ophthalmology. 2003;121:218–224

171.Bowd C, Zangwill LM, Medeiros FA, et al. Structure-function relationships using confocal scanning laser ophthalmoscopy, optical coherence tomography, and scanning laser polarimetry. Investigative Ophthalmology and Visual Science. 2006;47:2889–2895

172.Schlottmann PG, De Cilla S, Greenfield DS, et al. Relationship between visual field sensitivity and retinal nerve fiber layer thickness as measured by scanning laser polarimetry. Investigative Ophthalmology and Visual Science. 2004;45:1823–1829

173.Bowd C, Medeiros FA, Zhang Z, et al. Relevance vector machine and support vector machine classifier analysis of scanning laser polarimetry retinal nerve fiber layer measurements. Investigative Ophthalmology and Visual Science. 2005;46:1322–1329

174.Essock EA, Zheng Y, Gunvant P, et al. Analysis of GDx-VCC polarimetry data by Wavelet-Fourier analysis across glaucoma stages. Investigative Ophthalmology and Visual Science. 2005;46:2838–2847

175.Medeiros FA, Zangwill LM, Bowd C, et al. Fourier analysis of scanning laser polarimetry measurements with variable corneal compensation in glaucoma. Investigative Ophthalmology and Visual Science. 2003;44:2606–2612

176.Hoh ST, Greenfield DS, Liebmann JM, et al. Factors affecting image acquisition during scanning laser polarimetry. Ophthalmic Surgery and Lasers. 1998;29:545– 551

177.Bagga H, Greenfield DS, Feuer WJ, et al. Quantitative assessment of atypical birefringence images using scanning laser polarimetry with variable corneal compensation. American Journal of Ophthalmology. 2005;139:437–446

178.Bowd C, Tavares IM, Medeiros FA, et al. Retinal nerve fiber layer thickness and

visual sensitivity using scanning laser polarimetry with variable and enhanced corneal compensation. Ophthalmology. 2007;114:1259–1265

179. Medeiros FA, Bowd C, Zangwill LM, et al. Detection of glaucoma using scanning laser polarimetry with enhanced corneal compensation. Investigative Ophthalmology and Visual Science. 2007;48:3146–3153

180. Cioffi GA, Liebman JM, Johnson CA, Weinreb RN. Structural-functional relationship of the optic nerve in glaucoma. Journal of Glaucoma. 2000; 9:3-4

181. Johnson CA, Cioffi GA, Liebmann JM. The relationship between structural and functional alterations in glaucoma: a review. Seminars in Ophthalmology. 2000; 15:221- 223

182. Quigley HA, Dunkelberger GR, Green WR. Retinal ganglion cell atrophy correlated with automated perimetry in human eyes with glaucoma. American Journal of Ophthalmology. 1989;107:453–464

183. Kerrigan-Baumrind LA, Quigley HA, Pease ME, et al. Number of ganglion cells in glaucoma eyes compared with threshold visual field tests in the same persons. Investigative Ophthalmology and Visual Science. 2000;41:741–748

184. Artes PH, Iwase A, Ohno Y, et al. Properties of perimetric threshold estimates from Full Threshold, SITA Standard, and SITA Fast strategies. Investigative Ophthalmology and Visual Science. 2002;43:2654–2659

185. Keltner JL, Johnson CA, Levine RA, et al. Normal visual field test results following glaucomatous visual field end points in the Ocular Hypertension Treatment Study. Archives of Ophthalmology. 2005;123:1201–1206

186. Keltner JL, Johnson CA, Anderson DR, et al. The association between glaucomatous

visual fields and optic nerve head features in the Ocular Hypertension Treatment Study. Ophthalmology. 2006;113:1603–1612

187. Heijl A, Leske MC, Bengtsson B, et al. Measuring visual field progression in the Early Manifest Glaucoma Trial. Acta Ophthalmologica Scandinavia. 2003;81:286–293

188. Gordon MA, Beiser JA, Brandt JA et al. The Ocular Hypertension Treatment Study: baseline factors that predict the onset of primary open angle glaucoma. Archives of Ophthalmology. 2002; 120:714-720

189. Johnson CA, Sample PA, Zangwill L et al. Structure and function evaluation (SAFE): II. Comparison of optic disc and visual field characteristics. American Journal of Ophthalmology. 2003; 135:148-154

190. Bengtsson B, Heijl A. Evaluation of a new perimetric threshold strategy, SITA, in patients with manifest and suspect glaucoma. Acta Ophthalmologica Scandinavia. 1998;76:268–272

191. Dacey DM, Lee BB. The "blue-on" opponent pathway in primate retina originates from a distinct bistratified ganglion cell type. Nature. 1994; 367:731-735

192. Wild J. Short wave automated perimetry. Acta Ophthalmologica Scandinavica. 2001;79: 546-559.

193. Frisen L. High resolution perimetry: central field neuroretinal correlates. Vision Research. 1995; 35:293-301

194. Drance SM, Lakowski R, Schulzer M, Douglas GR. Acquired colour vision changes in glaucoma: use of 100 Hue test and Pickford anomaloscope as predictors of glaucomatous field change. Archives of Ophthalmology. 1981; 99:829-831

195.Adams AJ, Rodic R, Husted R, Stamper R, Spectral sensitivity and colour discrimination changes in glaucoma and glaucoma suspect patients. Investigative Ophthalmology and Visual Science. 1982;23:516-524

196.Stiles WS. The directional sensitivity of the retina and the spectral sensitivities of the rods and cones. Proceedings of the Royal Society, London (series B). 1939; 127:64-105

197.Stiles WS. Colour vision: the approach through increment threshold sensitivity. Proceedings of the National Academy of Science USA. 1959;45:100-114

198.Johnson CA. Selective versus non selective losses in glaucoma. Journal of Glaucoma. 1994; 3:S32-S44

199.Quigley H. Are some ganglion cells killed by glaucoma before others? In: Krieglstein GK (ed), Glaucoma Update III. Berlin: Springer-Verlag; 1987:23-26

200.Quigley HA, Dunkelberger GR, Green WR. Chronic human glaucoma causing selectively greater loss of large optic nerve fibres. Ophthalmology. 1988; 95; 357-363

201.Sample PA, Weinreb RN. Progressive color visual field loss in glaucoma. Investigative Ophthalmology and Visual Science 1992; 33:240-243

202.Sample PA, Weinreb RN. Colour perimetry for assessment of primary open angle glaucoma. Investigative Ophthalmology and Visual Science. 1990; 31:1869-1875

203.Johnson CA, Brandt JD, Khong AM, Adams AJ. Short wavelength automated perimetry in low-, medium-, and high-risk ocular hypertensive eyes. Initial baseline results. Archives of Ophthalmology. 1995; 113:70-76

204.Johnson CA, Adams AJ, Casson EJ, Brandt JD. Blue-on-yellow perimetry can predict the development of glaucomatous visual field loss. Archives of

Ophthalmology. 1993; 111:645-650

205.Sample PA. Short wavelength automated perimetry: It's role in the clinic and for understanding ganglion cell function. Progress in Retinal Research. 2000; 19:369-383

206.Sample PA, Taylor JDN, Martinez GA, Lusky M, Weinreb RN. Short wavelength colour visual fields in glaucoma suspects at risk. American Journal of Ophthalmology. 1993; 115:225-233

207.Sample PA, Weinreb RN. Variability and sensitivity of short wavelength colour visual field in normal and glaucoma eyes. In: Non invasive Assessment of the visual System. Archives of Ophthalmology. 1993; 293-295

208.Wild JM, Cubbidge RP, Pacey IE, Robinson P. Statistical aspects of the normal visual field in short-wavelength automated perimetry. Investigative Ophthalmology and Visual Science. 1998; 39:54-63

209.Wild JM, Moss ID. Baseline alterations in blue-on-yellow normal perimetric sensitivity. Graefe's Archive for Clinical and Experimental Ophthalmology. 1996; 234:141-149

210.Johnson CA, Adams AJ, Casson EJ, Brandt JD. Progression of early glaucomatous visual field loss for blue-on-yellow and standard white-on-white automated perimetry. Archives of Ophthalmology. 1993; 111:651-656.

211.Demirel S, Johnson CA. Incidenceand prevalence of short wavelength automated perimetry defects in ocular hypertensive patients. American Journal of Ophthalmology. 2001; 120:714-730

212.Johnson CA, Sample PA, Zangwill L et al. Structure and function evaluation

(SAFE):II, Comparison of optic disc and visual field characteristics. American Journal of Ophthalmology. 2003; 135: 148-154

213. Sanchez-Galeana C, Bowd C, Zangwill L, Sample PA, Weinreb RN. Short wavelength automated perimetry results are correlated with optical coherence tomography retinal nerve fibre layer thickness in glaucomatous eyes. Ophthalmology. 2004; 111:1866-1872

214. Teesalu P, Vihanninjoki K, Airaksinen PJ, Tuulonen A. Correlation of blue-yellow visual fields with scanning confocal laser optic disc measurements. Investigative Ophthalmology and Visual Science. 1997; 38:2452-2459

215. Yamagisji N, Anton A, Sample PA, Zangwill L, Lopez A, Weinrb RN. Mapping structural damage to the optic disc to visual field in glaucoma. American Journal of Ophthalmology. 1997; 123:667-676

216. Girkin CA, Emdadi A, Sample PA et al. Short wavelength perimetry and standard automated perimetry in the detection of progressive optic disc cupping. Archives of Ophthalmology. 2000; 188:1231-1236

217. Bengtsson B, Heijl A. Normal intersubject variability and normal limits of SITA-SWAP and full threshold SWAP perimetric programs. Investigative Ophthalmology and Visual Science. 2003; 44:5029-5034

218. Sample PA, Genaro MA, Weinreb RN. Short wavelength automated perimetry without lens density testing. American Journal of Ophthalmology. 1994; 118:632- 641

219. Blumenthal EZ, Sample PA, Zangwill L. Comparison of long term variability for standard and short wave automated perimetry in stable and glaucoma patients. Ophthalmology. 2000; 129:309-313

220.Kwon YH, Park HJ, Jap A, Ugurlu S, Caprioli J. Test retest variability of blue-on-yellow perimetry is greater than white on white perimetry in normal subjects. American Journal of Ophthalmology. 1998; 126:29-36

221.Maddess T, Henry G. Performance of non linear visual unit in ocular hypertension and glaucoma. Clinical Visual Science. 1992; 7:371-383

222.Sample PA, Bosworth CF, Blumenthal EZ, Girkin C, Weinreb RN. Visual function-specific perimetry for indirect comparison of different ganglion cell populations in glaucoma. Investigative Ophthalmology and Visual Science. 2000; 41:1783-1790

223.Maddess T, Bedford S, James A, Rose KA. A multiple frequency, multiple region pattern electroretinogra invesstigation of non linear retinal signals. Australian and New Zealand Journal of Ophthalmology. 1997; 25: S94-S97

224.Kelly DH. Non linear responses to flickering sinusoidal gratings. Journal of Optical society of America. 1981; 71: 1051-1055

225.Ansari EA, Morgan JE, Snowden RJ. Psychophysical characterisation of early functional loss in glaucoma. British journal of Ophthalmology. 2002; 6:1131-1135

226.Johnson C, Samuels S. Screening of glaucomatous visual field loss with frequency doubling perimetry. Investigative Ophthalmology and Visual science. 1997; 38: 413-425

227.Maddess T, Severt WL. Testing for glaucoma with the frequency doubling illusion in the whole, macular and eccentric visual fields. Australian and New Zealand Journal of Ophthalmology. 1999; 27: 194-196

228.Brusini P, Salvetat M, Zepieri M, Parisi L. Frequency doubling technology perimetry with the Humphrey Matrix 30-2 test. Journal of Glaucoma 2006; 15:77-83

229.Quigley HA. Identification of glaucoma related visual field abnormalities with the screening protocol of frequency doubling technology. American Journal of Ophthalmology. 1998; 125:819-829

230.Fabre K, Michelis I, Zeyer T. The sensitivity and specificity of TOP, FDP, GDx in screening for early glaucoma. Bulletin of the Belgium Society of Ophthalmology. 2000; 275: 17-23

231.Chauhan BC, Johnson CA. Test-retest variability of frequency doubling perimetry and conventional perimetry. Investigative Ophthalmology and Visual Science. 1999; 40:648- 656

232.Iester M, Capris P, Pandolfo A, Zingairian M, Traverso CE. Learning effect, short term fluctuation and long term fluctuation in frequency doubling technique. American Journal of Ophthalmology. 2000; 130:160-164

233.deMonaseterio FM. Asymmetry of on- and off- pathways of blue sensitive cones of the retina of macaque. Brain Research. 1979; 166:39-48

234.Trible JR, Schultz RO, Robinson C, Rothe TL. Accuracy of glaucoma detection with frequency doubling perimetry. American Journal of Ophthalmology. 2000; 129:740-745

235.Delgado MF, Nguyen NT, Cox TA et al. Automated perimetry: a report by the American Academy of Ophthalmology. Ophthalmology. 2002; 109:2362-2374

236.Spry P, Hussain H, Sparrow J. Glaucoma detection and the standard achromatic perimetry. British Journal of Ophthalmology. 2005; 91:933-938

237.Burganski – Eliash Z, Kagemann L, Dilworth W, Schuman J. Glaucoma detection with matrix and standard achromatic perimetry. British Journal of Ophthalmology.

2007; 91: 933-938

238. Medeiros FA, Sample PA, Zangwill L, Liebmann JM, Girkin CA, Weinreb RN. A statististical approach to the evaluation of covariate effects on the receiver operating characteristic curves of diagnostic tests in glaucoma. Investigative Ophthalmology and Visual Science. 2006; 47:2520-2527

239. Sakata LM, Deleon-Ortega J, Arthur SN, Monheit BE, Girkin CA. Detecting visual function abnormalities using the Swedish Interactive Threshold Algorithm and matrix perimetry in eyes with glaucomatous appearance of the optic disc. Archives of Ophthalmology. 2007; 125:340-345

240. Medeiros FA, Sample PA, Weinreb RN. Frequency doubling perimetry abnormalities as predictors of glaucomatous visual field loss. American Journal of Ophthalmology. 2004;137:863-871

241. Haymes SA, Hutchinson DM, McCormick TA et al. Glaucomatous visual field progression with frequency doubling technology and standard automated perimetry in a longitudinal prospective study. Investigative Ophthalmology and Visual Science. 2005; 46:547-554

242. Bayer AU, Erb C. Short wave automated perimetry, frequency doubling perimetry and pattern electroretinography for prediction of progressive glaucomatous standard visual field defects. Ophthalmology. 2002; 109:1009-1017

243. Artes PH, Hutchinson DM, Nicolela MT, LeBlanc RP, Chauhan BC. Threshold and variability properties of matrix frequency doubling technology and standard automated perimetry in glaucoma. Investigative Ophthalmology and Visual Science. 2005; 46: 241- 245

244.Wall M, Utzko KE, Chauhan BC. Variability in patients with glaucomatous visual field damage in patients with glaucomatous visual field damage is reduced using size V stimuli. Investigative Ophthalmology and Visual Science. 1997; 38:426-435

245.Landers J, Sharma A, Goldberg I, Graham S. Topography of the frequency doubling perimetry visual field compared with that of short wavelength and achromatic automated perimetry visual fields. British Journal of Ophthalmology. 2006; 90:70- 74

246.Contestible MT, Perdicchi A, Amodeo S, Recupero V, Recupero SM. The influence of learning effect on frequency doubling technology perimetry (Matrix). Journal of Glaucoma. 2007; 16:297-301

247.Blumenthal EZ, Haddad A, Horani A, Anteby L. The reliability of frequency doubling perimetry in young children. Ophthalmology. 2004; 435-439

248.Anderson AJ, Johnson CA. Frequency doubling technology perimetry and optical defocus. Investigative Ophthalmology and Visual Science. 2003; 44: 4147-4152

249.Johnson CA, Cioffi GA, Van Buskirk EM. Frequency doubling perimetry using a 24-2 stimulus presentation pattern. Optometry and visual Science. 1999; 76:571- 581

250.Anderson AJ, Johnson CA. Frequency doubling technology perimetry. Ophthalmology Clinic in North America. 2003; 16:213-225

251.Siddiqui MA, Azuara-Blanco A, Neville S. Effect of cataract extraction on frequency doubling perimetry in patients with glaucoma. British Journal of Ophthalmology. 2005; 89:1569-1571

252.Rodieck RW. Components of the electroretinogram – A reappraisal. Vision Research.1972; 12:773-780

253.Newman EA, Odette LL. Model of electroretinogram b-wave generation: a test of the

K+ hypothesis. Journal of Neurophysiology. 1984; 51:164-182

254. Stockton RA, Slaughter MM. B-wave of the electroretinogram: a reflection of bipolar cell activity. Journal of General Physiology. 1989; 93: 101-122

255. Newman EA. Regulation of extracellular potassium by glial cells in the retina. Trends in Neuroscience. 1985: 156-159

256. Karwoski CJ, Proenza LM. Relationship between Muller cell responses: a local transretinal potential and potassium flux. Journal of Neurophysiology. 1977; 40: 244-259

257. Graham S, Fortune B. Electrophysiology in glaucoma assessment. In: Shaarawy T, Sherwood MB, Hitchings RA, Crowston (eds), Glaucoma Volume I Medical diagnosis and therapy: Elseiver; 2009:151-170

258. Graham SL, Drance SM, Chauhan BC et al. Comparison of psychophysical and electrophysiological testing in early glaucoma. Investigative Ophthalmology and Visual Science. 1996; 37: 2651-2662

259. Cobb WA, Morton HB. A new component of the human electroretinogram. Journal of Physiology. 1954; 123: 36P-37P

260. Wachmeister L. Oscillatory potentials in the retina: what do they reveal. Progress in Retinal and Eye Research 1998; 17: 485-521

261. Viswanathan S, Frishman LJ, Robson JG. The uniform field and pattern ERG in macaques with experimental glaucoma: removal of spiking activity. Investigative Ophthalmology and Visual Science. 2000; 41: 2797-2810

262. Viswanathan S, Frishman LJ, Robson JG, Walters JW. The photopic negative response of the flash electroretinogram in primary open angle glaucoma. Investigative

Ophthalmology and Visual Science. 2001; 42: 514-522

263.Gur M, Zeevi YY, Bielik M, Neumann E. Challenges in the oscillatory potentials of the electroretinogram in glaucoma. Current Eye Research. 1987; 6:457-466

264.Colotto A, Falsini B, Salgarello T, Iarossi G, galan ME, Scullica L. Photopic negative response of the human ERG: losses associated with glaucomatous damage. Investigative Ophthalmology and Visual Science. 2000; 41: 2205-2211

265.Brodie SE, Frisch S, Siebold E et al. Fourier analysis of the oscillatory potentials in glaucoma and ocular hypertension. Investigative Ophthalmology and Visual Science. 1988; 29: 239

266.Wanger P, Persson HE. Pattern-reversal electroretinograms in unilateral glaucoma. Investigative Ophthalmology and Visual Science. 1983; 24: 749-753

267.Korth M, Nguyen NX, Horn F, Matus P. Scotopic threshold response and scotopic PII in glaucoma. Investigative Ophthalmology and Visual Science. 1994; 35:619- 625

268.Trick GL, Wintermeyer DH. Spatial and temporal frequency tuing of pattern- reversal retinal potentials. Investigative Ophthalmology and Visual Science. 1982; 23:774-779

269.Drasdo N, Aldebasi YH, Chiti Z, Mortlock KE, Morgon JE, North RV. The s-cone PHNR and pattern ERG in primary open angle glaucoma. Investigative Ophthalmology and Visual Science. 2001; 42: 1266-1272

270. Sieving PA, Nino C. Scotopic threshold response of the human electroretinogram. Investigative Ophthalmology and Visual Science. 1988; 28: 1608-1614

271.Frishman LJ, Reddy MG, Robson JG. Effects of background light of human dark adapted electroretinogram and psychophysical threshold. Journal of the Optical Society of America. 1996; 13:601-612

272.Saszik S, Frishman LJ, Robson JG. The scotopic threshold of the dark adapted electroretinogram of the mouse. Journal of Glaucoma. 2002; 543: 899-916

273.Glovinsky Y, Quigley HA, Drum B, Bissett RA, Jampel HD. A whole field scotopic retinal sensitivity test for the detection of early glaucoma. Archives of Ophthalmology. 1992; 110:486-490

274.Fortune B, Bui BV, Morrison JC et al. Selective ganglion cell functional loss in rats with experimental glaucoma. Investigative Ophthalmology and Visual Science. 2004; 45: 1854-1862

275.Frishman LJ, Shen FF, Du L et al. The scotopic electroretinogram of macaque after retinal ganglion cell loss from experimental glaucoma. Investigative Ophthalmology and Visual Science. 1996; 37:125-141

276.Bui BV, Edmonds B, Cioffi GA, Fortune B. The gradient of retinal functional changes during acute intraocular pressure elevation. Investigative Ophthalmology and Visual Science. 2005; 46:202-213

277.He Z, Bui BV, Vingrys AJ. The rate of functional recovery from acute IOP elevation. Investigative Ophthalmology and Visual Science. 2006; 47:4872-4880

278.O'Donaghue E, Arden GB, O'Sullivan F et al. The pattern electroretinogram in glaucoma and ocular hypertension. British Journal of Ophthalmology. 1992; 76:387-394

279.Harrison JM, O'Connor PS, Young RSL, Kincaid M, Bentley R. The pattern ERG in man following surgical resection of the optic nerve. Investigative Ophthalmology and Visual Science. 1987;28:492-49

280.Papst N, Bopp N, Schnaudigel OE. Pattern electroretinogram and visual evoked

cortical potentials in glaucoma. Graefe's Archives of Clinical and Experimental Ophthalmology. 1984; 222: 29-35

281. Porciatti V, Falsini B, Brunori S, Colotto A, Moretti G. Pattern-reversal electroretinogram as a function of spatial frequency in ocular hypertension and early glaucoma. Documenta Ophthalmologica. 1987; 65:349-355

282. Trick GL, Bickler-Bluth M, Cooper DG, Kolker AE, Nesher R. Pattern- reversal electroretinogram (PRERG) abnormalities in ocular hypertension: correlation with glaucoma risk factors. Current Eye Research. 1988; 7:201- 206

283. Parisi V, Miglior S, Manni GL, Centofanti M, Bucci MG. Clinical ability of pattern electroretinograms and visual evoked potentials in detecting visual dysfunction in ocular hypertension and glaucoma. Ophthalmology. 2006; 113:216-228

284. Lam BL (ed) Electrophysiology of vision. Boca Raton: Taylor and Francis group; 2005.

285. Dawson WW, Parmer R, Hope GM, Trick GL. Excitation and inhibition of the pattern evoked retinal response in a foveate animal. Documenta Ophthalmologica. 1984; 40:11- 20

286. Maffei L, Fiorentini A. Electroretinographic responses to alternating gratings before and after section of the optic nerve. Science. 1981; 211:953-955

287. Bach M. Electrophysiological approaches for early detection of glaucoma. European journal of Ophthalmology. 2001; 11:S41-S49

288. Trick G. Pattern-reversal retinal potentials in ocular hypertensives at high and low risk of developing glaucoma. Documenta Ophthalmologica.1987; 65:79-85

289. Bach M, Hiss P, Rover J. Check-size specific changes of pattern electroretinogram in

patients with early open-angle glaucoma. Documenta Ophthalmologica. 1988; 69: 315-322

290. Watanabe I, Iijima H, Tsukahara S. The pattern electroretinogram in glaucoma: an evaluation by relative amplitude from the Bjerrum area. British journal of Ophthalmology. 1989; 73:131-135

291. Holder GE. Significance of abnormal pattern electroretinography in anterior visual pathway dysfunction. British Journal of Ophthalmology. 1987;71:166- 171

292. Howe JW, Mitchell KW. Visual evoked cortical potential to paracentral retinal stimulation in chronic glaucoma, ocular hypertension and an age-matched group of normals. Documenta Ophthalmologica. 1986; 63:37-44

293. Papst N, Bopp M, Schnaudigel OE. The pattern evoked electroretinogram associated with elevated intraocular pressure. Graefe's Archives for Clinical and Experimental Ophthalmology. 1984; 222;34-37

294. Wanger P, Persson HE. Pattern-reversal electroretinograms in ocular hypertension. Documenta Ophthalmologica. 1985; 61:27-31

295. Bowd C, Tafreshi A, Vizzeri G, Zangwill L, Sample PA, Weinreb RN. Repeatability of pattern electroretinogram using a new paradigm optimized for glaucoma detection. Journal of Glaucoma. 2009; 18:437-442

296. Otto T, Bach M. Retest variability and diurnal effects in the pattern electroretinogram. Documenta Ophthalmologica. 1996; 92:311-323

297. Maddess T, James AC, Goldberg I, Wine S, Dobinson J. A spatial frequency-doubling illusion-based pattern electroretinogram for glaucoma. Investigative Ophthalmology and Visual Science. 2000; 41:3818-3826

298.Holopigian K, Snow J, Seiple W, Siegel I. Variability of the pattern electroretinogram. Documenta Ophthalmologica. 1988; 70:103-115

299.Regan RD. Human Brain Electrophysiology: Evoked Potentials and Evoked Magnetic Fields in Science and Medicine. New York; Elseiver Science Publishing; 1989

300.Sokol S. Visual Evoked Potentials: theory, techniques and clinical applications. Survey of Ophthalmology. 1976; 21:18-44

301.Yiannikas C, Walsh JC. The variation of the pattern shift visual evoked response with the size of the stimulus field. Electroencephalography and Clinical Neurophysiology. 1983; 55:427-435

302.Weinstein G, Arden G, Hitchings R, Ryan S, Calthorpe C, Odom J. The pattern electroretinogram in ocular hypertension and glaucoma. Archives of Ophthalmology. 1988; 106:923-928

303.Harter MR. Evoked cortical responses to checkerboard patterns: effect of check-size as a function of retinal eccentricity. Vision Research. 1970; 10:1365-1376

304.Bach M, Hoffman MB. Update on the pattern electroretinogram in glaucoma. Optometry and Vision Science. 2008; 85:386-395

305.Bach M, Unsoeld AS, Phillippin H et al. Pattern ERG as an early glaucoma indicator in ocular hypertension: a long term prospective study. Investigative Ophthalmology and Visual Science. 2006; 47:4881-4887

306.Porciatti V, Ventura LM. Normative data for a user friendly paradigm for pattern electroretinogram. Ophthalmology. 2004; 111:161-168

307.Towle VL. Moskowitz A, Sokol S, Schwartz B. The visual evoked potential in glaucoma and ocular hypertension: effects of check size, field size, and stimulation

rate. Investigative Ophthalmology and Visual Science. 1983; 24:175-183

308.Schmeisser ET, Smith TJ. Flicker visual evoked potential differentiation of glaucoma. Optometry and Visual Science. 1992; 69:458-462

309.Nyaken H, Raitta C. The correlation of visual evoked potential and visual field indices in glaucoma and ocular hypertension. Acta Ophthalmologica. 1989; 67:393- 395

310.Hood DC, Frishman LJ, Saszik S, Viswanathan S et al. Retinal origins of the primate multifocal ERG: implications for the human response. Investigative Ophthalmology and Visual Science. 2002; 43:1673-1685

311.Hood DC, Frishman LJ, Viswanathan S, Ahmed J, Robson JG. Evidence for a ganglion cell contribution to the primate electroretinogram (ERG): Effects of TTX on the multifocal ERG in macaque. Visual Neuroscience. 1999; 16:411-416

312.Hood DC, Greenstein V, Frishman L et al. Identifying inner retinal contributions to human multifocal ERG. Vision Research.1999; 39:2285-2291

313.Sutter EE, Bearse MA. The optic nerve head component to the human ERG. Vision Research. 1999; 39:419-436

314.Hood DC, Bearse MAJ, Sutter EE, Viswanathan S, Frishman LJ. The optic nerve head component of the monkey's (Macaca mulatta) multifocal electroretinogram (mERG). Vision Research. 2001; 41:2029-2041

315.Hood DC, Greenstein VC, Holopigian K et al. An attempt to detect glaucomatous damage to the inner retina with the multifocal ERG. Investigative Ophthalmology and Visual Science. 2000; 41:1570:1579

316.Lai TY, Chan WM, Lai RY, Ngai JW, Li H, Lam DS. The clinical applications of multifocal electroretinography: a systemic review. Survey of Ophthalmology. 2007;

52:61-96

317.Kretschmann U, Bock M, Gockeln R, Zrenner E. Clinical application of multifocal electroretinography. Documenta Ophthalmologica. 2000; 100:99-113

318.Fortune B, Johnson CA, Cioffi GA. The topographic relationship between multifocal electroretinographic and behavioural perimetric measures of function in glaucoma. Optometry and Vision Science. 2001; 78:206-214

319.Palmowski AM, Allgayer R, Heinemann-Vemaleken B. The multifocal ERG in open angle glaucoma – a comparison of high and low contrast recordings in high and low tension open angle glaucoma. Documenta Ophthalmologica. 2000; 101:35-49

320.Hasegawa S, Takagi M, Usui T, Takada R, Abe H. Waveform changes of the first-order multifocal electroretinogram in patients with glaucoma. Investigative ophthalmology and visual Science. 2000; 41: 1597-1603

321.Hood DC, Zhang X. Multifocal ERG and VEP responses and visual fields: comparing disease related changes. Documenta Ophthalmologica. 2000; 100:115- 137

322.Hare WA, Ton H, Ruiz G, Feldmann B, Wijono M, WoldeMussie E. Characterisation of retinal injury using ERG measures obtained with both conventional and multifocal methods in chronic ocular hypertensive primates. Investigative Ophthalmology and Visual Science. 2001; 42:127-136

323.Bearse MA, Sutter EE, Stamper RL. Detection of glaucomatous dysfunction using a global flash multifocal electroretinogram (mERG) paradigm. OSA technical digest Series, Optical Society of America, Washington DC. Vision Science and its Applications. 2001; 1:14-17

324.Sutter EE, Shimada Y, bearse MAJ. Mapping inner retinal function through

enhancement of adaptive components in the mERG. Vision Science and its applications, OSA Technical Digest Series. Washington DC. 1999; 52-55

325. Fortune B, Cull B, Wang L, Van Buskirk EM, Cioffi GA. Factors affecting the use of multifocal electroretinogram to monitor function in a primate model of glaucoma. Documenta Ophthalmologica. 2002; 105:151-178

326. Fortune B, Bearse MA, Cioffi GA, Johnson CA. Selective loss of an oscillatory component from temporal retinal multifocal ERG responses in glaucoma. Investigative Ophthalmology and Visual Science. 2002; 43:2638-2647

327. Palmowski AM, Allgayer R, Heinemann-Vernaleken B, Ruprecht KW. Multifocal electroretinogram with a multiflash stimulation technique in open angle glaucoma. Ophthalmic Research. 2002; 34:83-89

328. Stiefelmeyer S, Neubauer AS, Berninger T. The multifocal pattern electroretinogram in glaucoma. Vision Research. 2004;44:103-112

329. Harrison WW, Viswanathan S, Malinovsky VE. Multifocal pattern electroretinogram: Cellular origins and clinical implications. Optometry and Vision science. 2006; 83:473- 485

330. Regan D. Evoked potentials specific to spatial patterns of luminance and colour. Vision research 1973; 13:1933-1941

331. Hubel DH, Wiesel TN. Receptive fields and functional architecture of the monkey striate cortex. Journal of Physiology (London). 1968; 195:215-243

332. Bodis-Wollner I. Electrophysiological and psychophysical testing of vision in glaucoma. Survey of Ophthalmology. 1989; 33 (suppl):301-307

333. Schmeisser ET, Smith TJ. High-frequency flicker visual evoked potential losses in

glaucoma. Ophthalmology. 1989;96:620-623

334.Ducatti A, Fava E, Motti EDF. Neuronal generators of the visual evoked potentials: Intracerebral recordings in awake humans. Electroencephalography and Clinical Neurophysiology. 1988; 71: 89-99

335.Maier J, Dagrielle G, Spekreije H, van Duk BW. Principal component analysis for source localisation of VEPs in man. Vision Research. 1987; 27:165-171

336.Murray I, Parry NRA, Carden D, Kulikowski JJ. Human visual evoked potentials to chromatic and achromatic gratings. Clinical Vision Sciences. 1987; 1:258-263

337.Watts MT, Good PA, O'Neil EC. The flash stimulated VEP in the diagnosis of glaucoma. Eye. 1989; 3:732-737

338.Gray LG, Galetta SL, Siegal T, Schartz NJ. The central visual field in homonymous hemianopia. Evidence for unilateral foveal representation. Archives of Neurology. 1997; 54:312-317

339.Weinstein GW, Odom JV, Cavender S. Visual evoked potentials and electroretinography in neurologic evaluation. Review. Neurologic Clinic. 1991; 9:225-242

340.Fritsches K, Rosa M. Visuotopic organisation of striate cortex in the marmoset monkey. Journal of Comparative Neurology. 1996; 54:312-317

341.Accornero N, Gregori B, Galie E, De Feo A, Agnesi R. A new colour VEP procedure discloses asymptomatic visual impairments in optic neuritis and glaucoma suspects. Acta Neurologica Scandinavica. 2000; 102:258-263

342.Bradham MS, Montgomery DM, Evans AL et al. Objective detection of hemifield and quadrantic field defects by visual evoked cortical potential. British journal of

Ophthalmology. 1996; 80:297-303

343.Baseler HA, Sutter EE, Klein SA, Carney T. The topography of visual evoked response properties across the visual field. Electroencephalography and Clinical neurophysiology. 1994; 90:65-81

344.Patten J. Neurological differential diagnosis. London: Springer; 1995

345.Sutter E. The Fast m-Transform: A Fast Computation of Cross-Correlations with Binary m-Sequences. SIAM Journal of Computing. 1991; 20:686-691

346.Sutter E, Tran D. The field topography of ERG components in man – I. The photopic luminance response. Vision Research. 1992; 32:433-446

347.Baseler HA, Sutter EE. M and P components of the VEP and their visual field contribution. Vision Research. 1997; 37:675-790

348.Horton JC, Hoyt F. The representation of the visual field in the human striate cortex. Archives of Ophthalmology. 191; 109:816-824

349.Sutter E. Imaging visual function with the multifocal m sequence technique. Vision Research. 2001; 39:1241-1255

350.Sutter E. A deterministic approach to non-linear systems analysis. In: Pinter RB NB (ed), Nonlinear vision: Determination of neural receptive fields, functions and networks. Cleveland: CRC press 1992; 171-220

351.Victor JD. Non linear systems analysis in vision: overview of kernel methods. In: Pinter RB NB (ed), Nonlinear vision: Determination of neural receptive fields, functions and networks. Cleveland: CRC press 1992; 1-37

352.Klistorner AI, Graham SL. Early magnocellular loss in glaucoma demonstrated using the pseudorandomly stimulated flash visual evoked potential. Journal of Glaucoma.

1999; 8:140-148

353.Sutter E. The interpretation of multifocal binary kernels. Documenta Ophthalmologica. 2000; 100:49-75

354.Klistorner AI, Graham SL. Electroencephalogram based scaling of multifocal visual evoked potentials: effect on intersubject amplitude variability. Investigative Ophthalmology and Visual Science. 2001; 42:2145-2152

355.Erikoz B, Jusuf PR, Percival KA, Grunert U. Distribution of bipolar input to midget and parasol cells in the marmoset retina. Visual Neuroscience. 2008; 25:67-76

356.Klistorner AI, Graham SL, Grigg JR, Billson FA. Multifocal topographic visual evoked potential: improving objectivedetection of the local visual field defects. Investigative Ophthalmology and Visual Science. 1998; 39:937-950

357.Graham SL, Klistorner A, Grigg JR, Billson FA. Objective perimetry in glaucoma-recent advances using multifocal stimuli. Survey in Ophthalmology. 1999; 43: s199-209

358.Hood DC, Zhang X, Hong JE, Chen CS. Quantifying the benefits of additional channels of multifocal VEP recording. Documenta Ophthalmologica. 2002;104:303-320

359.Meigen T, Kramer M. Optimizing electrode positions and analysis strategies for multifocal VEP recordings by ROC. Vision Research. 2007; 47:1445-1454

360.Klistorner AI, Graham SL, Grigg J, Billson F. Electrode position and the multifocal visual evoked potential. Australian and New Zealand Journal of Ophthalmology. 1998; 26:S91-94

361.Klistorner AI, Crewther D. Separate magnocellular and parvocellular contributions

from temporal analysis of the multifocal VEP. Vision Research. 1997; 37: 2161-9.

362. Arvind H, Klistorner A, Graham S, Grigg J, Goldberg I, Billson FA. Dichoptic stimulation improves detection of glaucoma with multifocal visual evoked potentials. Investigative Ophthalmology and Visual Science. 2007; 48:4590- 4596

363. Arvind H, Klistorner A, Graham S, Grigg J. Multifocal visual evoked responses to dichoptic stimulation using the virtual reality goggles: multifocal VER to dichoptic stimulation. Documenta Ophthalmologica. 2006; 112:189- 199

364. Graham SL, Klistorner AI, Grigg JA, Bilson FA. Objective VEP perimetry in glaucoma: asymmetry analysis to identify early defects. Journal of Glaucoma. 2000;9:10-19

365. Hood DC, Zhnag X, Greenstein VC et al. An interocular comparison of the multifocal VEP: a possible technique for detecting local damage to the optic nerve. Investigative Ophthalmology and Visual Science. 2000; 41:1580-1587

366. Fortune B, Demirel S, Bui BV. Multifocal visual evoked potentials to pattern reversal, pattern offset and sparse pulse stimuli. Visual Neuroscience. 2009; 26:227-235

367. Zhang X, Hood DC, Chen CS, Hong JE. A signal to noise analysis of multifocal VEP responses: an objective definition of poor records. Documenta Ophthalmologica. 2002; 104:303-320

368. Maddess T, James AC, Bowman EA. Contrast response of temporally sparse dichoptic multifocal visual evoked potential. Visual Neuroscience. 2005; 22:153- 162

369. James AC, Ruseckaite R; maddess T. Effect of temporal sparseness and dichoptic presentation on multifocal visual evoked potentials. Visual Neuroscience. 2005; 22:45-54

370.Klistorner AI. Graham SL. Effect of eccentricity on pattern-pulse multifocal VEP. Documenta Ophthalmologica. 2005; 110:209-218

371.James AC, The pattern-pulse multifocal visual evoked potential. Investigative Ophthalmology and Visual Science. 2003; 44:879-890 372.Pieh C, Hoffman MB, Bach M. The influence of defocus on multifocal visual evoked potentials. Graefe's Archives for Clinical and Experimental Ophthalmology. 2005; 243:38-42

373.Winn BJ, Shin E, Odel JG, Greenstein VC, Hood DC. Interpreting the multifocal visual evoked potential: the effects of refractive errors, cataracts and fixation errors. British Journal of Ophthalmology. 2005; 89:340-344

374.Whitehouse GM. The effect of cataract on Accumap multifocal objective perimetry. American journal of Ophthalmology. 2003; 136:209-212

375.Fortune B, Goh K, Demirel S et al. Detection of glaucomatous visual field loss using multifocal VEP. IPS Proceedings 2002/2003. The Hague:Kugler Publication; 2004:251- 260

376.Sarwate, Pursley. Cross correlation properties of pseudorandom and related sequences.

Proceedings of IEEE. 1980; 68:593-619

377.Shimada Y, Horiguchi M, Nakamura A. Spatial and temporal properties of inter ocular timing differences in multifocal visual evoked potential. Vision Research. 2005; 45:365- 371

378.Maddess TT, Goldberg I, Wine S, Dobinson J, Welsh AH, james AC. Testing for glaucoma with the spatial frequency doubling illusion. Vision Research. 1999;39:4258- 4273

379.Hood DC, Greenstein VC. The multifocal VEP and ganglion cell damage: Applications and limitations for the study of glaucoma. Progress in Retinal Eye Research. 2003;22:201-251

380.Dandekar S, Ales J, Carney T, Klein SA. Methods for quantifying intra- and inter-subject variability of evoked potential data applied to the multifocal visual evoked potential. Journal of Neuroscience Methods. 2007; 165:270-286

381.Gallager AE, Chen CS, Hood DC. A comparison of multifocal visual evoked potentials recorded with different electrode positions. Investigative Ophthalmology and Visual Science. 2002;43:E-abstract 2172

382.Zhang X, Hood DC. A principal component analysis of multifocal pattern reversal VEP. Journal of Vision. 2004; 4:32-43

383.Goldberg I, Graham SL, Klistorner A. Multifocla objective perimetry in the detection of glaucomatous field loss. American Journal of Ophthalmology. 2002; 133:29-39

384.Fortune B, Demeril S, Zhang X, Hood DC, Johnson CA. Repeatability of normal multifocal VEP: implications for detecting progression. Journal of Glaucoma. 2006; 15: 131-141

385.Chen CS, Hood DC, Zhang X, Repeat repeatability of the multifocal visual evoked potential in normal and glaucomatous eyes. Journal of Glaucoma. 2003; 12:399-408

386.Klistorner A, Graham SL. Intertest variability of mfVEP amplitude: reducing its effect on the interpretation of sequential tests. Documenta Ophthalmologica. 2005; 111:159-167

387.Wangsupadilok B, Bereenstein VC, Kanadani FN et al. A method to detect progression of glaucoma using the multifocal visual evoked potential technique.

Documenta Ophthalmologica. 2009; 118:139-150

388.Fortune B, Hood DC. Conventional pattern-reversal VEPs are not equivalent to summed multifocal VEPs. Investigative Ophthalmology and Visual Science. 2003; 44:1367-1375

389.Balachandran C, Graham SL, Klistorner A, Goldberg I. Comparison of objective diagnositic tests in glaucoma – Heidelberg retinal tomography and multifocal visual evoked potentials. Journal of Glaucoma. 2006; 15:110-116

390.Grove LK, Hood DC, Ghadali Q et al. A comparison of multifocal and conventional visual evoked potential techniques in patients with optic neuritis /multiple sclerosis. Documenta Ophthalmologica. 2008;117:121-128.

391. Hoffmann MB. Straube S, Bach M. Pattern onset stimulation boosts central multifocal VEP responses. Journal of Vision. 2003; 3:432-439

392.Gardiner SK, Demirel S. Assessment of patient opinions of different clinical tests used in the management of glaucoma. Ophthalmology. 2008; 115:2127-2131

393.Klistorner AI, Graham S, Grigg J, Balachandran C. Objective perimetry using the multifocal visual evoked potential in the central pathway lesions. British Journal of Ophthalmology. 2007;89:739-744

394.Semela l, Yang EB, Hedges TR, Vuong L, Odel JG, Hood DC. Multifocal visual evoked potential in unilateral compressive optic neuropathy. British Journal of Ophthalmology. 2007; 91:445-448

395.Denesh Meyer HV, Carroll SC, Gaskin BJ, Gao A. Gamble GD. Correlation of the multifocal visual evoked potential and standard automated perimetry in compressive optic neuropathies. Investigative Ophthalmology and Visual Science. 2006;47:1458-

1463

396. Balachandran C, Klistorner A, Billson F. Multifocal VEP perimetry in children: its maturation and clinical application. British Journal of Ophthalmology. 2004:88:226-232

397. Odel JG, Winn BJ, Chen CS, Hong JE, Behrens MM, Hood DC. The multifocal visual evoked potential in a neuro-ophthalmology practice. Investigative Ophthalmology and Visual Science 2003; 44: E-abstract 2711

398. Hattenhauer MG, Johnson DH, Ing HH, Herman DC, Hodge DO, Yawn BP, et al. The probability of blindness from open-angle glaucoma. Ophthalmology. 1998;105:2099–104

399. Broman AT, Quigley HA, West SK, Katz J, Munoz B, Bandeen-Roche K, et al. Estimating the rate of progressive visual field damage in those with open-angle glaucoma, from cross-sectional data. Investigative Ophthalmology and Visual Science. 2008;49:66–76

400. Heijl A, Leske MC, Bengtsson B, Hyman L, Bengtsson B, Hussein M. Early Manifest Glaucoma Trial Group. Reduction of intraocular pressure and glaucoma progression: results from the Early Manifest Glaucoma Trial. Archives of Ophthalmology. 2002;120:1268–79

401. Leske MC, Heijl A, Hyman L, Bengtsson B. Early Manifest Glaucoma Trial: design and baseline data. Ophthalmology. 1999;106:2144–53

402. Heijl A, Bengtsson B, Hyman L, Leske MC. Early Manifest Glaucoma Trial Group. Natural history of open-angle glaucoma. Ophthalmology. 2009;116:2271–6

403. The effectiveness of intraocular pressure reduction in the treatment of normal-tension

glaucoma. Collaborative Normal Tension Glaucoma Study Group. American Journal of Ophthalmology. 1998;126:498–505

404. Langenegger J S, Funk J and Toteberg-Harms M. Reproducibility of retinal nerve fibre layer thickness measurements using the eye tracker and the retest function of Spectralis SD-OCT in glaucomatous and healthy control eyes. Invest Ophthalmol Vis Sci. 2011; 52:3338-3344.

405. Gupta N, Weinreb RN. New definitions of glaucoma. Curr Opin Ophthalmol. 1997;8:38– 41

406. A.J. Sit, F.A. Medeiros, R.N. Weinreb. Short-wavelength automated perimetry can predict glaucomatous standard visual field loss by ten years. Semin Ophthalmol. 2004; 19:122–124

407. L. Racette, P.A. Sample. Short-wavelength automated perimetry. Ophthalmol Clin North Am. 2003; 16:227–236

408. A.J. Anderson, C.A. Johnson. Frequency-doubling technology perimetry. Ophthalmol Clin North Am. 2003; 16:213–225

409. S. Kogure, Y. Toda, S. Tsukahara. Prediction of future scotoma on conventional automated static perimetry using frequency doubling technology perimetry. Br J Ophthalmol. 2006; 90:347–352

A. Ferreras, V. Polo, J.M. Larrosa et al. Can frequency-doubling technology and short-wavelength automated perimetries detect visual field defects before standard automated perimetry in patients with preperimetric glaucoma? J Glaucoma. 2007; 16:372–383

410. Quigley HA, Dunkelberger GR, Green WR. Retinal ganglion cell atrophy correlated

with automated perimetry in human eyes with glaucoma. American Journal Ophthalmology. 1989;107:453–464

411. Monhart M. What are the options of psychophysical approaches in Glaucoma? Surv Ophthal. 2007; 52:S127-S133

412. Jeoung JW, Kim TW, Weinreb RN, Kim SH, Park KH, Kim DM. Diagnostic ability of Spectral-domain versus Time-domain Optical Coherence Tomography in Glaucoma. J Glaucoma. 2013 Jan 31. (Epub ahead of print)

413. Balachandran C, Grahan SL, Klistorner A, Goldberg I. Comparison of Objective diagnostic tests in glaucoma: Heidelberg Retinal Tomogaphy and Multifocal Visual Evoked Potentals. J Glaucoma. 2006; 15:110-116

414. Klistorner A, Graham SL. Objective perimetry in glaucoma. Ophthalmology. 2000;107:2283–2299

415. Graham SL, Klistorner AI, Grigg JR, Billson FA. Objective VEP perimetry in glaucoma: asymmetry analysis to identify early deficits. J Glaucoma. 2000; 9:10–19

416. Hood DC, Zhang X. Multifocal ERG and VEP responses and visual fields: comparing disease-related changes. Doc Ophthalmol. 2000; 100:115–137

417. Hood DC, Zhang X, Greenstein VC, et al. An interocular comparison of the multifocal VEP: a possible technique for detecting local damage to the optic nerve. Invest Ophthalmol Vis Sci. 2000;41:1580–1587

418. Arvind H, Graham S, Leaney J, Grigg J, Goldberg I, Billson F, Klistorner A. Identifying preperimetric functional loss in glaucoma: a blue-on-yellow multifocal visual evoked potentials study. Ophthalmology. 2009; 116:1134-1141

419. Arvind H, Klistorner A, Grigg J, Graham SL. Low-luminance contrast stimulation is

optimal for early detection of glaucoma using multifocal visual evoked potentials. Invest Ophthalmol Vis Sci. 2011 Jun 1; 52(6):3744-50

420. Leeprechanon N, Giaconi J A, Manassakorn A, Hoffman D, Caprioli J. Frequency Doubling Perimetry and Short-Wavelength Automated Perimetry to detect Early Glaucoma. Ophthalmol. 2007; 114:931-937

421. Regan D. Human brain electrophysiology: evoked potentials and evoked magnetic fields in science and medicine. Elsevier, New York, 1989. pp 431–441

422. Hood DC, Greenstein VC. Multifocal VEP and ganglion cell damage: applications and limitations for the study of glaucoma. Progress in Retina and Eye Research. 2003; 22:201–251

423. Baseler HA, Sutter EE, Klien SA, Carney T. The topography of visual evoked response properties across the visual field. Electroencephalography and Clinical Neurophysiology. 1994; 90:65–81

424. Daniel PM, Whitteridge D. The representation of the visual field on the cerebral cortex in monkeys. Journal of Physiology.1961; 159:203–221

425. Riggs LA, Wooden BR. Electrical measures and psychophysical data on human vision. In: Jamison D, Hur- vich LM (eds) Handbook of sensory physiology, vol 7/4. Springer, New York, 1972. pp 690–731

426. Yiannikas C, Walsh JC (1983) The variation of the pattern shift visual evoked response with the size of the stimulus field. Electroencephalography and Clinical Neurophysiology. 1983; 55:427–435

427. Brigell MG (2001) The visual evoked potential. In: FIshman GA, Birch DG et al (eds) Electrophysiological testing in disorders of the retina, optic nerve and visual

pathway. American Academy of Ophthalmology, San Francisco, pp 237–279

428.Ebers GC. Optic neuritis and multiple sclerosis. Archives of Neurology. 1985; 42:702– 704

429.Jones SJ, Brusa A. Neurophysiological evidence for long-term repair of MS lesions: implications for axon pro- tection. Journal of Neurological Science. 2003; 206:193–198

430.Hood DC, Ohri N, Yang EB, Rodarte C, Zhang X, Fortune B, Johnson CA. Determining abnormal latencies of multifocal visual evoked potentials: a monocular analysis. Documenta Ophthalmologica. 2004; 109:189–199

431.Hood DC, Zhang X, Rodarte C, Yang EB, Ohri N, Fortune B, Johnson CA. Determining abnormal interocular latencies of multifocal visual evoked potentials. Documenta Ophthalmologica. 2004; 109:177–187

432.Klistorner A, Graham SL. Effect of eccentricity on pattern-pulse multifocal VEP. Documenta Ophthalmologica. 2005; 110: 209–218

433.Graham SL, Klistorner A, Grigg JR, Billson FA. Objective VEP perimetry in glaucoma: asymmetry analysis to identify early deficits. Journal of Glaucoma. 2000; 9:10–19

434.Klistorner , Graham SL. Electroencephalogram- based scaling of multifocal visual evoked potentials: effect on intersubject amplitude variability. Investigative Ophthalmology and Visual Science. 2001; 42:2145–2152

435.Goldberg I, Graham SL, Klistorner A. Multifocal objective perimetry in the detection of glaucomatous field loss. American Journal of Ophthalmology. 2002; 133:29–39

436.Klistorner A, Fraser C, Garrick R, Graham SL, Arvind H. Correlation between

fullfield and multifocal VEPs in optic neuritis. Documenta Ophthalmologica. 2008; 116:19–27

437.Hubel DH, Wiesel TN, Ferrier lecture. Functional architecture of macaque monkey visual cortex. Proceedings of the Royal Society of London. 1977; 198:1–59

438.Parry NRA, Murray IJ, Hadjizenonos C. Spatio- temporal tuning of VEP: effect of mode of stimulation. Vision Research. 1999; 39:3491–3497

439.Fortune B, Hood DC.Conventional pattern-reversal VEPs are not equivalent to summed multifocal VEPs. Investigative Ophthalmology and Visual Science. 2003; 44:1364–1375

440.Waxman SG. Altered distributions and functions of multiple sodium channel subtypes in multiple sclerosis and its models. In: Waxman SG (ed) Multiple sclerosis as a neuronal disease. Elsevier, Amsterdam. 2005; pp 101–118

441.Martin M, Hiltner TD, Wood JC, Fraser SE, Jacobs RE, Readhead C. Myelin deficiencies visualized in vivo:visually evoked potentials and T2-weighted magnetic resonance images of shiverer mutant and wild-type mice. Journal of Neuroscience Research. 2006; 84:1716–1726

442.Klistorner A, Graham SL, Fraser C, Garrick R, Nyugen T, Paine M, O'Day J, Grigg JR, Arvind H, Billson FA. Electrophysiological evidence for heterogeneity of lesions in optic neuritis. Investigative Ophthalmology and Visual Science. 2007; 48:4549–4556

443.Halliday AM, McDonald WI, Mushin J. Delayed visual evoked response in optic neuritis. Lancet. 1972; 1: 982–985

444.McDonald WI. Pathophysiology of conduction in central nerve fibres. In: Desmedt JE

(ed) Visual evoked potentials in man. Clarendon Press, Oxford. 1977; pp 427–437

445. Halliday AM, Darbett G, Blumhardt. The macular and submacular components of pattern evoked response. In: Lehman D, Callaway E (eds) Human evoked potentials. Plenum Publishing, New York. 1979; pp 135–151

446. Klistorner A, Graham SL, Grigg JR, Billson FA. Multifocal topographic visual evoked potential: improvingobjective detection of local visual field defects. Investigative Ophthalmology and Visual Science. 1998; 39(6):937–950

447. Hood DC, Odel JG, Zhang X. Tracking the recovery of local optic nerve function after optic neuritis: a multifocal VEP study. Investigative Ophthalmology and Visual Science. 2000; 41(12):4032–4038

448. Graham SL, Klistorner A, Goldberg I. Clinical application of objective perimetry using multifocal visual evoked potentials in glaucoma practice. Archives of Ophthalmology. 2005; 123:729–739

449. Laron M, Cheng H, Zhang B, Schiffman JS, Tang RA, Frishman LJ. Assessing visual pathway function in multiple sclerosis patients with multifocal visual evoked potentials. Multiple sclerosis. 2009; 15:1431–1441

450. Yang EB, Hood DC, Rodarte C, Zhang X, Odel JG, Behrens MM. Improvement in conduction velocity after optic neuritis measures with the multifocal VEP. Investigative Ophthalmology and Visual Science. 2007; 48:692–698

451. Lassmann H. Pathology of neurons in multiple sclerosis. In: Waxman SG, ed. Multiple sclerosis as a neuronal disease. Amsterdam: Elseiver, 2005; 153-164

452. Youl BD, Turano G, Miller DH, et al. The pathophysiology of acute optic neuritis. An association of gadolinium leakage with clinical and electrophysiological deficits.

Brain. 1991;114: 2437–2450

453.Trip A, Schlottmann PG, Jones SJ, et al. Optic nerve atrophy and retinal nerve fibre layer thinning following optic neuritis: evidence that axonal loss is a substrate of MRI-detected atrophy. Neuroimage 2006;31:286–293.

454.Sergott RC, Frohman EM, Glanzman R, Al-Sabbagh A. Optical coherence tomography in multiple sclerosis: expert panel consensus. J Neurol Sci 2007;263:3–14

455.Nuver MR. Evoked potentials. In: Cook SD, ed. Handbook on multiple sclerosis. New York: Taylor & Francis, 2006:243–269.

456.456. Gelfand, J.M., et al., Retinal Axonal Loss Begins Early in the Course of Multiple Sclerosis and Is Similar between Progressive Phenotypes. PloS ONE, 2012. 7: p. e36847

457.Gundogan, F.C., S. Demirkaya, and G. Sobaci, Is optical coherence tomography really a new biomarker candidate in multiple sclerosis? Invest Ophthalmol Vis Sci, 2007. 48: p. 5773-5781

458.Evangelou, N., et al., Size-selective neuronal changes in the anterior optic pathways suggest a differential susceptibility to injury in multiple sclerosis. Brain, 2001. 124: p. 1813-1820

459.Ganter, P., C. Prince, and M.M. Esiri, Spinal cord axonal loss in multiple sclerosis: a post-mortem study. Neuropathol Appl Neurobiol, 1999. 25: p. 459- 467

460.Matthews, M.R. and e. al, Transneuronal cell degenerationin the lateral geniculate nucleus of the Macaque monkey. J Anat, 1960. 94: p. 145-168

461.Johnson, H. and A. Cowey, Transneuronal retrograde degeneration of retinal

ganflion cells following restricted lesions of striate cortex in the monkey. Exp Brain Res, 2000. 132: p. 269-275

462. Weller, R.E. and J.H. Kaas, Parameters affecting the loss of ganglion cells of the retina following ablation of striate cortex in primates. Vis Neurosci, 1989. 3: p. 327-349

463. Mehta, J.S. and G.T. Plant, Optical coherence tomography findings in congenital / long- standing homonymous hemianopia. Am J Ophthalmol, 2005. 140: p. 727-729

464. Cowey, A., I. Alexander, and P. Stoerig, Transneuronal retrograde degeneration of retinal ganglion cells and optic tract in hemianopic monkeys and humans. Brain, 2011. 134: p. 2149-2157

465. Jindahra, P., A. Petrie, and G.T. Plant, Retrograde trans-synaptic retinal ganglion cell loss idenfified by optical coherence tomography. Brain, 2009. 132: p. 628-634

466. Bridge, H., et al., Imaging reveals optic tract degeneration in hemianopia. Invest Ophthal Vis Sci, 2011. 52: p. 382-388

467. Ciccarelli, O., et al., Optic radiation changes after optic neuritis detected by tractography- based group mapping. Hum Brain Map, 2005. 25: p. 308-316

468. Barboni, P., et al., Microcystic macular degeneration from optic neuropathy: not inflammatory, not trans-synaptic degeneration. Brain, 2013. Advance Access: p. e1

469. Gelfand, J.M., et al., Microcystic macular oedema in multiple sclerosis is associated with disease severity. Brain, 2012. 135: p. 1786-1793

470. Hollander H, Bisti S, Maffei L, Hebel R. Electroperinographic re- sponses and

retrograde changes of retinal morphology after intra- cranial optic nerve section. Experimental Brain Research. 1984;55:483–493

471. Komaromy AM, Brooks DE, Kallberg ME, et al. Long-term effect of retinal ganglion cell axotomy on the histomorphometry of other cells in the porcine retina. Journal of Glaucoma. 2003;12:307–315

472. Weber AJ, Chen H, Hubbard WC, Kufman PL. Experimental glau- coma and cell size, density and number in the primate lateral nucleus. Investigative Ophthalmology and Visual Science. 2000;41:1370–1379

473. Yu cel YH, Zhang Q, Gupta N, Kaufman PL, Weinreb RN. Loss of neurons in magnocellular and parvocellular layers of the lateral geniculate nucleus in glaucoma. Archives of Ophthalmology. 2000;118:378 – 384

474. Yucel YH, Zhang Q, Weinreb RN, Kaufman PL, Gupta N. Effect of retinal ganglion cell loss on magno-, parvo-, koniocellular pathways in the lateral geniculate nucleus and visual cortex in glaucoma. Progress in Retinal and Eye Research. 2003;22:465–481

475. Gupta N, Ly T, Zhang O, et al. Chronic ocular hypertension induces dendrite pathology in the lateral geniculate nucleus of the brain. Experimental Eye Research. 2007;84:176– 184

476. Green IJ, McQuaid S, Hauser SL, Allen IV, Lyness R. Ocular pathology in multiple sclerosis: retinal atrophy and inflammation irre- spective of disease duration. Brain. 2010;133:1591–1601

477. Lei Y, Garraban N, Hermann B, et al. Quantification of retinal transneuronal degeneration in human glaucoma: a novel multiphoton DAPI approach.

Investigative Ophthalmology and Visual Science. 2008;49:1940– 1945

478.Gundogan FC, Demirkaya S, Sobaci G. Is optical coherence tomog- raphy really a new biomarker candidate in multiple sclerosis? Investigative Ophthalmology and Visual Science. 2007;48:5773–5781

479.Calabresi PA, Balcer LJ, Frohman EM. Retinal pathology in multiple sclerosis: insight into the mechanisms of neuronal pathology. Brain. 2010;133:1575–1577

480.Williams RR, Cusato K, Raven MA, Reese BE. Organization of the inner retina following early elimination of the retinal ganglion cell population. Visual Neuroscience. 2001;18:233–244

481.Blumenthal EZ, Parikh RS, Pe'er J, et al. Retinal nerve fiber layer imaging compared with histological measurements in a human eye. Eye. 2009;23:171– 175

482.Bagci AM, Shahidi M, Ansari R, et al. Thickness profiles of retinal layers by optical coherence tomography image segmentation. American Journal of Ophthalmology. 2008;146:679–686

483.Loduca A, Cjang C, Zelkha R, Shahidi M. Thickness mapping of retinal layers by spectral-domain optical coherence tomography. American Journal of Ophthalmology. 2010;150:848–855

484.McDonald WI, Compston A, Edan G, et al. Recommended diagnostic criteria for multiple sclerosis: guidelines from the International Panel on the diagnosis of the multiple sclerosis. Ann Neurol. 2001;50:121–127

485.Nakajima H, Hosokawa T, Sugino M, et al. Visual field defect of optic neuritis in neuromyelitis optica compared with multiple sclerosis. BMC Neurol. 2010;10:45.

486.Evangelou N, Konz D, Esiri MM, et al. Size-selective neuronal changes in the anterior

optic pathways suggest a differential sus- ceptibility to injury in multiple sclerosis. Brain. 2001;124:1813– 1820

487. Ciccarelli O, Toosy AT, Hickman SJ, et al. Optic radiation changes after optic neuritis detected by tractography based group mapping. Human Brain Mapping. 2005;25:308– 316

488. Johnson H, Cowey A. Transneuronal retrograde degeneration of retinal ganglion cells following restricted lesions of striate cortex in the monkey. Experimental Brain Research. 2000;132:269–275

489. Jindahra P, Petrie A, Plant GT. Retrograde trans-synaptic retinal ganglion cell loss idenfified by optical coherence tomography. Brain. 2009;132:628–634

490. Brandt AU, Oberwahrenbrock T, Ringelstein M, et al. Primary retinal pathology in multiple sclerosis as detected by optical co- herence tomography. Brain. 2011;134:e193

491. Wang M, Hood DC, Cho JS, et al. Measurement of local retinal ganglion cell layer thickness in patients with glaucoma using frequency-domain optical coherence tomography. Archives of Ophthalmology. 2009;127:875–881

492. Quigley HA, Dunkelberger GR, Green WR. Retinal ganglion cell atrophy correlated with automated perimetry in human eyes with glaucoma. American Journal of Ophthalmology. 1989;107:453–464

493. Toussaint D, Perier O, Verstappen A, Bervoets S. Clinicopathological study of the visual pathways, eye and cerebral hemisperes in 32 cases of disseminated sclerosis. Journal of Clinical Neuroophthalmology. 1983; 3:211–220

494. Brusa A, Jones SJ, Kapoor R, Miller DH, Plant GT. Long-term recovery and fellow

eye deterioration after optic neuritis, deter- mined by serial visual evoked potentials. Journal of Neurology. 1999;246:776 – 782

495. Martin PR, Grunert U. Soatial density and immunoreactivity of bipolar cells in the Macaque monkey retina. Journal of Computational Neurology. 1992;323:269 –287

496. Krebs W, Krebs IP. Quantitative morphology of the central fovea of the of the primate retina. American Journal of Anatomy. 1989;184:225–236

497. BridgeH, JindahraP, BarburJ, PlantGT. Imaging reveals optic tract degeneration in hemianopia. Investigative Ophthalmology and Visual Science. 2011;52:382–388

498. Coupland SG, Kirkham TH. Flash electroretinogram abnormalities in patients with clinically definite multiple sclerosis. Canadian Journal of Neurological Sciences. 1982;9:325–330

499. Forooghian F, Sproule M, Westall C, et al. Electroretinigraphic abnormalities in multiple sclerosis: possible role for retinal auto-antibodies. Documenta Ophthalmologica. 2006;113:123–132

500. Velten IM, Horn FK, Korth M, Velten K. The b-wave of the dark-adapted flash electroretinogram in patients with advanced asym- metrical glaucoma and normal subjects. British Journal of Ophthalmology. 2001; 85:403– 409

MACQUARIE UNIVERSITY

Research Office
Research Hub, Building C5C East
MACQUARIE UNIVERSITY NSW 2109

Phone +61 (0)2 9850 8612
Fax +61 (0)2 9850 4465
Email ro@vc.mq.edu.au

Ethics
Phone +61 (0)2 9850 6848
Email ethics.secretariat@vc.mq.edu.au

Macquarie University Ethics Review Committee (Human Research)

Human Research Ethics Committee

External Application Approval Form

When to use this form:

USE THIS FORM if you have submitted an ethics application to an external NH&MRC registered Human Research Ethics Committee (excluding the NSW Department of Education Approval) from any of the following:

- Another University
- NSW Health Human Research Ethics Committees or Lead Human Research Ethics Committees http://www.health.nsw.gov.au/ethics/research/contactshrec.asp
- Cancer Institute NSW Clinical Research Ethics Committee http://www.cancerinstitute.org.au/cancer_inst/research/ethics.html
- Area Health Service Ethics Committees
- Hospital Human Research Ethics Committees

IF you have already submitted an ethics application to one of these committees you can complete this MQ External Human Research Ethics Committee Application Approval Form and you WILL NOT BE REQUIRED to submit a full Macquarie University Ethics Review Committee (Human Research) ethics application.

How to use this form:

1. Complete the External Human Research Ethics Committee Application Approval Form (on the following page)
2. Attach the completed form with:
   - The **external ethics application form** (i.e. the application form submitted to one of the Human Research Ethics Committees above)
   - The **final approval letter** from the external Human Research Ethics Committee
   - **All correspondence** between you and the external Human Research Ethics Committee.
3. Please submit all hard copies printed **double sided** if possible.

OFFICIAL USE ONLY
SURNAME:
REF. NO.:

External Application Approval Form

Please attach this page ONLY to your external HREC application form, final approval letter and all correspondence.

1. Project Title: "Optimizing the detection of early glaucoma targeting specific visual pathways in combination with structural measures."

2. Indicate whether the project is a staff or student application

Staff: **Student: Yes**
Staff no: **Student no: 41680367 (John Leaney)**

3. External HREC Name: University of Sydney

4. External HREC Approval Number: 05-2009/11594

5. Name/s and details of all Investigator/s (extra rows in final page if necessary)

Name and Academic Qualifications	Investigator (Chief 1,2,3 etc., or Associate)	Positions held		Faculty	Department	Contact details	
		Staff	Student			Telephone	Email
A/Prof Sasha Klistorner (ASAM – Ophthalmology and Medicine Sydney Uni)	Chief	x		ASAM	Ophthalmology	0408267250	sasha@eye.usyd.edu.au
Professor Stuart Graham (ASAM – Ophthalmology)	Chief	x		ASAM	Ophthalmology	0416060862	Stuart.Graham@asam.mq.edu.au
Dr Hemamalini Arvind	1	x			Ophthalmology	0432107400	hema@eye.usyd.edu.au
Dr John Leaney	1		x	ASAM	Ophthalmology	0410641616	John.leaney@students.mq.edu.au
Dr Prema Sriram	1		x	ASAM	Ophthalmology		Premasriram@gmail.com

6. Student's Supervisor and contact details (if applicable):

Professor Stuart Graham
A/Prof Sasha Klistorner

7. Duration of project:

Commencement date: November 2009

Completion date: May 2014

IMPORTANT NOTICE: ELECTRONIC SUBMISSION OF THIS FORM IS EQUIVALENT TO YOUR SIGNATURE AND THAT OF YOUR SUPERVISOR (IF APPLICABLE).

Name/s and details of all Investigator/s (any additions to Q5 from previous page)

Name and Academic Qualifications	Investigator (Chief 1,2,3 etc., or Associate)	Positions held		Faculty	Department	Contact details	
		Staff	Student			Telephone	Email
